University of Padua
Technical University of Denmark

Environmental Engineering Department

EVALUATION OF THE METHANE MITIGATION AT THE AV MILJØ PILOT BIOCOVER SYSTEM

Master Student Candidate
CASSINI FILIPPO

Internal Supervisor: Mantovani Antonio
External Supervisor: Kjeldsen Peter

There is a *driving force* more powerful than steam, electricity and nuclear power: *the will*.

- Albert Einstein -

Fairy Tales are more than *true*; not because they tell us that *dragons exist*, but because they tell us that *dragons can be beaten*.

- Gilbert K. Chesterton -

ABSTRACT

In the last years, EU landfill policies force European countries to reduce the quantity of organic waste diverted to landfilling. Consequently, landfill gas generation from landfills is intended to be drastically reduced in the future, making economically unfeasible the realization of landfill gas extraction systems. In these circumstances, is fundamental to: 1) develop low-cost alternative technology for LFG management, as methanotrophic oxidation in biofilters, and 2) optimize monitoring techniques to evaluate methane oxidation performances. The aim of this study was to assess the methane oxidation efficiency of the biofilter implemented at AV Miljø landfill (Denmark) and evaluate the reliability of the Tracer Mass Balance Approach as a tool to calculate biofilter performances. The achieved average methane oxidation performance of the biofilter was 18 $g \cdot m^{-2} \cdot d^{-1}$. A substantial difference was observed between the oxidation performance of the area near the gas inlet (50 $g \cdot m^{-2} \cdot d^{-1}$) and the farther area (10 $g \cdot m^{-2} \cdot d^{-1}$) of the biofilter. The scarceness of landfill gas in the farther biofilter volume produced this gap, but the exact cause of this inhomogeneous distribution has not been identified. On the other hand, methane emissions were proved to be considerably low (0-0.16 $g \cdot m^{-2} \cdot d^{-1}$), without the substantial presence of emission hot spots. The average oxidation efficiency of 99.7 % measured on January 25th proved the robustness of AV Miljø biofilter, able to obtain high performances also during the winter season. The biofilter was be able to adapt its conformation depending to atmospheric pressure and temperature variation, maintaining a constant methane oxidation performance. This flexibility is guaranteed by the constant presence of O_2 at every depth and by the thermal insulation of the methanotrophic active layer. The Tracer Mass Balance Approach has been proved to be more reliable than the Carbon Mass Balance Approach if applied with low methane superficial fluxes, due to its simple methodology and data interpretation. Future studies could focus on investigate the causes of the scarce LFG distribution in the farther volume, assess the biofilter performances with different environmental conditions and redesign the pilot plant to guarantee LFG distribution in whole biofilter.

KEYWORDS: *Landfill gas emissions; Methanotrophs; Biocovers; Biofilters; Methane oxidation; Mass Balance.*

ACKNOWLEDGMENTS

I would like to express my full gratitude to Professor Peter Kjeldsen and Professor Charlotte Scheutz for the great opportunity to do my Master Thesis at DTU and for their assistance during the whole period. I want to thank also Professor Antonio Mantovani for the availability of supervising me from Italy.

This thesis would not have been possible without the daily help and commitment of Mou Zishen. He watched over me in every field experience, from the preparation to the realization. His contribution to my work was definitely essential. I could not have found a better friend.

A special thank to Bent Henning Skov, Technician in charge for this project, for his flexibility and for his practical skills. I'm grateful to the whole staff of AV Miljø for the assistance in critical situations and for their hospitality during the cold Danish nights.

I am highly indebted with all my friends, both here in Denmark and in Italy. I want to thank Jan De Schoenmaeker, Christian Pilegaard Jespersen and Stefan Danielsson for their friendship, with them also the harder work was a joke. How not to mention all my international friends living with me, they actually made this time of my life unforgettable. Especially I want to cite Franco Ly, George Tanev and Tatiana Katsaiti for their patience in correcting my thesis.

I would like to express my appreciation to my parents and my brother, they always drove me through every problem and pushed me to work hard. If in this moment I'm writing this piece, it's thank to them.

In the end, a special mention to my best friend and fiancee Elena Lavanda. I just want to thank her because, although I know that the fairy tale world does not exists, when we are together I can feel it is real.

CONTENTS

LIST OF FIGURES

LIST OF TABLES

ACRONYMS

HFC-134a 1,1,1,2-Tetrafluoroethane

EPS Exopolymeric Substances

FID Flame Ionization Detection

GHG Greenhouse Gases

GWP Global Warming Potential

HDPE High Density Polyethylene

LFG Landfill Gas

MBT Mechnical Biological Treatment

MLPGS Multi Level Probes for Gas Sampling

MO Methane Oxidation

NDIR Non Dispersive Infrared

PMOB Passive Methane Oxidation Biocover

PVC Polyvinyl Chloride

SAR Surface Area Ratio

1

INTRODUCTION AND AIM OF THE THESIS

The work presented in this Master Thesis has been carried out as part of the project which involves the collaboration between DTU (Danmarks Tekniske Universitet) and AV Miljø Landfill. The final aim is to develop an alternative tool to landfill gas extraction systems, in order to manage methane emissions from landfills. Several parallel studies have been done between September 2012 and January 2013 to evaluate AV Miljø biofilter design and performances.

Particularly, the study presented in this Thesis is focused on three points. The first aspect is related to emissions monitoring, with the reliability evaluation of preliminary methodologies and of Mass Balance Approaches. The second point is the proper assessment of Methane oxidation performances and efficiencies of the biofilter. In the end, the analysis of biofilter behavior has been done, also considering the correlation with external factors.

The reliability analysis concerning the use of biocovers and biofilters as landfill gas management tools, is of considerable importance in the Waste Management panorama. In fact, landfilling is still a fundamental ring to close the loop of Waste Management Systems (Cossu, 2009). However, EU landfill policies (1999/31/EC) force European countries to reduce the quantity of organic waste diverted to landfilling (Bogner et al., 2008). Consequently, landfill gas generation from landfills is intended to be drastically reduced in the future, making economically unfeasible the realization of landfill gas extraction systems. In these circumstances, the development of a low-cost alternative technology as methanotrophic oxidation in compost covers is fundamental.

Chapter 2 introduces the thesis topic, with a general overview on landfilling and landfill impacts management. Methanotrophic oxidation and the role of biofilters is then presented, to explain the importance of this technology in the waste management panorama. Chapter 3 summarizes the state of art of this technology, presenting the main biofilter designs and methane oxidation performances reported in previous studies. Moreover, a general description of AV Miljø landfill and biofilter are provided.

Chapter 4 gives detailed description of all the methodologies and analysis carried out during the monitoring and measurement activities. Chapter 5 presents raw data collected in this study, observing if it's possible to detect methanotrophic activities in the biofilter. In the second part of the chapter, the elaboration of this data is reported.

In the end, chapter 6 summarizes the thesis conclusions, trying to give a future prospective of this study and underlining the role of this study in methanotrophic based technologies development.

Strengths of this thesis are certainly the Tracer Mass Balance Approach assessment and the evaluation of AV Miljø biofilter flexibility and robustness from the point of view of methane oxidation.

2

GENERAL BACKGROUNDS

2.1 LANDFILL IMPACT

Waste management related to environment preservation is going to be one of the main issues of our time. Till few decades ago, the only available waste treatment was the disposal in open dumps. Only in the last years, developed countries have understood the importance of correct waste management and the safeguard of the environment. Several techniques for proper waste management have been developed in the last years, as waste recycling, incineration and biological and mechanical treatment Mechnical Biological Treatment (MBT). However, the use of underground waste disposal techniques is still widespread all over the world. All of the countries are trying to increase the percentage of recycled waste, using incineration technologies and landfilling as last option. The main criteria for the decision between incineration and landfilling is still the available space that a country has (Cossu, 2009a). That's the main reason why countries as the United States, Australia, South Africa, Canada and China use landfilling as primary choice, instead of countries such as Denmark, Japan, Singapore and many others rely more on incineration techniques. Nevertheless, also in those countries in which the national policy is based mainly on incineration, landfills are used for residues and incineration ashes disposal. Can be concluded that, despite all the technologies and studies conducted to date, as a matter of fact landfilling is still a fundamental ring to close the loop of our waste management systems (Cossu, 2009).

For this reason, it's important to understand how to reduce as much as possible the negative impact that landfills have on the surrounding environment and on the population living in closer areas. Obviously nowadays landfills have radically changed from the original open dumps, going to compose the "sanitary landfill" category (at least in developed countries). With the use of proper technologies, as bottom and top liners, embankment construction and Landfill Gas Landfill Gas (LFG) extraction systems, it's feasible to transform landfills from a strongly challenged way to treat waste into a positive tool to subtract carbon from the atmosphere and give it back to the ground. Due to the strong resistance of several compounds inside waste as lignin and cellulose, more than a half of the carbon stored in landfills cannot be degraded (Bogner et al., 2008). This theory is known with the name of Carbon Sink and is a fundamental point of

view to reassess the positive role of landfills in our waste management system.

Unfortunately, landfills still have several safety problems which originate impacts on the surrounding environment:

- Atmospheric emission of *LFG* containing methane and carbon dioxide, both Greenhouse Gases responsible of the overheating of the earth;
- Underground infiltration of *LFG* along preferential pathways, with risk of explosions in the surrounding living areas in case of sparks presence;
- Leachate underground infiltration with consequent groundwater pollution. The release of underground contaminants in the groundwater, can bring severe consequences for the population of the surrounding areas due to groundwater contamination;
- Landslides risk, due to mobilization of a great mass of waste, as consequence of increased moisture content. This impact can bring to severe consequences for local population, as in Payatas landslide with more than 200 victims.

Figure 1 shows a schematic representation of these possible harms, which need to be considered to assess the real landfill risk.

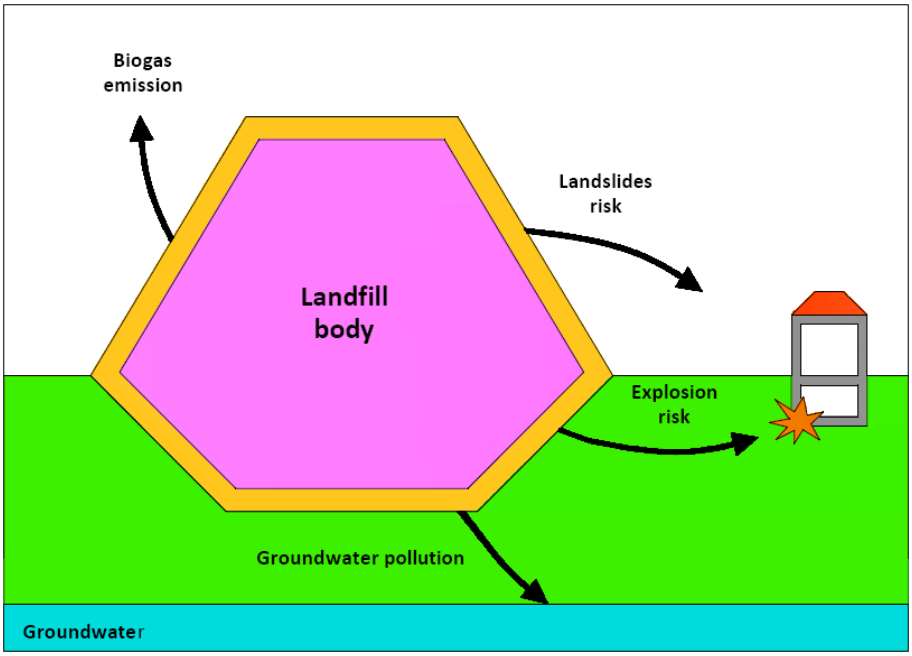

Figure 1: External impacts of a landfill((Kjeldsen, 1996), modified)

2.2 LANDFILL GAS IMPACT

One of the most dangerous and challenging impact is *LFG* emission. Biogas is dangerous for the environment and also for the population living around the emission point: the main damages involved are then described afterward.

It's known that *LFG* is constituted by several compounds generated by the anaerobic degradation of the organic substances. Between all these gases, Methane (CH_4) and Carbon Dioxide (CO_2) are those with greater concentrations (Scheutz et al., 2011). Moreover, it's well known the so called "Global Warming" phenomena, which consists in the continuous overheating of the atmosphere due to the increasing accumulation in the atmosphere of Greenhouse Gases Greenhouse Gases (GHG). Carbon Dioxide and Methane are both considered GHG, but Methane is generally considered as more dangerous for the atmosphere overheating. In fact, Global Warming Potential for Methane over a 100-years period (GWP_{100}) is 25 times the Global Warming Potential (GWP) for Carbon Dioxide. Methane is accounted to contribute about 14% to the total GHGs emission (Rogner, 2007). The waste sector has a great influence in the world methane emission. The estimated CH_4 contribution deriving from landfills and wastewater is approximately 18% of the total anthropogenic methane emission, and the total contribution to Global Warming is approximately 2.8% (Bogner et al., 2008). Landfills emissions have been accounted to 800 Mt CO_2-eq. in 2015 on a total GHGs emission of 49 Gt CO_2-equivalent. Moreover it's estimated to reach emissions greater than 4,000 Mt CO_2-eq. in 2050 (Bogner et al., 2008). The role of landfill biogas in Global Warming phenomena can't be considered just marginal. On the contrary, has to be considered a priority, also considering the realistic future increase of waste production and landfilling use due to the unavoidable increase of worldwide population.

Regarding *LFG* hazard, another fundamental impact is the risk of explosion. *LFG* usually has a relevant percentage of methane, ranging between 55-60% v/v (Fredenslund et al., 2010). Methane, in concentrations between 5 and 15% and in solution with atmospheric air, creates an explosive mixture. Consequently to *LFG* production inside the landfill body due to anaerobic conditions, an internal pressure buildup can be observed. Several factors are involved, at this point, in *LFG* behavior. First of all, geological factors (for example the presence of cracks or low permeability layers), and secondly meteorological factors (for example atmospheric pressure variation or soil moisture content). In the end landfill characteristics are also involved (for example the presence of gas ventilation pipes) (Kjeldsen, 1996). A combination of these factors, with an inefficient or in-existent landfill bottom and edges lining system, can bring to lateral migration of *LFG*. The *LFG* channeled into lateral cracks, low permeable soils or

also pipes, can diffuse in the surrounding subsoil, reaching nearby urban areas and fill closed underground environments. At this point every electric contact with the right mixture of air and methane can bring to an explosive event, as happened near Skellingsted landfill (Kjeldsen and Fischer, 1995).

Another factor that shouldn't be underestimated is fire hazard inside or in the surrounding areas of a landfill. Possible causes that may lead to this event are explosion due to *LFG* ignition, due to accidental events or high landfill temperatures. In case of fire, the presence of a continuous methane flux from the landfill body can generate harmful conditions for the nearby population due to:

- The difficulty of extinguish a fire continuously fed by methane;
- The possible extension of this phenomena;
- The unsafe generation of flue gas from waste burning.
- damages to the local flora can be caused by the presence of methane and carbon dioxide in the soil nearby plant's roots.

Damages to the local flora can be caused also by the excessive concentration of methane in the soil, due to vegetation asphyxia. Figure 2 shows a schematic representation of possible risks related to *LFG* uncontrolled emission from a landfill.

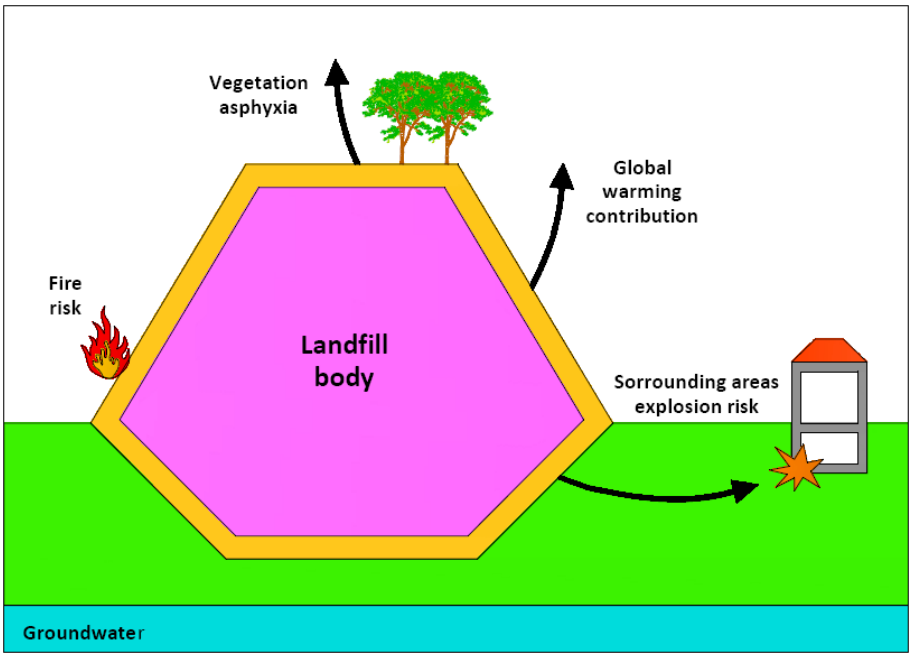

Figure 2: External impacts of *LFG* ((Kjeldsen, 1996), modified)

Standard levels of CO_2 in soils range between 0.04% and 2% and can be acceptable until 5% (Nagendran et al., 2006). In case that CO_2 concentration exceeds 20% of the soil-gas phase, carbon dioxide becomes phytotoxic causing diseases and chlorosis (Gendebien, 1992).

Contrarily, methane it's not phytotoxic for plants but can generate growth problems. Oxygen, which is needed from plants in concentrations between 5% and 10%, is replaced by methane and CO_2 causing asphyxia. Besides, the scarce oxygen presence inside the soil generates the appearance of bacteria working in anaerobic conditions, which are responsible of soil acidification and of the C/N ratio imbalance(Gendebien, 1992).

2.3 *LFG* MANAGEMENT: TECHNOLOGIES AND ISSUES

Consequently to all previous considerations, during the last decades several methods have been developed for a proper and safe *LFG* management. The main technology applied in this field is *LFG* extraction from biogas detection wells, with the consequent reuse of *LFG* for energy and heat production. In the life of a landfill we can identify different periods with different *LFG* extraction efficiencies. During the operational period we can obtain an extraction efficiency of 35% with an active *LFG* recovery system. The recovery efficiency can be increased to 65% during the temporary cover period and reach a maximum of 90% during the active aftercare period (Spokas et al., 2006). In figure 3, the different phases and the total recoveries of *LFG* extraction can be observed.

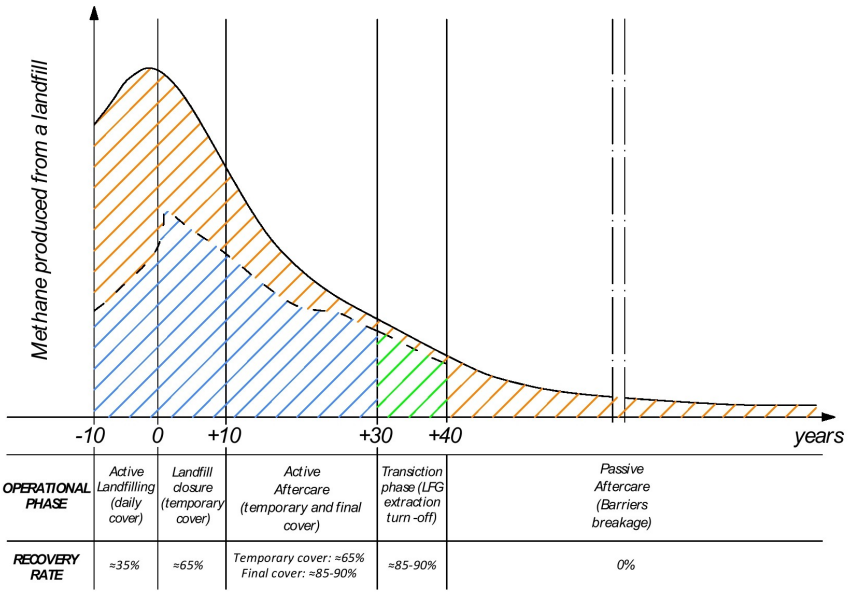

Figure 3: Landfill Gas recovery and dispersion ((Huber-Humer et al., 2008), modified)

It's easy to understand that the quantity of methane not recovered with the extraction system is not negligible. Moreover, there is plenty

of reasons not to consider this technology acceptable from the point of view of *LFG* recovery efficiency.

One of the main reasons is related to *LFG* emissions from a landfill body. *LFG* has the propensity to exit from preferential pathways as landfill leachate wells (Fredenslund et al., 2010), soil cracks and landfill slopes (Scheutz et al., 2011a). *LFG* emissions in two Danish landfills have been measured, showing that methane escaped from leachate wells is respectively the 27% and 44% of the total methane emitted from the landfill (Fredenslund et al., 2010).

Another important reason is strictly related with economical aspects connected to the realization of a *LFG* extraction system. The *LFG* extraction plant is a very expensive technology that following requires a gain. This is the main reason why it's considered unaffordable for small landfills or for landfills sited in developing countries. In fact, developing countries often don't have enough funds to invest in the waste management system, leaving to citizens the task to manage and dispose waste. Moreover, usually there is not a cultural attitude and education to consider waste not only as garbage but as a resource.

Conclusively, another weakness of the *LFG* extraction system are the old waste disposal sites, present all over the developed countries, which include old landfills and small dumping sites. For all these waste sites the *LFG* peak production period has elapsed, but they are still producing methane as shown in figure 3 for landfills in the aftercare period. Obviously, the possibility of setting up a new *LFG* extraction system is unfeasible. *LFG* emission and percentage of methane in the *LFG* is so low that turns out to be economically and technically unfeasible to install an extraction system. That happens when *LFG* flow falls below 30-50 m^3 per hour and methane percentage in *LFG* falls below 35-40% (Huber-Humer et al., 2008).

All these previous considerations bring to the necessity of finding an alternative method to integrate the *LFG* extraction system, replace it in certain cases and solve the problem of methane emission. This need is more than ever overriding in Europe, also as consequence of the EU landfill directive (1999/31/EC) which forces all European countries to reduce the quantity of organic waste diverted to landfilling below 35% by 2016 (Bogner et al., 2008). Lower organic content means lower *LFG* production, corresponding to growing in *LFG* extraction systems installation and management.

2.4 *LFG* ALTERNATIVE MANAGEMENT: METHANE OXIDATION

One of the most effective system, which can be used to avoid previously explained issues, is biological oxidation of methane. Methane is oxidized in different steps by methanotrophs, a group of aerobic bacteria which is able to use methane as a source of carbon and en-

ergy. The chemical pathway for CH_4oxidation is represented in the following equations.

$$\begin{aligned} CH_4 + \tfrac{1}{2}O_2 &\longrightarrow CH_3OH \\ CH_3OH + \tfrac{1}{2}O &\longrightarrow CHOH + H_2O \\ CHOH + \tfrac{1}{2}O_2 &\longrightarrow CHOOH \\ CHOOH + \tfrac{1}{2}O_2 &\longrightarrow CO_2 + H_2O \end{aligned}$$

The overall accepted reaction for methanotrophic methane oxidation is:

$$CH_4 + 2O_2 \longrightarrow CO_2 + 2H_2O + heat$$

Mainly two categories of bacteria are differentiated, named Type I and Type II (Bowman et al., 1994). The first category, labeled Type I, best fits to grow in soil areas with high concentration of oxygen and low concentrations of CH_4, almost comparable with atmospheric concentrations (1.7 ppmv). Conversely the second category, labeled Type II, prefers ambient conditions with high supply of CH_4 and low oxygen presence (Scheutz et al., 2009). These considerations lead to the fact that is probable to find a bacteria community of Type I in the shallowest soil, while a bacteria community of Type II is more easily adaptable with deeper soil layers conditions. Obviously, not only $CH_4$and O_2 concentrations directly influence methanotrophic bacteria performances, but several external factors need to be considered as well in this analysis. Main factors are shortly described in the following section, but a more accurate and deep analysis can be easily found in literature (Scheutz et al., 2009).

The first factor is the soil temperature. It's overall known that biological activity is strictly influenced by temperature variation, and this is no exception for methanotrophic bacteria. Different optimal temperature ranges have been found for methanotrophic; generally this range is around 25-30 °C (Scheutz et al., 2011) or 30-40 °C (Streese and Stegmann, 2003). Temperatures of the soil subjected to methane oxidation activities can be influenced by different factors:

- Methanotrophic bacteria pathway is an exothermic reaction. Consequently, soil temperature can be increased by a strong bacteria community activity;
- Seasonal variation of outdoor environmental temperature has a strong influence on soil temperature, with reported cases of variation from 60 °C to 48°C during warm and cold season respectively (Dever et al., 2011),(Humer and Lechner, 2001);
- The inflow LFG, coming from the high temperatures inside the landfill body, can be considered a strong influence factor for top cover methane oxidation soils (Dever et al., 2011).

A second relevant factor is soil moisture content. A consistent presence of water inside the soil is needful for bacteria activity for several reasons: water is necessary for chemical reactions, indispensable for nutrients transportation and also fundamental for waste compounds removal (Scheutz et al., 2011). At the same time, an excessive presence of water inside the soil can limit LFG diffusion and inhibit methanotrophic bacteria activity, in case of low oxygen and methane presence. Moisture content of soil is directly influenced by rainfall; in indoor studies with a missing periodic supply of water, bacteria activity can leads to soil desiccation and consequently to the inhibition of oxidation performances (Haubrichs and Widmann, 2006). Another important factor affecting methane oxidation is soil porosity and permeability. This soil characteristics are primarily determined by the soil type itself, but are also affected by moisture content and Exopolymeric Substances (i.e. EPS) formation. Exopolymeric Substances (EPS) it's a high molecular weight compound, which accumulates inside the soil after long LFG exposure. This substance is probably generated by bacteria as a form of anchorage to soil particles, and is highly responsible for pores clogging (Scheutz et al., 2009). The pores clogging brings to a relevant methane oxidation efficiency decrease, which can be avoided by periodically turning the soil material (Wilshusen et al., 2004) or aerating periodically the methanotrophic substrate to prevent carbon excess (Scheutz et al., 2009).

In order to analyze the correlation of these phenomena with methane oxidation and to optimize this technology, several studies have been carried out in the last years. The methodologies applied for these studies can be subdivided in two main branches: the branch of laboratories studies (with batch or continuous flow experiments) and the branch of field trials. Several types of field studies have been carried out, which can be summarized in four categories (Huber-Humer et al., 2008):

- Biocover, the most elementary configuration for methane oxidation, consists in the installation on a landfill of a soil layer as top cover, which has the correct characteristics to allow bacteria growth and to maximize oxidation efficiency. Biocover technology is used as a temporary cover for low organic content landfills and can be substituted, after waste stability achievement, with a final waterproof capping;

- Biofilter is a technology very similar to the one used for odors and organic contaminants removal. It consists of the installation of a fixed-bed reactor (Huber-Humer et al., 2008) combined with a final landfill proof top capping and extraction system; LFG extracted from the landfill body is then pumped, in up-flow or down-flow mode, inside the biofilter in which methane is subjected to bacteria oxidation;

- Biowindow is also a technology used in combination with a final top capping. It consists in a special window embedded in the capping surface, used as biocover. LFG produced inside the landfill body is prevented to escape in the atmosphere with a gas proof capping and is forced to reach the biowindow. With this technology, methane flowing inside the biowindow can be oxidized without substituting the whole landfill capping;
- Biotarps are used for landfills during the operational period, when sectors are not already closed with temporary or final covers. This technology consists mainly in the daily installation of a tarp soaked of methanotrophic bacteria (Huber-Humer et al., 2008) that, receiving LFG form the bottom, is able to oxidize the exiting methane.

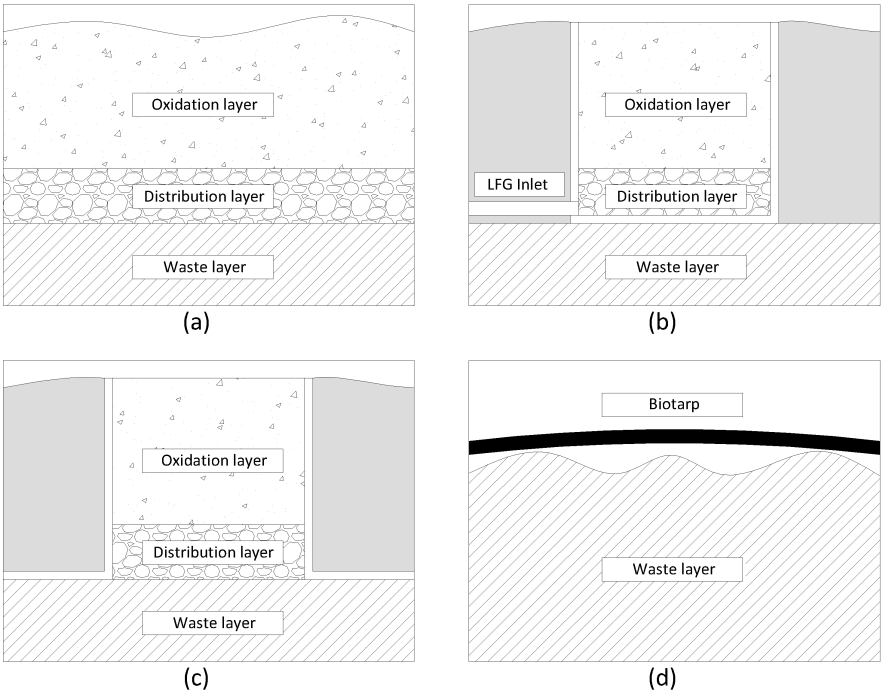

Figure 4: Conceptual schemes of a biocover (a), a biofilter (b), a biowindow (c), and a biotarp (d).

3

THEORETICAL AND PROJECT BACKGROUNDS

Biofilters are one of the possible approaches to field scale methane oxidation plants. Several studies have been carried out so far on this type of pilot plant, different designs have been adopted and different methane oxidation efficiencies have been achieved. In the following chapter a general theoretical overview will be presented in order to show the main features of several of these studies. A general background overview will be carried out regarding theoretical methods for results calculation. Moreover a general background overview will be given regarding AV Miljø landfill and AV Miljø biofilter, in order to present the starting point of this thesis. In the end of this chapter, a short presentation of all the existing methods used for biofilter monitoring will be made.

3.1 BIOFILTERS DESIGN REVIEW

Gebert and Gröngröft (2006) designed a field-scale passively vented biofilter. The biofilter was subdivided in several layers made of different materials. The upper layer was 10 cm high and made of loamy sand, with a lower layer 1.5 cm high made with sand. At sand layer bottom, a 1.5 cm gravel layer was settled with an underlying layer made of crushed porous clay 67 cm height. In the end on the bottom was placed a gravel layer, ranging between 10 and 30 cm, made of gravel. The purpose of this last layer was to guarantee the correct drainage of internal moisture and of water entering into the biofilter. The authors decided to use a purely mineral substrate as porous clay as filter material. The use of inorganic substrates is different from the common materials used for this purpose, which are generally made of organic soils as compost. The adopted porous clay material has a very high bulk pore volume of 83% and was chosen to avoid the internal degradation of compost or the establishment of anaerobic conditions in the filter material in case of high moisture content. The pH of the material was around 7, which is in the optimal range to guarantee a good methanotrophic activity, and the biofilter was heated and moisted just by natural atmospheric and LFG conditions. The biofilter was embedded in the re-cultivation layer of the landfill and built in a polyethylene tank. The biofilter substrate was then placed into two chambers respectively of 6 and 9 m^3, independently one from the other. The LFG was extracted from 2 gas venting wells sited in different sectors of the landfills and then mixed, to create a unique biogas composition. In the end, the mixed LFG was subdivided in

two streams directed each one in a different chamber of the biofilter and distributed in a homogeneous way using horizontal and parallel slotted pipes positioned in the bottom drainage.

Streese and Stegmann (2003) operated with a bench scale plant and a biofilter pilot plant. The pilot plant consisted in 12 biofilters subdivided in 4 columns, for a total biofilter volume of 4 m^3. Mainly three types of materials were adopted in this study. The first material which was used was yard waste compost, used for its attitude in nutrient supply to bacteria. The second material adopted was peat, useful for water storage, and lastly squeezed spruce wood fibers were used to increase filter material air voids and avoid EPS (i.e. Exopolymeric substances) clogging. Then these materials were composed in different ways into the four columns, in order to test the efficiencies of the different settings. The first column was filled with pure yard waste compost. The second one was composed mainly by two layers: one distribution layer of wood fibers and one layer with the real filter material. The distribution layer was 2 cm thick and was disposed every 15 cm of compost, forming a multilayer biofilter (Streese and Stegmann, 2003). The third column was filled with an equal quantity of compost, wood fibers and peat. In the end, the fourth column was filled with yard waste compost and spruce wood fibers with a volume ratio respectively of 2:1. The calculated pH of the mixture filter material was around 5.7 with a bulk density of 434 kg/m^3. The LFG, with a composition around 65-70% methane and 30-35% carbon dioxide, was extracted from a gas well embedded in the landfill body. Thus, was mixed in a mixing chamber with atmospheric air, creating a diluted biogas with a percentage composition of atmospheric oxygen. Before entering the biofilter in down-flow, the mixture was humidified in an up-flow wet scrubber in order to maintain a constant moisture content inside the biofilter. The ambient air was also previously heated during the colder periods, in order to reach an acceptable inflow temperature. The exiting gas was recirculated inside the biofilter in a quantity corresponding to 30% of the outflow, with the specific purpose of lowering the temperature and moisture losses.

Cabral et al. (2010) reported the experience of passive methane oxidation biocover Passive Methane Oxidation Biocover (PMOB), named PMOB-2, at a Canadian landfill. The biofilter material was composed of different layers. The first layer, the real filter material, was 80 cm thick and consisting of a compost and sand mixture. On the bottom of the filter material, two distribution layers were settled: the first layer 10 cm thick was made of 6.4 mm gravel while the second layer was 30 cm thick and made of 12.7 mm gravel. The filter material was the mixture of a 12 mm sieved compost and coarse sand, with a volume ratio respectively of 5:1. The biofilter substrate material was compacted in 20 cm layers in order to achieve a bulk density of 8.4 $kg/m^3 3$ and a filter porosity of 63%. The biofilter, embedded in the existing 2.7 m

silty clay top cover, had a depth of 2.45 m and a length of 9.45 m. The whole biofilter material was lined on the boundaries by using a 1.5 mm thick HDPE geomembrane and on the sides by a 15 cm thick polystyrene foam layer. These two materials were used for specific purposes. The HDPE geomembrane was used to seal the biofilter from the surrounding clay liner, in order to avoid water and LFG exchange or leakages from one material to the other. The polystyrene foam was used to thermally isolate the biofilter from the outside soil, in order to avoid moisture exchange from clay to compost due to different thermal gradients. The biofilter, built with a slope of 3.5%, was endowed with a drainage system on the lower side, in order to let the excess moisture leave. The inflow LFG was extracted from the landfill body from a gas well and, without any gas addition, injected inside the biofilter body from three distribution points. The LFG distribution system was made up of 5 cm diameter pipes in acrylonitrile butadiene styrene (ABS) and embedded in the bottom LFG distribution layer. The inflowing LFG composition were measured. The LFG was constituted by about 60-65% methane and 35-45% carbon dioxide.

A new experimental setup was then built in the same Canadian landfill and results reported in Roncato and Cabral (2012). This biofilter, named PMOB-3B, was composed as the previous one by three layers but with different materials and thicknesses. The upper layer, the proper filter material, was 30 cm thick and constituted by an equal mixture of the previous compost-sand substrate with 6.4 mm gravel. The second layer, used as LFG distribution material, was 10 cm thick and composed by 6.4 mm gravel. In the end, the third layer was composed by 80 cm of 12.7 mm coarse gravel, with the final purpose of increasing the air penetration and increase of oxygen concentration inside the soil. The substrate was compacted as for the previous biofilter, reaching a bulk density of 1.43 kg/m^3 and a porosity of 48%. This biofilter maintains the previous configuration regarding the High Density Polyethylene (HDPE) geomembrane liner and the temperature isolation on the sides made by polystyrene. Also the biofilter dimensions and the LFG distribution system were preserved. The inflowing LFG composition had the same composition of the one used for PMOB-2 because the used extraction well and distribution system were the same.

Philopoulos et al. (2008)investigated different biofilter design characteristics, by building three pilot plants in a Canadian landfill. The built biofilters were embedded in the top cover soil, letting the biogas reach the biofilter in a passive way without the necessity of a LFG collection system. The biofilters were constructed with a specific material stratification. The upper layer, consisting in the real filter material, was designed 150 cm deep, in order to obtain a good thermal insulation of the deeper layers. At the bottom of the medium was settled the LFG distribution layer composed by 80 cm of tire shreds. The

distribution layer was disposed on the top of the landfill waste in a slightly sloped mood from the center to the external edge. In the end, the landfill was proofed on the top with a geomembrane, in order to secure the LFG conveying inside the biofilter medium. The geomembrane was also used to cover the tank containing the biofilter medium, in order to avoid LFG losses and moisture exchanges. The main criteria adopted for biofilter design was the surface ratio Surface Area Ratio (SAR), which can be defined as the ratio between the areal surface of covered waste and the areal surface of the filter. The criteria determines the retention time of LFG inside the biofilter and consequently the contact time between methane, oxygen and the methanotrophic bacteria community acting inside the biofilter medium (Philopoulos et al., 2008). Two biofilters were designed with a SAR of 10.8, while the last one was built with a SAR of 4.8. The last biofilter was designed with a higher SAR in order to test its increase in the oxidizing capacity, considering that it was built on the top of a gas ventilation well. The gas ventilation well was designed with a central Polyvinyl Chloride (PVC) pipe embedded in waste layer and slotted in the first meters, in order to collect the generated LFG and collect it to the surface.

Dever et al. (2011) designed four biofilters system at an Australian landfill. The biofilter was composed by four squares with 3 m side and vertically composed by several layers. The biofilter was designed with a special layering, the upper layer used as substrate material and the lower layer used as distribution layer. For each biofilter a different type of substrate material was used, in particular: composted garden organic with 10% (v/v) of woodchip was used for the first biofilter, composted municipal solid waste with 10% (v/v) of woodchips was used for the second biofilter and pure composted garden organic was used for the third biofilter. For the last biofilter a mixture of composted municipal solid waste with 20% (v/v) of woodchips was used. Different types of drainage materials were used also for the biofilters, made by crushed concrete and crushed brick, with sizes ranging from 10 to 70 mm. Each biofilter was fed by 2 separate gas drainage pipes, collecting biogas from the surroundings areas of the landfill. Each pipe was designed to be 20 m long, and made by 100 mm diameter polyethylene. Moreover the pipes were embedded in trenches with the dimension of 60 cm of depth and 60 cm of width, filled with 70 mm crushed concrete or 70 mm crushed brick.

3.2 BIOFILTERS OXIDATION PERFORMANCES REVIEW

Haubrichs and Widmann (2006) worked with a column biofilter increasing progressively the methane flow injected in the compost biofilter. The experimental testing was to be divided in four periods, in which changes happened both in injected flux and in total methane

oxidation efficiency. During the first period, from day 1 to day 65, a stable CH_4load of 144 $g/m^2 \cdot d$ (5.1 $g/(m^3 \cdot h)$ was applied and the oxidation efficiency was estimated to be stable around 100%. The methane oxidation dropped around 32% percent from day 66 to 91 even if the methane load was maintained constant. This important decrease has been attributed to the lack of moisture detected in the compost and to the formation of EPSs. From day 92 these problems were solved and the methane oxidation became 100% again, also with the increased maximum rate of 813 $g/m^2 \cdot d$ (28.8 $g/m^3 \cdot h$) around day 223. The last period started at day 240 when the methane oxidation efficiency dropped again and reached the final value of 95%. For this study it was established that the maximum achievable methane oxidation can be considered around 770 $g/m^2 \cdot d$ (27.3 $g/m^3 \cdot h$), which is the maximum load born from this biofilter.

Streese and Stegmann (2003) directed a study with a column biofilter and a large-scale experiment, using a time increasing methane load. During the first bacteria adaptation period, the maximum oxidation efficiency was calculated to be between 212 and 282 $g/m^2 \cdot d$ (15 and 20 $g/m^3 \cdot h$) for the column test and between 218 and 436 $g/m^2 \cdot d$ (10 and 20 $g/m^3 \cdot h$) for the large-scale experiment. After 100 days of adaptation the methane injection flow was increased and maximum values around 875 $g/m^2 \cdot d$ (62 $g/m^3 \cdot h$) were found for the compost based biofilter, while for a mixed and multi-layer biofilter (see paragraph 2.1- Biofilter design review) the maximum measured efficiencies were around 564 $g/m^2 \cdot d$ and 424 $g/m^2 \cdot d$ (30 and 40 $g/m^3 \cdot h$) respectively. The maximum methane oxidation efficiency for the large-scale experiment was calculated to be around 873 $g/m^2 \cdot d$ (40 $g/m^3 \cdot h$), with peaks around 1,090 $g/m^2 \cdot d$ (50 $g/m^3 \cdot h$).

Gebert and Gröngröft (2006) designed a pilot scale biofilter and injected a quantity of methane increasing progressively. The different methane oxidation efficiencies depended mainly from the observation season and consequently from the biofilter and inlet gas temperature. Considering the annual evaluation of the biofilter methane efficiency, they found that in the 70% of cases the biofilter oxidation capacity was higher than the methane injected. Only in the 30% of the cases the biofilter was overloaded. Calculating the annual fluxes, they found that the 38% of the methane escaped and only the 62% of the injected methane was oxidized. In the end, they concluded that the maximum load of methane born from the biofilter was 1,280 $g/m^2 \cdot d$ (80 $g/m^3 \cdot h$), which is a considerably high value as oxidation efficiency, but in this case strongly fluctuating and inconstant.

Philopoulos et al. (2008) designed three biofilters embedded in the landfill top cover. They calculated average methane fluxes during the testing period around 37.4 $g/m^2 \cdot d$ for biofilter 1, 53.5 $g/m^2 \cdot d$ for biofilter 2 and finally 1.2 $g/m^2 \cdot d$ for biofilter 3. The average measured methane oxidation efficiencies were 76% (28.4 $g/m^2 \cdot d$) for biofilter

1, 68% (36.4 $g/m^2 \cdot d$) for biofilter 2 and 35% (0.5 $g/m^2 \cdot d$) for biofilter 3. During almost all the monitoring campaign, emission values for all the three biofilters were below 15 $g/m^2 \cdot d$. Only in two cases the measured oxidation efficiencies were really low. In the first case they found low oxidation efficiencies but high oxidation rates: 24 % (35 $g/m^2 \cdot d$) for biofilter 1 and 29% (57 $g/m^2 \cdot d$) for biofilter 2. In the second case, oxidation rates were found around 0 $g/m^2 \cdot d$ also with average methane loads. The best oxidation rate measured in this study can be considered to be 57 $g/m^2 \cdot d$.

Roncato and Cabral (2012) carried out a study on two biofilters, described in the previous paragraph. In the first biofilter, called PMOB 2, they injected methane increasing the load from 8 $g/m^2 \cdot d$ to 580 $g/m^2 \cdot d$. They achieved maximum oxidation efficiencies for maximum methane loads around 99% (576 $g/m^2 \cdot d$) .In the second biofilter, PMOB 3B, they increased the methane load starting from 20 $g/m^2 \cdot d$ and reaching, after three weeks, the final load of 352 $g/m^2 \cdot d$. The maximum efficiency they obtained was 100% (352 $g/m^2 \cdot d$). An oxidation rate around 804 $g/m^2 \cdot d$ was expected from biofilter PMOB 3B, as found in previous studies, but a hole in the geomembrane prevented the biofilter to reach the needed pressure for this flow.

Wilshusen et al. (2004) performed a biofilter experiment using different types of substrate material in four testing columns. The first column, filled with leaf compost, showed the higher oxidation performance with an efficiency of 360-400 $g/m^2 \cdot d$. Two other testing columns, filled with municipal solid waste compost and woodchip compost, showed lower oxidation efficiencies and higher adaptation times for bacteria; the maximum oxidation efficiency obtained in these two columns was around 270-300 $g/m^2 \cdot d$. The last material, which consisted in Home Depot garden compost, showed no relevant oxidation activity. All these oxidation performances decreases with time during the experiment reaching performances around 100 $g/m^2 \cdot d$ after 200 days. This phenomena is due to EPS building inside the biofilter and can be avoided turning periodically the adopted substrate inside the biofilter.

An important study carried out by Dever et al. (2011) on four biofilters, showed different results depending on the different monitoring seasons. During the first monitoring season, carried out between September and May, methane oxidation efficiency of the biofilters varied between 0 and more than 90 % (corresponding to a methane oxidation performance of 0-360 $g/m^2 \cdot d$). In the second monitoring phase, carried out from July to January, the oxidation efficiency decreased to 25% but with a methane oxidation performance increased to 600 $g/m^2 \cdot d$.

3.3 THE MASS BALANCE APPROACH

The final purpose of this thesis is the evaluation of the methane oxidation efficiency of a biofiltration system installed in AV Miljø, a Danish landfill. One of the most reliable methods, which can be used for the evaluation of the oxidation potential, is the Mass Balance Approach.

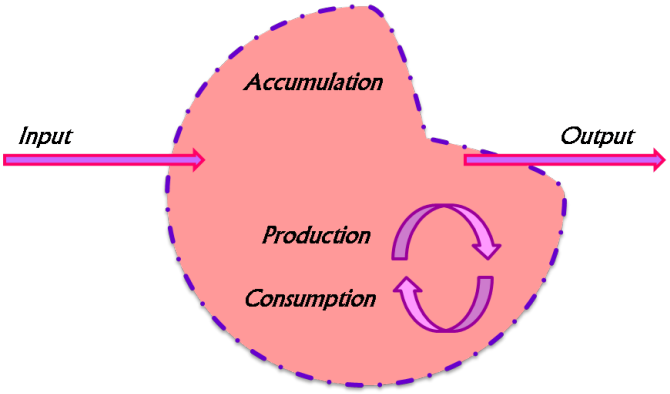

Figure 5: Mass Balance Approach concept.

In this thesis two different types of Mass Balance are adopted, in order to compare the reliability of obtained results: the Carbon Mass Balance Approach and the Tracer Mass Balance Approach.

3.3.1 *The Carbon Mass Balance Approach*

The first approach described is the Carbon Mass Balance. This important approach was previously used in other studies and described in Christophersen (2001) and Scheutz (2011a). This method is based on the following assumptions:

- Steady state of infiltrating gas inside soil pores;
- No carbon dioxide is dissolved inside the seepage water;
- There is no gas production inside the substrate soil (CH_4 in anaerobic zones and CO_2 for bacteria respiration).

The main equation of the Carbon Mass Balance approach is expressed in this form:

$$J_{LFG,bot} = J_{CO_2,bot} + J_{CH_4,bot} = J_{CO_2,sur} + J_{CH_4,sur} \quad (1)$$

where:

$J_{LFG,bot}$	LFG flow $(mol\,C/d \cdot m^2)$
$J_{CO_2,bot}$	CO_2 flow at the bottom of the biofilter $(mol\,C/d \cdot m^2)$
$J_{CH_4,bot}$	CH_4 flow at the bottom of the biofilter $(mol\,C/d \cdot m^2)$
$J_{CO_2,surf}$	CO_2 flow at the surface of the biofilter $(mol\,C/d \cdot m^2)$
$J_{CH_4,surf}$	CH_4 flow at the surface of the biofilter $(mol\,C/d \cdot m^2)$

In order to calculate the bottom flux on methane, it's necessary to previously calculate the concentrations of methane and carbon dioxide at the bottom of the biofilter substrate layer and their relative surface fluxes. Methane and carbon dioxide concentrations can be obtained analyzing the concentration of gas inside the soil. To calculate the surface fluxes of these gases it's possible to use the flux chamber method, which consists in the installation of a closed chamber on the soil surface and the consequent measurement of several parameters. This method is one of the most common to calculate gas fluxes and has been used in several previous studies for this purpose ((Roncato and Cabral, 2012),(Stern et al., 2007),(Einola et al., 2009),(Borjesson et al., 2000),(Christophersen and Kjeldsen, 2001)). The formula adopted for the calculation of surface gas fluxes is the following one.

$$J_{CH_4,sur} = \frac{V}{A} \cdot \frac{\partial C}{\partial t} \cdot \frac{P \cdot M}{T \cdot R} \quad \left[\frac{m^3}{m^2} \cdot \frac{l}{s \cdot m^3} \cdot \frac{atm \cdot \frac{g}{mol}}{K \cdot \frac{atm \cdot l}{K \cdot mol}} \right] \tag{2}$$

where:

$J_{CH_4,sur}$	CH_4 flux $(g/s \cdot m^2)$
V	flux chamber volume (m^3)
A	Areal surface (m^2)
$\partial C/\partial t$	Slope of the line generated by interpolation of methane concentration data $(l/s \cdot m^3)$
P	Atmospheric pressure (atm)
M	Methane molar mass (g/mol)
T	Temperature (K)
R	Gas constant $(atm \cdot l/K \cdot mol)$

Once these quantities have been calculated, it's possible to obtain the original flux of methane at the bottom:

$$J_{CH_4,bot} = (J_{CO_2,sur} + J_{CH_4,sur}) \cdot \frac{C_{CH_4,bot}}{C_{CH_4,bot} + C_{CO_2,bot}} \tag{3}$$

In the end, it's likely easy to calculate the theoretical methane oxidation efficiency, using the difference of methane flux between top and bottom:

$$J_{CH_4,oxi} = J_{CH_4,bot} - J_{CH_4,sur} \quad (4)$$

3.3.2 *Tracer Mass Balance Approach*

A new and innovative method for the calculation of methane reduction considers the additional injection of an inert gas inside the biofilter body. The inert gas, called tracer, needs to be mixed with the inflow LFG. Inlet and surface fluxes need to be measured. The basic equation for a general mass balance is the following one:

$$J_{out} = J_{in} - J_{consumed} + J_{produced} \quad (5)$$

Assuming that tracer gas is inert, the general mass balance formula can be expressed also by the ratio of two general gases:

$$\frac{J_{in,1}}{J_{in,2}} = \frac{J_{out,1}}{J_{out,2}} \quad (6)$$

The Tracer Mass Balance is based on the following assumptions:

- Steady state of infiltrating gas inside the soil pores;
- In case of no gas production or consumption inside the soil, methane and tracer gas diffuse with the same rate;
- In case of no gas production or consumption inside the soil, the ratio between the flux of methane and tracer gas is always constant;
- Tracer gas is not subjected to production or consumption.

With these instruments, it's possible to calculate the ratio between methane and tracer gas in the inlet. It's also possible to calculate the same ratio on the biofilter surface, using the flux chamber method previously described in the chapter above. Comparing results and considering all the previously stated assumptions, it's possible to identify if any methane oxidation has occurred inside the biofilter. The final formula which needs to be used for this mass balance is here illustrated.

$$MO = \frac{\left(J_{CH_4}/J_{C_2H_2F_4}\right)_{inlet} - \left(J_{CH_4}/J_{C_2H_2F_4}\right)_{surface}}{\left(J_{CH_4}/J_{C_2H_2F_4}\right)_{inlet}} \quad (7)$$

3.4 LANDFILL AV MILJØ

AV Miljø is a landfill site for the disposal of low organic content waste and is sited south of Copenhagen, Denmark. The filling of the first cell was started in 1992 and operations are still in progress. The total landfill available volume is estimated to be around 2 million $m^3$and is formed by 22 sectors (Scheutz et al., 2011b).

Figure 6: AV Miljø landfill plant view. Green areas represent finally top covered sectors, light gray areas represent the administration zone, yellow areas represent gravel roads, and dark gray areas represent paved roads (KøbenhavnsAMT, 2006).

This landfill is receiving low organic content waste as shredded waste, ashes from incineration, asbestos, contaminated soils, waste from street sweeping and residues. The different classes of waste received at AV Miljø are reported in table 1.

Table 1: Tons of waste collected to AV Miljø. Of these quantities, only 1,579,870 tons have been landfilled (AVMiljø, 2011).

Waste supply (tons)	*2007*	*2009*	*2011*	*1989-2011*
Landfill waste	21,725	21,316	16,388	574,358
Waste suitable for incineration	80,665	34,037	0	668,647
Residues	-	-	-	240,121
Slag / fly ash sludge	1.,570	1,153	664	94,886
Ash sludge	0	0	0	71.523
Contaminated soil + debris	3,042	714	1.525	101,941
Street sweeping	9,953	10,343	3,914	237,043
Asbestos	3,075	5,100	11,496	60,341
Shredded waste	48,882	39,687	44,982	440,854
Total	168,912	112,350	78,969	2,489,714

The landfill has been sited on a reclaimed land in Køge Bay, very close to the sea, and no bottom liner is present except for natural clay. Landfilled waste are generally disposed in layers of 0.5 meters with an average total height for each sector of 5.5 meters. When the maximum allowed disposal height has been reached, each sector is closed with a final top cover, consisting in 0.2 meters of gravel, 1 meter of compacted clay and finally 0.2 meters of natural soil.

Due to the fact that a proper bottom lining system is missing and the top cover is not installed in all the closed sectors, leachate is mainly originated from rainfall and sea water infiltration. The leachate drainage system is independent for each sector. Leachate is collected all together and, with the use of pumps, sent to the treatment. The treatment of leachate consists of an on-site pollutant abatement; after it's sent to the near wastewater treatment plant. Several leachate wells are located inside the landfill body, in order to control the leachate level. Moreover, due to the absence of a proper biogas extraction system, these wells have the important role of release the few methane generated inside the landfill body, avoiding the pressure buildup inside the landfill and several problems related with it. The total landfill methane emission estimated with measurements every six months has been estimated about 7.6 ± 1 kg CH_4 per hour (AVMiljø, 2011).

The sector on which the biocover has been sited is numbered as 2.2.2. and has a total volume of 61,133 m^3. Waste disposal started in 1998 and the sector has been filled mainly with materials discarded from waste recycling, industrial waste, sand coming from grit chamber tank of wastewater treatment plants and combustible waste.

3.5 AV MILJØ BIOFILTER DESIGN

The plant view of the biofilter is represented in figure 7.

Figure 7: Plant view of biofilter at AV Miljø.

The biofilter designed for AV Miljø is composed by several parts:

- LFG collection points;
- Mixing chamber;
- Biofilter.

The LFG is collected from three leachate wells sited in sector 2.2.2 and 2.1.4. and stored in black collection buildings. These boxes are properly proofed in order to reduce as much as possible the gas exchange from outside to inside. The choice of designing the *LFG* collection system in this way derives from several previous studies, which showed how leachate wells can be preferential pathways for methane escape from landfill body to the atmosphere. A previous study carried out at Fakse landfill, another Danish disposal site, has showed that on a total landfill emission estimated of 740 kg $CH_4 \cdot d^{-1}$ circa (Scheutz et al., 2011c), a quantity around 211 and 351 kg $CH_4 \cdot d^{-1}$ were released from leachate wells (Fredenslund et al., 2010). An important mass balance was realized also on sector 2.2.2. of AV Miljø, resulting in a total emission of 21 kg $CH_4 \cdot d^{-1}$. Moreover, was estimated that about 15 kg $CH_4 \cdot d^{-1}$are released from leachate collection wells, resulting in 67% of total methane exiting from leachate wells (Scheutz et al., 2011b). The main reason of the presence of this preferential pathway is that the sector has been already closed with a compacted clay top cover, forcing LFG to exit from leachate wells. In figure 8, some pictures of leachate wells and LFG collection boxes are presented.

(a) (b)

Figure 8: (a): Collection point installation on a leachate well, (b): LFG collection point installed.

Every collection point is endowed with a pump, which has the role to collect the stored LFG to the mixing chamber. The LFG collection pump characteristics are listed in table 2.

Table 2: Characteristics of pumps used for LFG collection.

Characteristic	*Pump 1*	*Pump2*	*Pump 3*	*Unit*
Theor. airflow	35-42	80	35-42	*l/min*
Daily airflow	51	82	49	m^3/d
Max. Pressure	7	7	7	*bar*
Power	0,35	-	0,35	*kW*
V	200-400	-	200-400	*V*
A	1.9-1.5	-	1.9-1.5	*A*
rpm	1,425-1,725	-	1,425-1,725	-
Producer	Kawake Airvac	-	Kawake Airvac	-

LFG is transported to the mixing chamber through 3 PVC pipes and then naturally mixed inside the chamber. In order to avoid shortcuts of the injected LFG, a vertical septum was located in the middle of the mixing chamber: in this way LFG is obliged to overcome this barrier and mix. The homogeneous mixture of LFG reaches the outlet pipe, through which it will arrive to the biofilter distribution layer. In figure 9 a representation of mixing chamber main features is illustrated.

(a) (b)

Figure 9: (a): View of the mixing chamber already sealed, (b): LFG inlet pipes inside the mixing chamber.

After the LFG have left the mixing chamber, it instantaneously reaches the biofilter bottom. The distribution system was designed following the guidelines deriving from other previous experiences. In a previous Danish study a biowindow system was designed at Fakse landfill (Scheutz et al., 2011a). In this analysis the distribution system of 0.15 m of gravel was demonstrated to be insufficient to guarantee a homogeneous distribution of methane and avoid hot spots and biocover overloads. For this reason and according to other previous studies reported in paragraph 1.1, the biogas distribution system was

designed with 0.3-0.4 meters of gravel, in which 19 PVC perforated pipes are embedded. These pipes are placed every 2 meters. They are located at 0.1 meters from the bottom of the biofilter and they are 10 meters long. At the inlet of the distribution system there are 2 valves to have to possibility to switch off half of the pipes and obtain a more dispersed distribution system, with one pipe every 4 meters.

(a) (b)

Figure 10: (a): Front view of the biocover distribution layer, (b): Valves sites at biofilter distribution system inlet.

Over the distribution system, a layer of compost as substrate material was placed. The compost material was distributed without compaction, maintaining the soil porosity and the low density; in this way it's possible to obtain the wanted LFG and oxygen diffusion in the soil, necessary for methanotrophic bacteria feeding. The adopted compost layer is approximately 0.9 m thick and is expected to sustain the bacteria growth so that the majority of methane pumped in the biocover can be oxidized. Other important aspects to underline in the biofilter design are the water drainage system and the water locks.

The biofilter is provided with a drainage system placed on the bottom of the gravel distribution layer and embedded in the gravel itself. The water drainage system is made by a bottom slope and a holed collection pipe placed in the final spot of the slope. The final purpose of the drainage system is to avoid water buildup inside the biofilter due to rain seepage, in such a way of reduce soil porosity. To check periodically the water head on the bottom of the biofilter, a direct access was provided to the bottom drainage, installing vertical tubes connected with the drainage bottom pipe. At last two water locks were installed in the biofilter. A water lock is a water layer which is designed to avoid LFG from escaping. The first water lock has been installed on the bottom of the mixing chamber and the second one has been placed at the end of the biocover, on the Northern side. Adopted water locks at AV Miljø biofilter can be filled from outside with the use of small connection tubes and a vacuum pump or directly filled if

the water lock is not underground. Water locks are really important for biofilter proper functioning. They need to be checked regularly and filled in case of necessity.

The total area of the biofilter is 504 m^2, with a length of 42 m and a width of 12 m. In figures 11 and 12 the lateral and frontal sections of the biofilter are represented.

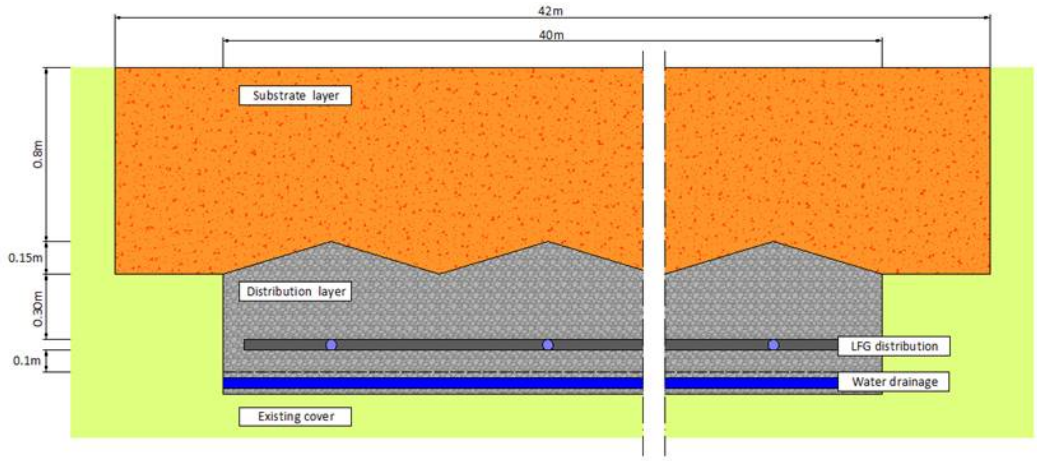

Figure 11: Lateral section (East-West) showing the biofilter inner structure.

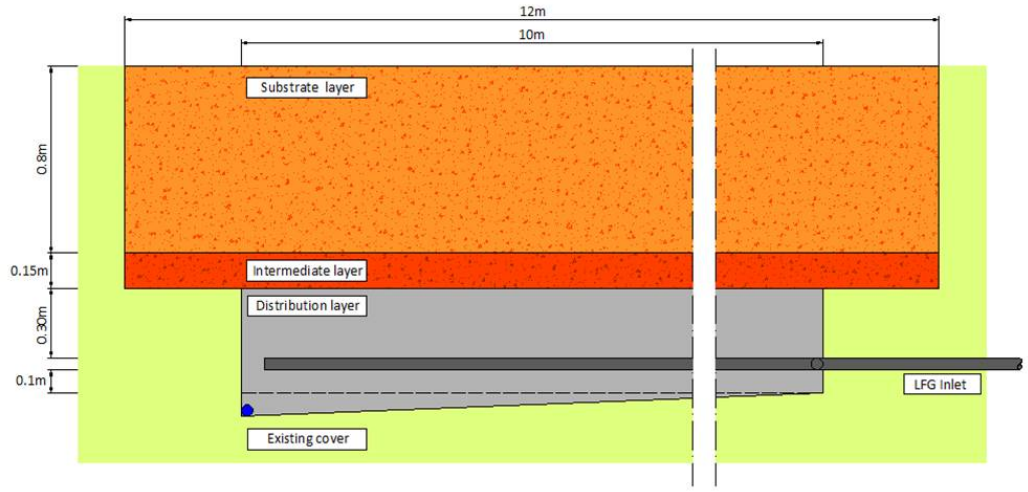

Figure 12: Front section (South-North) showing the biofilter inner structure.

3.6 METHODS AVAILABLE FOR MONITORING

It has been largely proved by several studies that biofilters can be used successfully for methane emissions oxidation (Cabral et al., 2010; Dever et al., 2011; Einola et al., 2009; Philopoulos et al., 2008; Scheutz et al., 2009; Streese and Stegmann, 2003). In order to implement this technology on field-scale and optimize the oxidation efficiency, the priority is to implement reliable methodologies, which can be used

to assess the oxidation capacity of a biofilter. Therefore several pilot projects have been carried out on this topic, to create new useful methods for methane emission calculation. The main methods, already described in several previous studies (Peter Kjeldsen and Charlotte Scheutz, 2011; Scheutz et al., 2009) are here introduced.

- Static and Dynamic flux chamber method: this method is carried out with the use of a cylindrical chamber installed on the ground surface. The methane flux in measured calculating the increasing concentration inside the chamber using equation (2). The main difference between static and dynamic method is that for the static analysis the chamber is sealed and gas sampling is quick as possible, while for dynamic analysis the chamber is flushed and sampling is carried for several hours. This methodology has been used in several studies (Borjesson et al., 2000; Cabral et al., 2010; Christophersen and Kjeldsen, 2001; Einola et al., 2009; Stern et al., 2007);

- Gradient technique: The subsoil CH_4 concentration and underground pressure have to be monitored. With these data and with diffusional equations, it's possible to calculate the ground surface flux (Scheutz et al., 2009);

- Tracer dilution method: a tracer inert gas (N_2O, SF_6 or CO) is released from the surface where methane flux wants to be calculated. The tracer gas is released with a known flux and measured downwind together with methane, using special instruments. In the end, the whole methane flux or the point flux from the surface is calculated using the ratio between tracer and methane upwind and downwind. This method has also been used in several last studies to calculate the total methane emission from landfills (Galle and Samuelsson, 1999; Fredenslund et al., 2010; Scheutz et al., 2011c);

- Micro-meteorological methods: a group of techniques based on turbulence models. Using the turbulence model it's possible to calculate the vertical flux of methane from the ground to the atmosphere. Methane concentration and atmospheric parameters are measured constantly and rapidly by sensors and data are then processed using the surface energy balance. It's a relatively unused technique due to expensive sensors and uncertainties derived from environmental factors (Scheutz et al., 2009; Peter Kjeldsen and Charlotte Scheutz, 2011).

4

MATERIALS AND METHODS

The final aim of this study is to evaluate methane oxidation efficiency of the biocover implemented at AV Miljø, a Danish landfill. In order to assess this parameter, several monitoring techniques have been established and monitoring campaigns have been carried out between September 2012 and January 2013. All these applied methodologies have been previously designed for particular purposes, in order to take into account all the factors related with methane emission. Briefly, inflowing methane concentration and flux has been measured constantly during the monitoring period in the collection boxes and in the mixing chamber. The LFG composition has been also measured inside the mixing chamber and inside the biofilter at different depths and in different points. As previously stated, soil temperature and moisture content are directly affected and have an influence on methane oxidation and methanotrophic bacteria activity (paragraph 2.4): for these reasons these parameters have been continuously monitored inside the biofilter. Moreover, weather condition was monitored at AV Miljø, recording atmospheric humidity, temperature, wind speed and atmospheric pressure. The outdoor temperature strongly influences the inlet LFG temperature and then biofilter temperature. Atmospheric pressure and wind speed have been largely proved to have a relevant effect on methane emission from landfill and soils. Methane emission is controlled by atmospheric pressure fluctuations, with an increase of CH_4 advective flux from the landfill in case of pressure decrease (Christophersen and Kjeldsen, 2001; Czepiel et al., 2003; Fredenslund et al., 2010; Peter Kjeldsen and Charlotte Scheutz, 2011). At the same time, wind creates a underground overpressure which fluctuates with wind speed change. This pressure fluctuation is one of the main factors of influence of gas emissions. In fact, it causes fluctuations in gas flux from the upper soil to the atmosphere (Poulsen and Moldrup, 2006). Characteristics of the soil surface, the deviation and the spectrum of fluctuations are the main factors affecting the behavior of this phenomena, always overestimated or neglected but with a relevant footprint on a field scale. Regarding the estimation of the biofilter efficiency, some campaigns were carried out using different procedures. First of all, a series of CH_4 and CO_2 surface screenings were carried out. These measurements were done to understand the general efficiency of the biofilter and eventually identify the presence of emission hotspots due to the presence of preferential emission pathways. Afterward, an inert gas was injected inside the biofilter until stability achievement. Flux cham-

ber measurements were performed at this point in order to calculate a point specific mass balance (using methods in paragraph 3.3). In the end, always using the flux chamber method, the realization of a total mass balance was achieved in order to understand the efficiency of the whole biofilter. In the following paragraphs, a detailed description of the methodologies and instruments adopted for these analysis will be provided.

4.1 INFLOW LFG COMPOSITION

The inflow LFG composition was monitored using different equipments. Methane concentration was monitored continuously inside the mixing chamber, while the composition of the LFG in the three inlet tubes and in the outlet was monitored weekly. The continuous monitoring was carried out using a OLCT IR infrared transmitter detector (Oldham, France), installed inside the mixing chamber and connected to a GP-HR TruTrack outdoor data logger (Intech, New Zealand).

(a) (b)

Figure 13: (a): OLCT IR gas detector placed inside the mixing chamber for methane concentration measurement, (b): GP-HR TruTrack outdoor data logger connected to the gas detector inside the mixing chamber.

The infrared detector works with the principle of infrared adsorption and is able to identify different gases including hydrocarbons and methane. The main characteristics of the GP-HR TruTrack and of the OLCT IR are reported in the tables below.

Table 3: Main features of GP-HR TruTrack methane data logger.

Characteristic	*Value*
Operating conditions	-30°C to +70°C
Time accuracy	±5 seconds per day at 20°C
Weight and dimensions	20 mm x 168 mm; 110 g

Table 4: Main features of OLCT IR infrared transmitter detector.

Characteristic	*Value*
Operating Range	0-100% of volume for CH_4
Sensitivity	1% of volume for CH_4
Accuracy	+/- 5% of the value
Humidity range	0 to 99%
Weight and dimensions	212 x 105 x 120 mm; 1.6 kg

The data logger was set to sample methane percentage concentration every 5 minutes, recording a maximum, a minimum and an average value. Calibration was done by the seller before the equipment installation. Stored data were downloaded and analyzed weekly.

Every week a complete analysis of LFG composition inside the mixing chamber was also carried out. Using the four tubes which connect the mixing chamber and the outdoor atmosphere (three inlet pipes and the outlet pipe) gas was sucked out using a specific equipment, and the concentration of CH_4, CO_2, O_2 (percentage) and H_2S (in ppm) was determined. For this purpose, a Biogas 5000 portable gas analyzer (Geotech, Warwickshire, UK) was used.

(a) (b)

Figure 14: (a): Biogas 5000 portable gas analyser used for LFG composition identification inside the mixing chamber (Geotech, 2011), (b): Biogas 5000 utilization to create vertical concentration gases profiles.

CO_2 and CH_4 are measured using a dual wavelength infrared sensor inside the equipment, while O_2 and H_2S are measured by an internal electrochemical sensor. The pump flow of Biogas 5000 is approximately 550 ml/min, with an operating temperature range from -10°C to +50°C. Two plastic tubes with water trap filters were used as

inlet and outlet pipes for extracted *LFG*. In table 5, equipment ranges and accuracy standards are presented.

Table 5: Biogas 5000 gas ranges and accuracies.

Characteristic	*Value*
CH_4 range	0 - 100%
CO_2 range	0 - 100%
O_2 range	0-25%
H_2S range	0-5,000 ppm or 0-10,000 ppm
Accuracy CH_4, CO_2 and O_2	From 0-25%: ±1.0 % (vol)
Accuracy H_2S	From 0-50 ppm: ±1.5 % FS

Th LFG contained inside the mixing chamber was sucked out for 10 seconds (which corresponds approximately to 92 ml of gas) and gas composition data collected after the equipment has reached the stability. After each sampling, the equipment was flushed with fresh air for 30 seconds in order to guarantee a complete cleaning from residual LFG.

4.2 LFG COMPOSITION INSIDE THE BIOFILTER

In order to measure the gas composition inside the biofilter, an innovative sampling device was designed and installed during the biofilter construction. This device is composed by 100 small tubes embedded in the biofilter soil at different depths and with different lengths, in order to cover almost all the biofilter volume. In figure 15 some pictures of the system are presented.

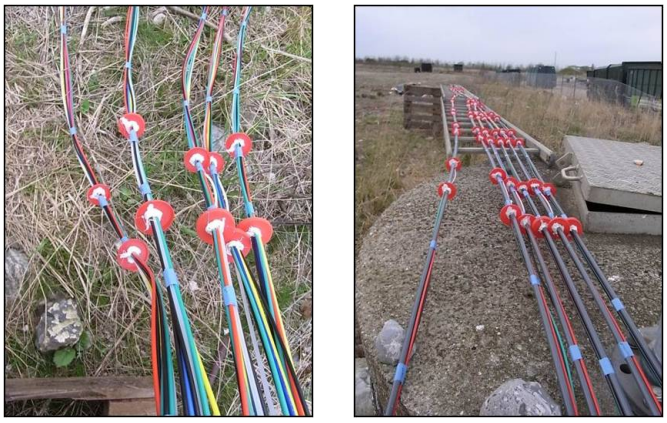

(a) (b)

Figure 15: (a): Close view of MLPGS tubes for biofilter underground gas sampling, (b): General view of the 100 tubes before laying.

The 100 probes, all located in the eastern part of the biofilter, were divided in two lines of 50 tubes, each embedded 3.5 meters from the surface boundary of the biocover (2.5 meters from the underground boundary). Then, each group of tubes was divided in 10 groups of 5 tubes and each of these groups layed with one of the extremities at different distances from the biofilter center.

The first group (n°10) of 5 tubes was placed 2 meters far from the biofilter center, the second group (n°9) was placed 4 meters from the center, the the third group (n°8) was placed 8 meters from the center, the fourth (n°7) 9 meters, the fifth group (n°6) 10 meters, the sixth group (n°5) 11 meters. The seventh group (n°4) was placed 12 meters from biofilter center, the eighth group (n°3) was placed 14 meters from biofilter center, the ninth group (n°2) 16 meters and the tenth group (n°1) 18 meters from biofilter center. Each tube of these groups was embedded at 5 different depth (-0.20 m, -0.50 m, -0.75 m, -1.00 m and -1.20 m) and labelled with a a letter (A, B, C, D, E) from the shallowest tube to the deepest. A schematic representation of these ports is presented in figure 16.

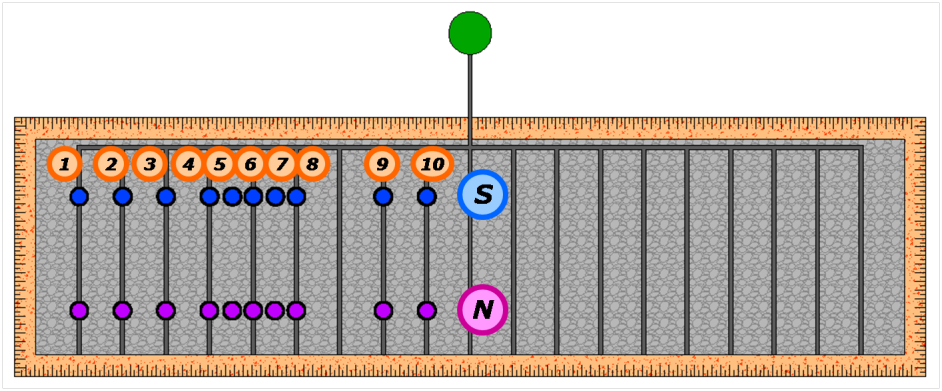

(a)

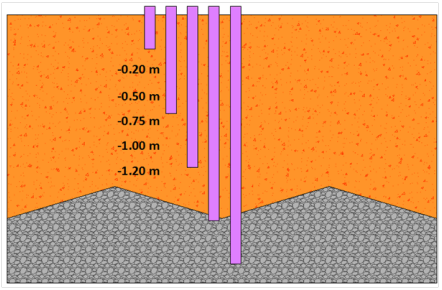

(b)

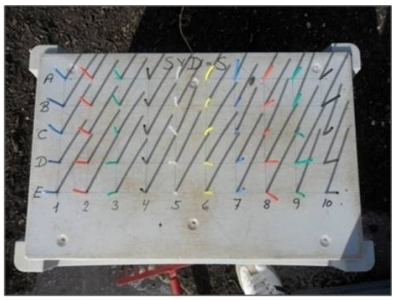

(c)

Figure 16: (a): Schematic plant distribution of the 100 sampling ports in the North and South line of the biofilter, (b): Schematic section distribution of the 100 ports with different depths, (c): Box with tubes used for gas sampling.

This system has been called Multi Level Probes for Gas Sampling Multi Level Probes for Gas Sampling (MLPGS) and is an innovative system which guarantees an optimal distribution of gas samples. The sampling monitoring was carried out by using the Biogas 5000 device, described accurately in the previous paragraph and applied also for mixing chamber sampling. The pump was set to run for 20 second, with a 30 seconds flushing at the end of every measurement. The suction time decision was made considering the necessity of sampling the gas concentration at the other extremity of the tube. The suction time was chosen considering the period which allows to sample the real gas concentration into soil at the tube extremity, avoiding to create an underpressure in the soil and measuring gases far from the sampled point. All the 100 ports were sampled every week during monitoring period (from September to December) and underground gases distribution profiles were produced using software. The geospatial mean distribution for all the sampled gases (CH_4, CO_2 and O_2) of the biofilter section was done with Surfer 8 (released by Golden Software Inc.), and Kriging was used to define isoconcentration curves. The Kriging method, already used in several previous studies (Cabral et al., 2010; Borjesson et al., 2000), has been proved to give the best representation compared to the other methods available. A pump was usually used to empty the 100 tubes from water when, moisture contained in the biofilter, seeped inside the tubes. Weekly collected data were recorded and processed.

4.3 SOIL TEMPERATURE AND MOISTURE CONTENT

Monitoring of soil parameters, as temperature and moisture, is relevant in understanding of processes involved in the biofilter. As previously explained, temperature and moisture content of the biofilter substrate are closely related and influenced by methanothropic activity. For these reasons, the monitoring of these parameters was done, in different points of the biofilter and at different depths. Three point were chosen to be monitored (represented in figure 17a) at 4 meters far from the biofilter center (n°1), at 6 meters far from the biofilter center (n°2) and at 16 meters far (n°3). For each point, three probes were installed at different depths (figure 17b). For point n°1 and n°3 probes were installed at -0.20 meters, -0.50 meters and -0.95 meters under the soil surface, while for point n°2 probes were installed at -0.20 meters, -0.50 meters and -0.75 meters. As it's possible to observe in figure 17b, all the probes are embedded in the substrate layer (orange colour in the figure) and no probes were placed in the gravel distribution layer (gray colour in the figure). The continuous monitoring was carried out with the 5TM probes (Decagon, Washington, Usa) and data were collected and recorded every 5 minutes by Em50 data loggers (Decagon, Washington, Usa). Accuracy of the probes for moisture con-

tent data was ± 0.01-0.02 m^3/m^3 (±1-2% Volumetric Water Content) and for temperature ±1°C. The probes range was between 1 and 80 for moisture and between -40°C to +50°C for temperature. Recorder data were downloaded from data loggers weekly in the study period and afterward elaborated.

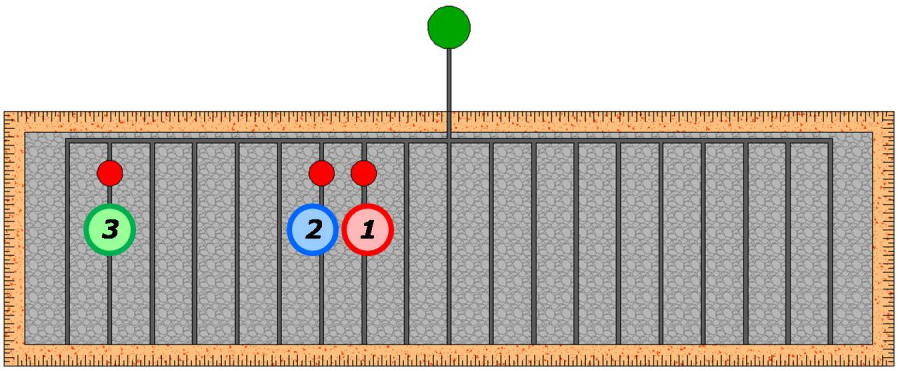

(a)

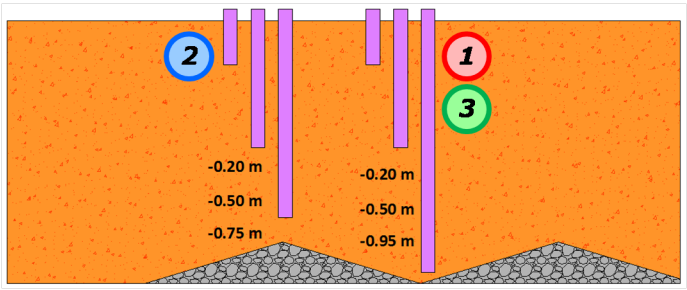

(b)

Figure 17: (a): Schematic plant distribution of the 9 sampling probes in the south east part of the biofilter, (b): Schematic section distribution of the 9 probes with different depths.

4.4 WEATHER PARAMETERS MONITORING

Weather data were monitored for the whole thesis period, in order to observe the correlation of several factors as atmospheric pressure, outdoor temperature and wind velocity on the biofilter behavior. The WS-3650 weather station (La Crosse Technology, Usa) was installed at AV Miljø, which is constituted by 3 devices (temperature detector, moisture detector and anemometer).

It's possible to obtain data about indoor and outdoor temperature (with maximum and minimum), indoor and outdoor humidity (with maximum and minimum), absolute and relative atmospheric pressure, wind velocity and direction measured with the anemometer. The detector is equipped with a wi-fi device which permits to record

all the data collected outdoor. The program Heavy Weather Pro 3600 (La Crosse Technology, Usa) has been used to download the recorded data and it can be used also to process data. The accuracy has been specified to be 0.1 °C for the temperature probe, 0.1 hPa for atmospheric pressure probe and 1% for the humidity sensor. The available range for temperature device is between – 40 °C and + 59.9 °C, while for humidity probe between 1% and 99%. Data recorded from the weather station were downloaded weekly and then analyzed.

(a) (b)

Figure 18: (a): Schematic representation of WS-3650 weather station, with all the used devices (LaCrosseTechnology, 2013 modified), (b): WS-3650 weather station installed at AV Miljø biofilter.

4.5 BIOFILTER SURFACE SCREENING

The biofilter surface screening was carried out to analyze the surface distribution of methane and carbon dioxide emissions. This analysis allows to:

- Find out the presence of CH_4 and CO_2 hot spots. Hot spots are specific points in which the emission flux of a gas is extraordinarily high compared to the average emission. These hot spots are generated from the presence of preferential pathways produced by soil inhomogeneities. These points need to be identified to establish the correct emission of gases from the monitored soil surface;
- Prove the symmetric distribution of LFG in the biofilter. Theoretically, the biofilter, considering CH_4 and CO_2 emissions, should be symmetrical relatively to the center . In fact, the biofilter inlet

pipe is placed in the very center of the pilot plant and the distribution system should guarantee the homogeneity of the LFG distribution;

- Prove the symmetric methanotrophic activity in the biofilter. Theoretically, with an homogeneous distribution of LFG in the biofilter, the methane oxidation activity carried out from methanotrophic bacteria should be also homogeneous or, at least, symmetric to the center. The surface screening of the biofilter allows to identity the conformation of methane oxidation activity (also comparing the emissions of methane with carbon dioxide emissions).

Methane screening was carried out using a Flame Ionization Detection Flame Ionization Detection (FID) device. The Thermo Scientific Vapor Analyzer 1000B or TVA1000B FID (ThermoScientific, 2008) was used for the surface screening campaigns. The range specified for FID is between 0.5 ppmv and 10,000 ppmv and for temperature is between 0°C and 40°C. Since during the measuring campaigns the environmental temperature was lower than 0°C, the device needed to run for a while and warm up before starting the measuring procedure. The methane screening has been done on November 14th, November 28th and December 3rd. The screening procedure consisted in crossing the biofilter surface with the FID device probe 5-10 cm far from the surface. The biofilter is located on the seaside and sometimes a very strong wind is present, which can affect the surface screening results. During all the days in which this analysis was carried out, the wind was so negligible that the use of a collection funnel was avoided. An ideal grid was created on the biofilter surface made by rectangular areas 2 meters high and 1 meter deep. The surface was crossed with the FID device and, for each ideal rectangular area, one value was recorded on a form. For each sampling point, the value shown on the FID screen has been waited to become stable for at least 5 seconds before being recorded. Every screening consists in the measurement of 252 samples. Usually the whole analysis took 4 hours to be completed, an acceptable time in which weather conditions change (as atmospheric pressure) can be assumed to be negligible. After the screening has been completed, collected data were processed with Surfer 8 (released by Golden Software Inc.), and Kriging was used to define isoconcentration curves.

Carbon dioxide screening was carried out using a silicon-based non-dispersive infrared Non Dispersive Infrared (NDIR) sensor. The GMP343 Carbon Dioxide Probe or Vaisala CARBOCAP® Sensor (Vaisala, 2009) was used for the surface screening campaigns. The measurement range specified by Vaisala for GMP343 is between 0 ppmv and 20,000 ppmv of Carbon Dioxide. The accuracy between 0 ppmv and 1,000 ppmv is guaranteed to be ±(3 ppm + 1 % of reading) while between 1,000 and 20,000 ppmv is ±(5 ppm + 2 % of reading). Measure-

ment campaigns were always carried out with temperatures lower than 0°C, which is considered a stable condition for GMP343 Vaisala Sensor. Carbon Dioxide screening has been done on November 18th, November 28th and December 4th. An ideal grid was created on the biofilter surface made by rectangular areas 1 meter high and 2 meters deep. The screening procedure consisted in crossing the biofilter surface with the Vaisala probe 5-10 cm far from the surface; the equipment was previously set to collect one sample every 15 seconds, so one sample was recorded for each rectangular area every 15 seconds. The total number of collected values for each screening was 252. Usually the whole analysis was completed in 4 hours assuming that, in this relatively short time, the change of carbon dioxide emission can be considered negligible. After the screening was completed, all the collected data were processed with Surfer 8 (released by Golden Software Inc.), and Kriging was used to define isoconcentration curves.

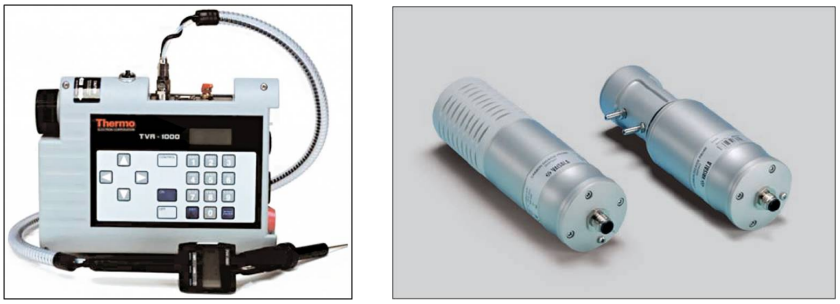

(a) (b)

Figure 19: (a): TVA1000B Flame Ionization Detection (FID) Vapor Analyzer (ThermoScientific, 2008), (b): GMP343 Carbon Dioxide Probe (Vaisala, 2009).

4.6 TRACER GAS INJECTION TEST

To obtain a reliable methane mass balance of the biofilter, a new method (described in paragraph 3.3.2) was used and a tracer gas has been injected inside the biofilter. The tracer gas adopted is scientifically known as 1,1,1,2-Tetrafluoroethane and commercially as 1,1,1,2-Tetrafluoroethane (HFC-134a). Its chemical formula is $C_2H_2F_4$ and is an inert gas usually used as refrigerant for domestic refrigerators and air conditioners.

This inert gas was injected inside the biofilter with a known flowrate and also methane flux entering the biofilter was measured. Then, fluxes from the biofilter surface of HFC-134a and methane have been measured. In the end, by means of the incoming and outgoing fluxes of methane and HFC-134a, a total ratio mass balance has been carried

out, using the method described more accurately in paragraph 3.3.2. Theoretically, assuming that methane and HFC-134 are both inert gases, the ratio between fluxes of these two gases has to be constant before and after the biofilter. But, as is overall known, methane could be subjected to oxidation by methanotrophic bacteria. This observation brings to the fact that, being HFC-134a an inert gas, a change in this ratio means that methane flux has changed inside the biofilter due to methane oxidation.

HFC-134a has been injected inside the biofilter in two measurement campaigns: the first carried out between the 17th and 18th of November and the second one between the 5th and the 9th of December. These campaigns had also a parallel purpose to evaluate the efficiency of the biofilter's distribution system by using the HFC compound as tracer. During the first period of monitoring, 9 ports of the Southern line and 6 ports of the Northern line have been sampled continuously in order to measure the breakthrough time (namely the time taken by the tracer gas to reach the stability inside biofilter voids). Figure 20 is an example of the breakthrough curve obtained during the monitoring period. Results of this measurements are presented in "Undersøgelser af gasfordeling i biocoveranlægget på AV Miljø affaldsdepotetanother", Bachelor Thesis written by Christian Jespersen and Stefan Danielsson at DTU.

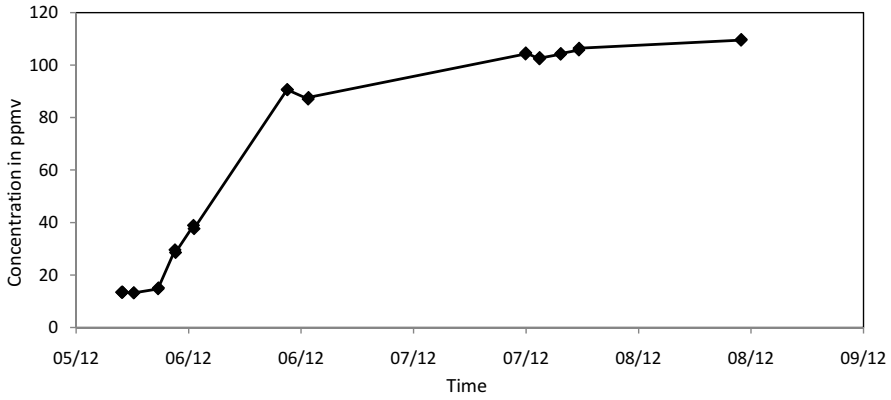

Figure 20: Breakthrough curve measured for HFC-134a at AV Miljø biofilter during the campaign of 05-09 December.

The HFC-134a gas was injected inside the outlet pipe of the mixing chamber using a vacuum pump. The tracer was stored in plastic gas bags with a capacity of 8 liters, which needed to be filled approximately every 8-10 hours. The flux was controlled by a meter placed between the vacuum pump and the inlet pipe, in order to guarantee a constant incoming flux to the biofilter. The meter, marked with numbers between 0 and 14, has been previously calibrated in order

to identify the corresponding fluxes in ml/second. The final adopted values were 4, corresponding to a flux of 0.185 ml/second. In the figure below we have the calibration line obtained for the meter. Generally, the use of a vacuum pump connected to a gas bag has to be preferred to the injection of gas directly from a gas cylinder, because the gas flux turns out to be more stable. The stability of tracer flux needs anyway to be continuously monitored, as it's one of the fundamental hypothesis for the tracer mass balance method.

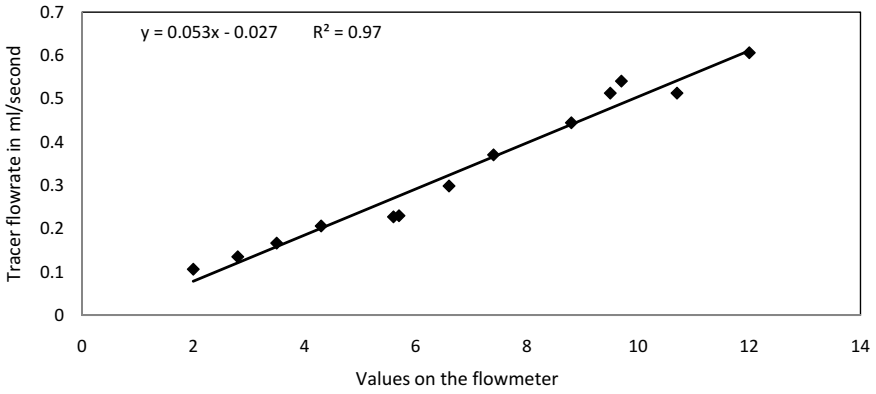

Figure 21: The curve obtained from the calibration procedure of the tracer injection meter is reported.

The concentration of methane, carbon dioxide and HFC-134a were monitored at several places and at different depths. During the first monitoring campaign (17-18 November), gases concentrations in tubes 1A, 1B, 1D, 5A, 5B, 5D, 10A, 10B, 10D in the South line and 1A, 1B, 1D,10A, 10B, 10D in the North line were measured. In the second monitoring campaign (05-09 December), gases concentrations in tubes 1A, 1B, 1D, 4A, 4B, 4D, 8A, 8B, 8D, 10A, 10B, 10D in the South line and 1A, 1B, 1D, 4A, 4B, 4D, 8A, 8B, 8D, 10A, 10B, 10D in the North line were measured. In order to measure the concentration of all these gases, specific equipment was adopted. A Photoacoustic Gas Monitor INNOVA 1412i (LumaSenseTechnologies, 2012) based on photoacoustic infrared detection methods was used. The temperature operating range specified for INNOVA 1412i is between +5°C and 40°C, then temperatures below 0°C (as were during the measurements campaigns) can affect the stability of the equipment. The equipment was connected with a pipe 4 meters long, used to connect the device to the sampling tubes. The flushing time for this pipe was 14 seconds. The pump was set to sample for 5 seconds (with a flowrate of 30 cm^3per second of gas). The sampling procedure consisted in connecting INNOVA 1412i with one of the tubes and each tube was sampled two times in order to verify the tested values. After one port

was completed, a sample was taken with fresh air in order to guarantee values accuracy. Usually the whole analysis took 2-3 hours to be completed, an acceptable time in which weather conditions change (as atmospheric pressure) can be assumed to be negligible.

(a) (b)

Figure 22: (a): Photoacoustic Gas Monitor INNOVA 1412i equipment (LumaSenseTechnologies, 2012), (b): INNOVA 1412i used for underground gas sampling at AV Miljø biofilter.

4.7 FLUX CHAMBER CAMPAIGNS WITH TRACER

In order to obtain surface fluxes from the biofilter of CH_4, CO_2 and $C_2H_2F_4$, measurements by using flux chamber method were carried out during the two measurement campaigns (17-18 November and 05-09 December). A static flux chamber was placed on the surface of the biofilter in the same points previously sampled with INNOVA 1412i. During the first campaign, concentrations in the flux chamber in points 1, 5, and 10 for the South line and in 1 and 10 for the North line were measured.

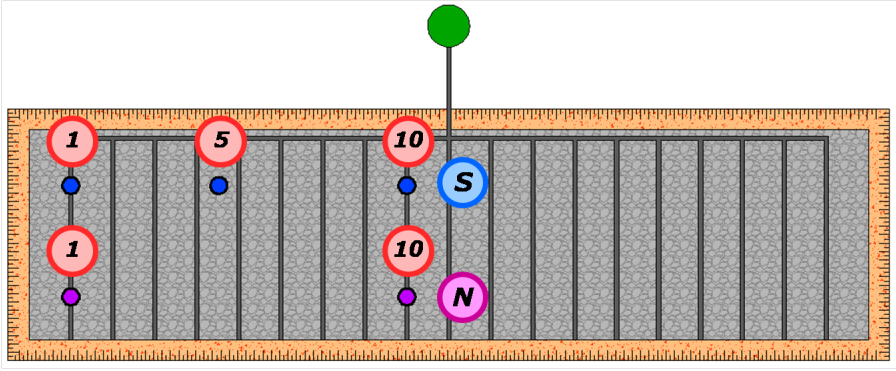

Figure 23: Schematic plant distribution of the 5 points where flux chamber test was performed during the first measurement campaign.

During the second campaign, concentrations in points 1, 4, 8 and 10 for the South line and in 1, 4, 8 and 10 for the North line were measured.

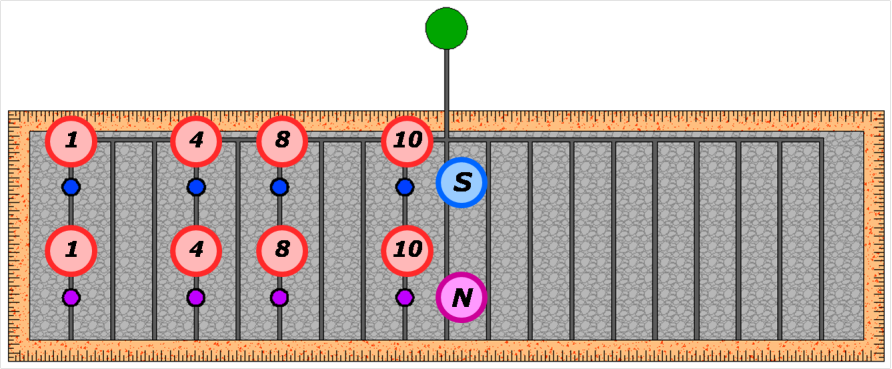

Figure 24: Schematic plant distribution of the 8 points where flux chamber test was performed during the second measurement campaign.

A cylindrical flux chamber 0.25 m high and with a diameter of 0.31 m (0.015 $m^3$of volume) was used for the static flux chamber analysis. The measurement was done by placing the flux chamber on the chosen point and by pressing it 5 cm inside the biofilter soil. Instantaneously, after pulling the chamber, all the measurement equipments were started to record CH_4, CO_2 and $C_2H_2F_4$ (tracer) concentrations inside the flux chamber. CH_4, CO_2 and $C_2H_2F_4$ increasing concentrations were measured and recorded using Photoacoustic Gas Monitor INNOVA 1412i (LumaSenseTechnologies, 2012) connected with a 1 meter tube to the flux chamber. INNOVA 1412i was set to sample gas inside the flux chamber just for 1 second and to take one sample every minute. CO_2 increasing concentrations and temperature inside were measured also by using the GMP343 Carbon Dioxide Probe (Vaisala, 2009) placed, through a hole, inside the chamber. GMP343 Carbon Dioxide Probe was set to measure CO_2 and temperature inside the flux chamber every minute. For each point and each flux chamber measurement, 5-6 samples were taken. During the sampling period, a small fan was manually turned inside the flux chamber to improve gas distribution and homogeneity.

Methane, Carbon Dioxide and HFC-134a concentrations were after plotted against time scale and dC/dt was considered acceptable for $R^2 \geq 0.8$. Fluxes were in the end calculated for every point and every compound. Values obtained from measurements of dC/dt for every gas compound and average temperature from Vaisala, were used in formula (2) presented in paragraph 3.3.1 to obtain surface fluxes. In figure 25, the flux chamber equipments and testing is showed.

(a)

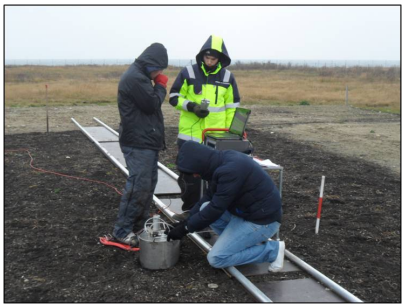

(b)

Figure 25: (a): Static flux chamber placed on the biofilter. It's possible to observe the cylindrical Vaisala probe and the tube connecting the chamber with INNOVA equipment , (b): One flux chamber test performed at AV Miljø biofilter.

4.8 EVALUATION OF BIOFILTER CH_4 OXIDATION EFFICIENCY

A measurement campaign using static flux chamber method has been carried out on January 24th and 25th. The final purpose of this analysis was completely different from all the previous ones. In fact, while the previous campaigns were carried out to understand the phenomena occurring in the biofilter, this specific measurement was done to evaluate the efficiency of the whole biofilter as a technology applicable on a large scale. From several previous studies it has been reported that the lower efficiency of the biofilter technology was recorded during winter season. Is therefore evident that the performing of this analysis during this particular season is equivalent to measuring the lower biofilter CH_4 oxidation efficiency. The static flux chamber method was applied in 60 point distributed homogeneously over the entire biofilter surface (see figure 26). Six of these points have been placed in the hot spot area localized with the FID scanning (South-East corner of the biofilter). To perform this measurement campaign, the same cylindrical flux chamber used for the previous surface analysis was adopted (height of 0.25 m, 0.31 m of diameter, 0.015 $m^3$of volume). The chamber was placed in the sampling point and pressed 5 cm in the biofilter. INNOVA 1412i device was used to extract gas from the chamber and to analyze the concentration of CH_4 and CO_2 inside. A small fan was turned manually inside the flux chamber to improve gas distribution and homogeneity. The increasing concentrations of gas recorded by Photoacoustic Gas Monitor INNOVA 1412i (LumaSenseTechnologies, 2012) have been then elaborated in order to calculate the fluxes of these two gases from every sampling point (in $mol \cdot m^{-2} \cdot d^{-1}$).

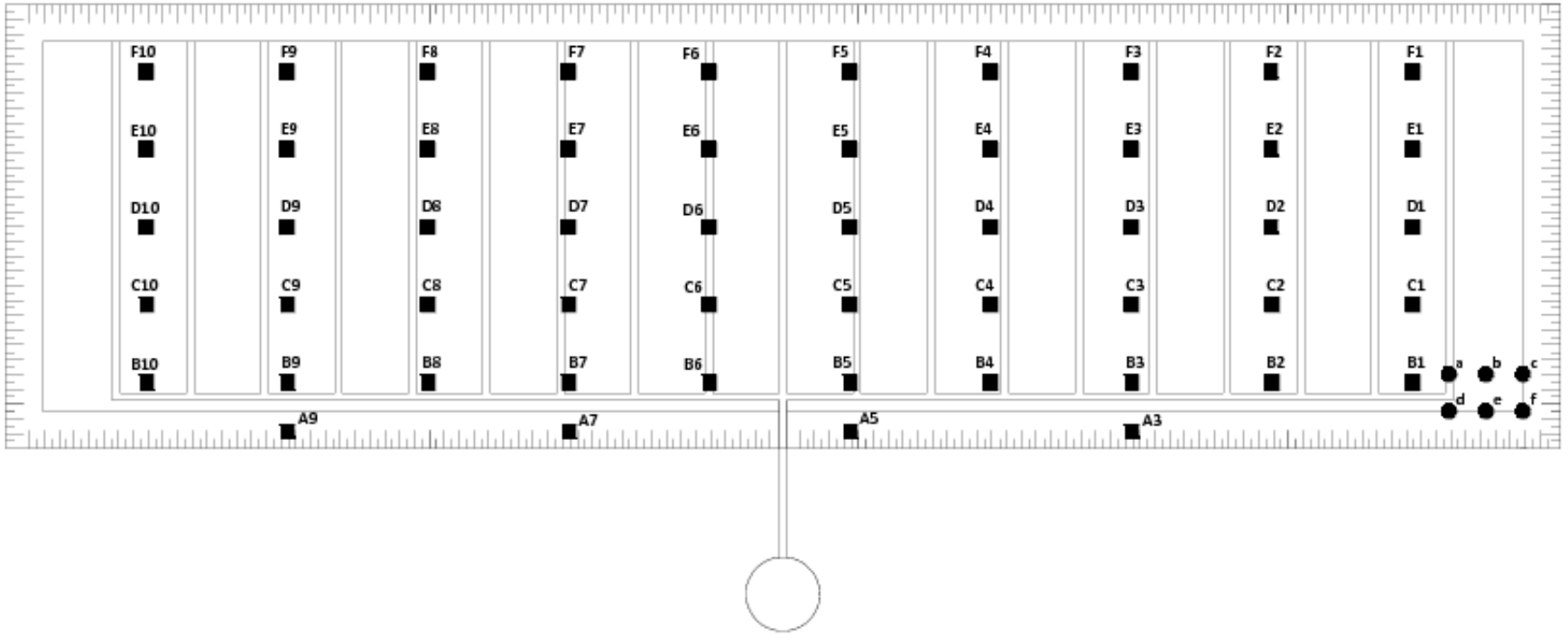

Figure 26: Planimetric distribution of points sampled with static flux chamber method on January 25th.

As for the previous analysis, dC/dt of methane and carbon dioxide was considered acceptable for $R^2 \geq 0.8$. In order to obtain a spatial 2D distribution of these two gases, Surfer 8 (released by Golden Software Inc.) software was adopted. From the analysis of the spatial distribution, emission areas with different flux values were obtained (m^2) and multiplied by the corresponding flux ($mol \cdot m^{-2} \cdot d^{-1}$). All the different emissions were then summed and the total biofilter emission were compared with the measured inflowing gas flux to estimate the biofilter efficiency. In figure 27, the performing of flux chamber test is represented.

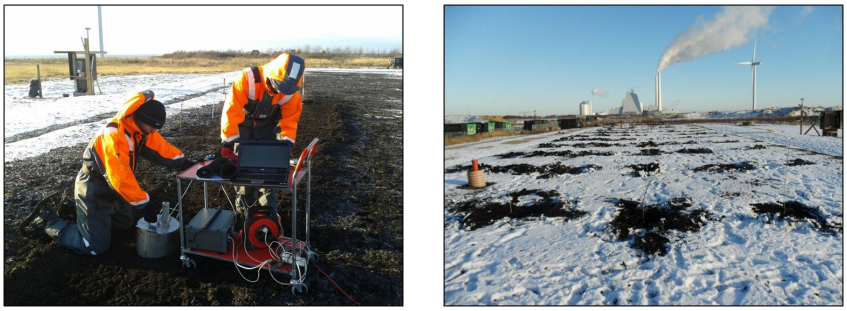

(a) (b)

Figure 27: (a): Static flux chamber test at AV Miljø biofilter. (b): Disposition of the 60 sampling points where the flux chamber test has been performed; the snow and the frozen soil have been previously removed from the top surface in order to let flow the biogas naturally.

5 RESULTS

Results obtained from measurement activities carried out from September 2012 to January 2013 are presented . The first part of the chapter introduces raw results while the second part concerns the interpretation of data.

5.1 RAW RESULTS

5.1.1 *MLPGS profiles of the biofilter*

METHANE IN BIOFILTER'S SOUTHERN AREA. From monitoring activities carried out using methodologies described in paragraph 4.2, it has been possible to draw biofilter profiles for CH_4, $CO_2$and O_2. The biofilter inlet valve was opened on September 22nd and LFG was allowed to flow from the mixing chamber to the biofilter distribution layer. During this period, methane increased its concentration (see figure 26) inside the biofilter, even though a mistake was committed. In fact, in the period between September 22nd and October 16th, the biofilter water lock remained open. Thus, LFG gas was allowed to flow inside the biofilter, but was also allowed to escape from the opposite side. However, this mistake brought interesting consequences that will be described later on in this report.

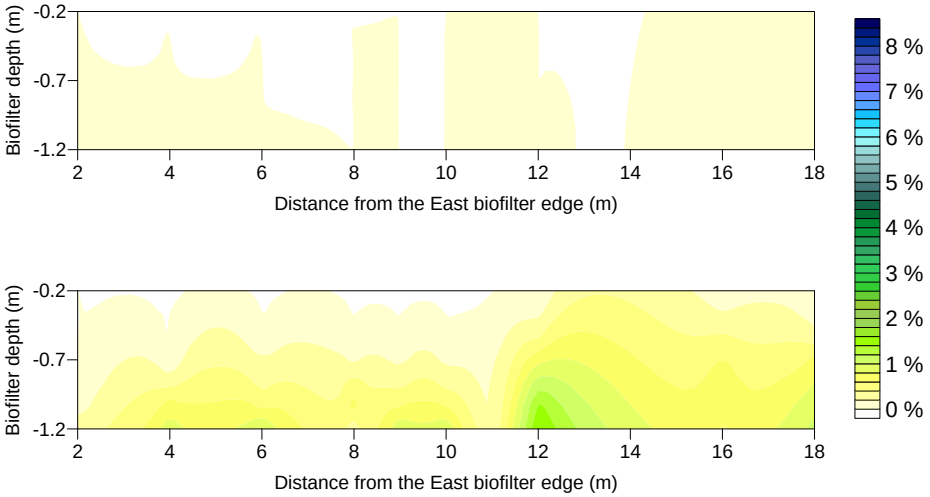

Figure 28: Southern section of the biofilter representing methane distribution from the Eastern edge (left) to the biofilter center (right). Measurements were carried out on September 23rd and September 26th, 2012.

On the third week after LFG flow opening, a certain stable conformation was reached in the biofilter, which is illustrated in the first graph of figure 27. On this day, water lock was detected to be open and sealed. Methane accumulated inside the biofilter all next week long, reaching relatively high concentrations, as showed in the second graph of figure 27. After two weeks from water lock sealing, methane distribution reverted to concentrations measured before biofilter locking (see figure 28). This fact can be this can be attributed to the presence of a methanotrophic community of bacteria in the biofilter that, after the overloading of methane, oxidized excess CH_4 accumulated to maintain a stable condition.

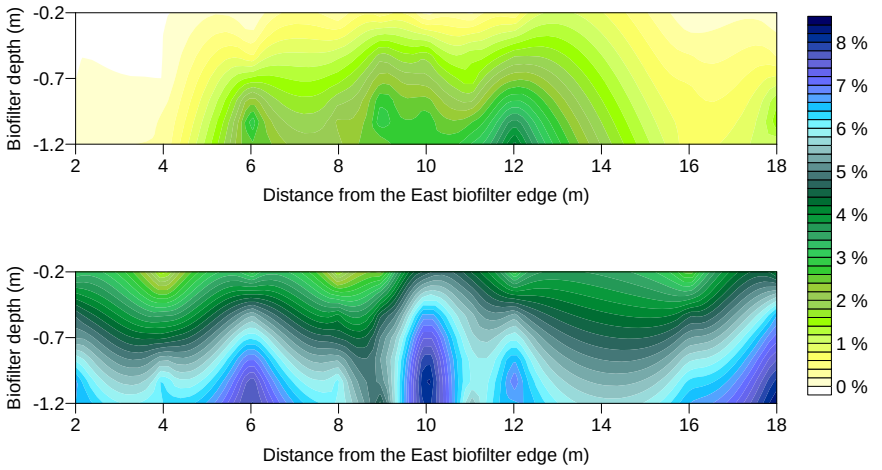

Figure 29: Southern section of the biofilter representing methane distribution from the Eastern edge (left) to the biofilter center (right). Measurements were carried out on October 10th and October 24th.

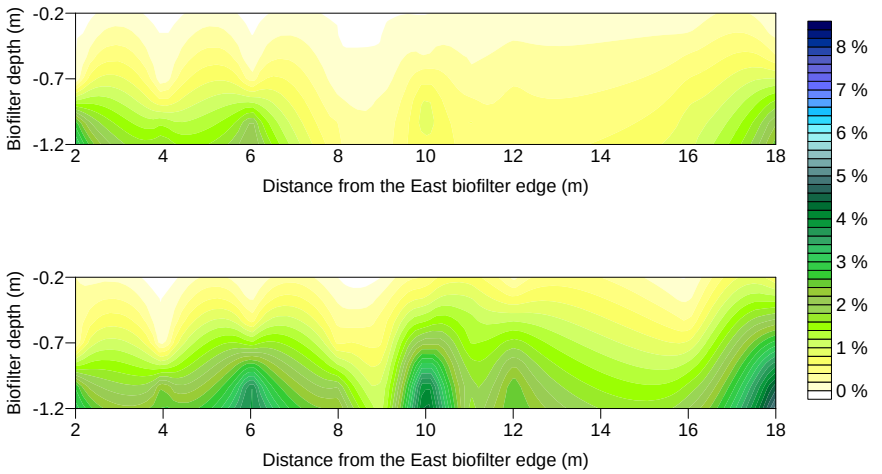

Figure 30: Southern section of the biofilter representing methane distribution from the Eastern edge (left) to the biofilter center (right). Measurements were carried out on October 31st and November 14th.

METHANE IN BIOFILTER'S NORTHERN AREA. In the Northern part of the biofilter, even though methane concentration was lower due to a lower efficiency of the distribution system, the same phenomenon was observed. A really low concentration, around 0.1%, was measured in the biofilter before water lock closure (see figure 29). After the closure of the water lock, methane concentration increased to 4-5% also in the deepest part of the biofilter (first graph of figure 30), as occurred in the Southern part of the biofilter. Then the concentration inside the biofilter decreased in one week reverting to the low stable concentrations (second graph of figure 30).

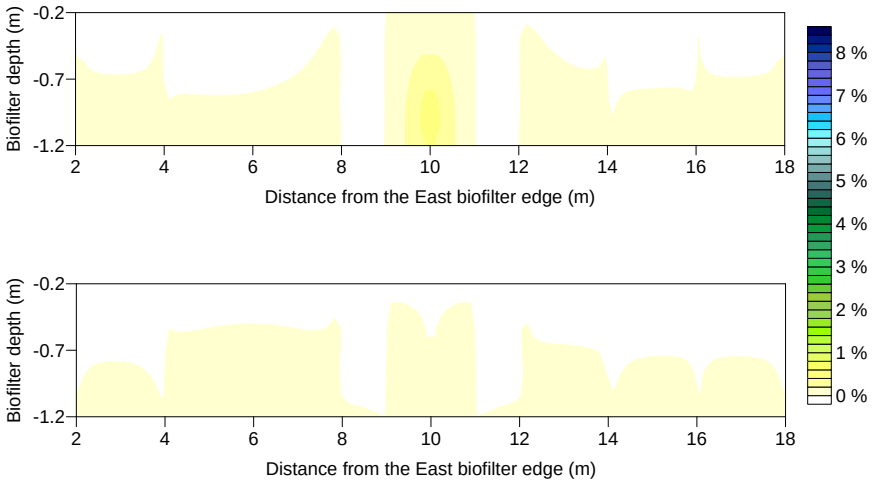

Figure 31: Northern section of the biofilter representing methane distribution from the Eastern edge (left) to the biofilter center (right). Measurements were carried out on September 23rd and October 10th.

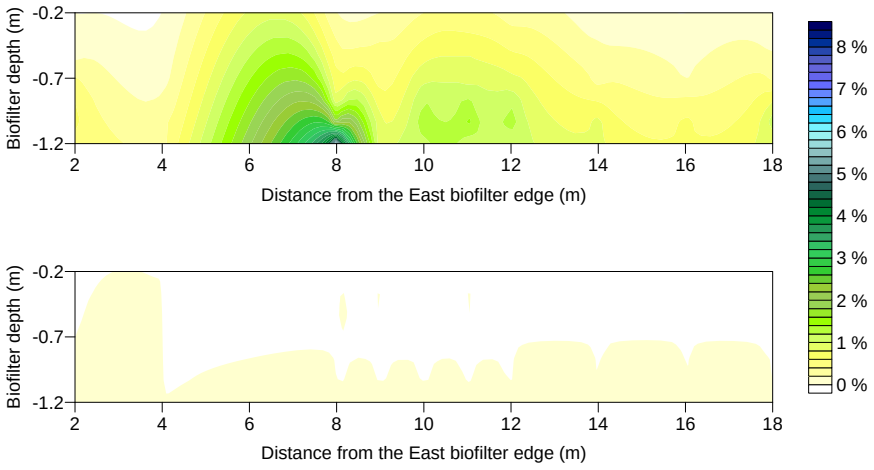

Figure 32: Northern section of the biofilter representing methane distribution from the Eastern edge (left) to the biofilter center (right). Measurements were carried out on October 24st and November 14th.

Also from these methane distribution sections, it's possible to state that a constant conformation for the biofilter is generally observed, with a stable CH_4 concentration equilibrium. If for some reasons (in this case the sealing of biofilter water lock) the concentration of methane tends to increase inside the biofilter substrate, methanotrophic bacteria play a fundamental role to reinstate the old constant conformation.

Moreover, the low concentration of methane in the north part of the biofilter can be attributed to different factors. The most probable cause is the low distribution efficiency of the gravel layer beneath the biofilter. However, that could only be a partial explanation as on October 24th very high concentrations were recorded. Then the low concentration of methane in the Northern part of the biofilter can also be ascribed to methanotrophic activity in the soil. Methanotrophic activity could be located inside the compost soil, but also inside the distribution layer.

CARBON DIOXIDE IN BIOFILTER'S SOUTHERN AREA. Carbon dioxide was also monitored during the testing period, and vertical profiles of the Eastern part of the biofilter were obtained. In figure 31 it's possible to observe CO_2 concentration before and after LFG flux opening. The first graph of figure 31 represents the standard distribution of carbon dioxide before LFG opening. Is possible to observe the presence of non homogeneous areas of carbon dioxide concentration, probably due to compost respiration.

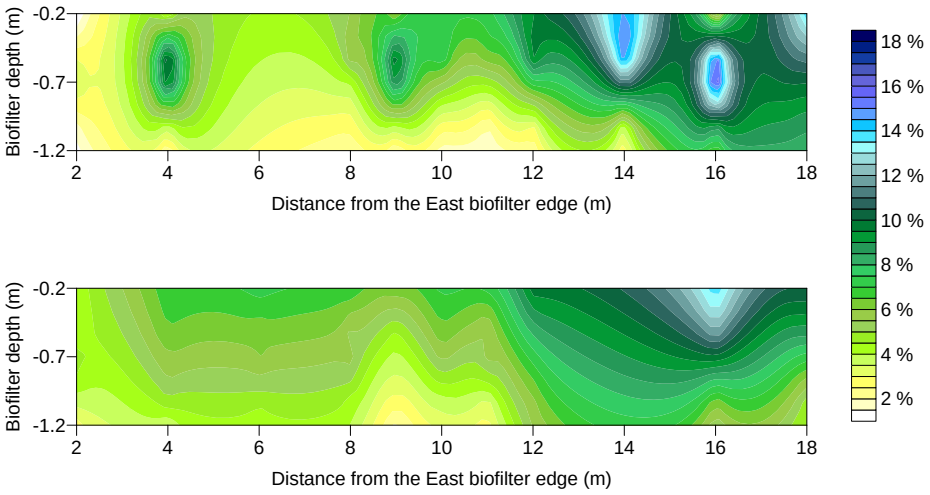

Figure 33: Southern section of the biofilter representing carbon dioxide distribution from the Eastern edge (left) to the biofilter center (right). Measurements were carried out on August 7th and October 16th.

The second graph, which represents carbon dioxide distribution after LFG flux opening, is easy to distinguish from the previous setting mainly due to the disappearance of CO_2 hot spots and the appearance of a concentration layering. In both conformations, the average value

of carbon dioxide is the same and the concentration in the central part of the biofilter is higher than in the external area.

After the water lock closure, carbon dioxide distribution changes radically. Concentration layering is accentuated, with the disappearing of different concentrations between the central and the external part. Carbon dioxide concentrations are doubled, from an average of 7% to an average of 14%. After water lock closure the concentration of carbon dioxide remains constant for all the following measurement, which means that some reactions which involve the generation of CO_2 are occurring. Considering that the only factor which changed from the previous period is the increase of methane presence inside the biofilter, it's probable that the CO_2 concentration increase could be attributed to methane oxidation activities carried out by methanotrophic bacteria.

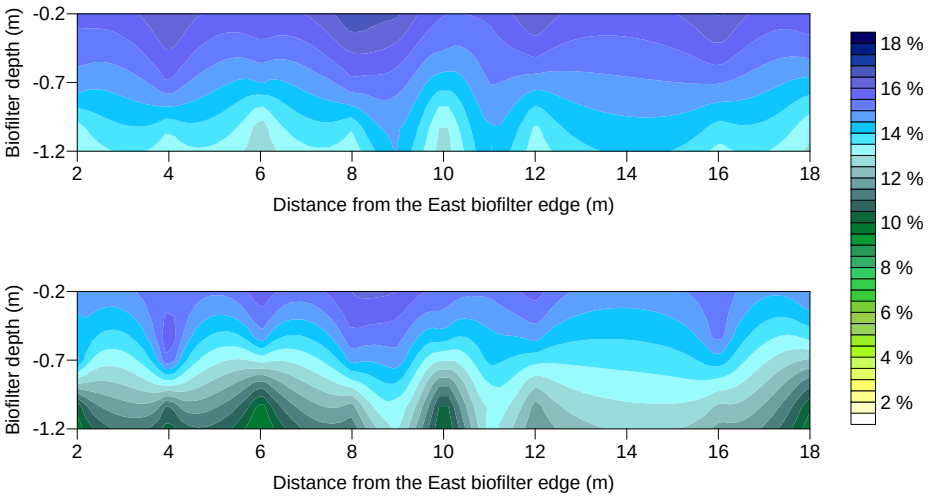

Figure 34: Southern section of the biofilter representing carbon dioxide distribution from the Eastern edge (left) to the biofilter center (right). Measurements were carried out on October 24th and November 14th.

CARBON DIOXIDE IN BIOFILTER'S NORTHERN AREA. In the Northern part of the biofilter it's possible to underline how the conformation before opening the LFG flux for CO_2 (first graph in figure 33) is similar to Southern part of the biofilter. After methane has started to flow inside the biofilter body, the classical stratification of concentrations (with higher concentrations in the shallowest part of the biofilter) happened. It's possible to observe also in this graph (second of figure 33) that carbon dioxide concentration is greater in the area close to the center than in areas near the biofilter edge.

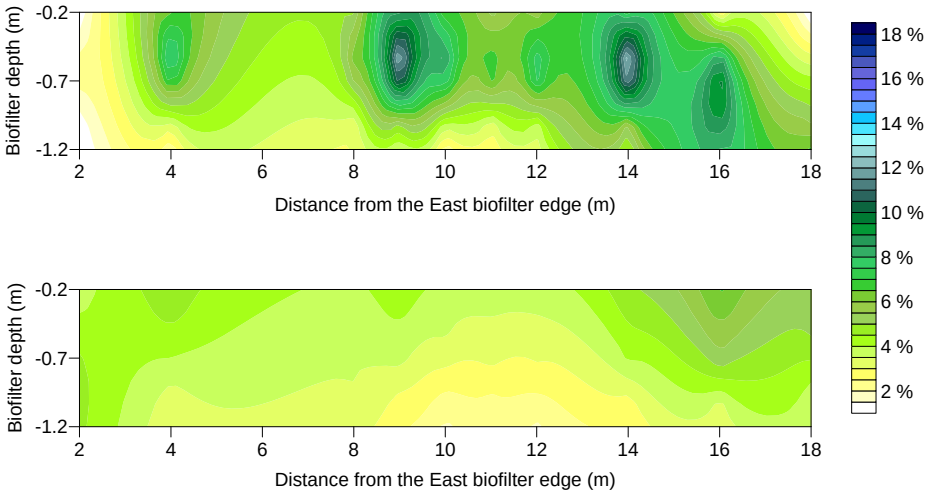

Figure 35: Northern section of the biofilter representing carbon dioxide distribution from the Eastern edge (left) to the biofilter center (right). Measurements were carried out on August 7th and October 16th.

After the closure of the water lock, the concentration of CO_2 increased suddenly in the north area on the biofilter, as happened for the south one. Concentrations of carbon dioxide increased from 4-5% to 13% the week after water lock sealing (see first graph of figure 34) and reached the constant average value of 10% in the next weeks (second graph of figure 34). As for the Southern part of the biofilter, it's possible to conclude that methane oxidation occurred in the biofilter body. Probably methanotrophic bacteria activity is the reason of this sudden increase of CO_2 concentration, as methane flow is the only factor of interest which is changed after October 16th.

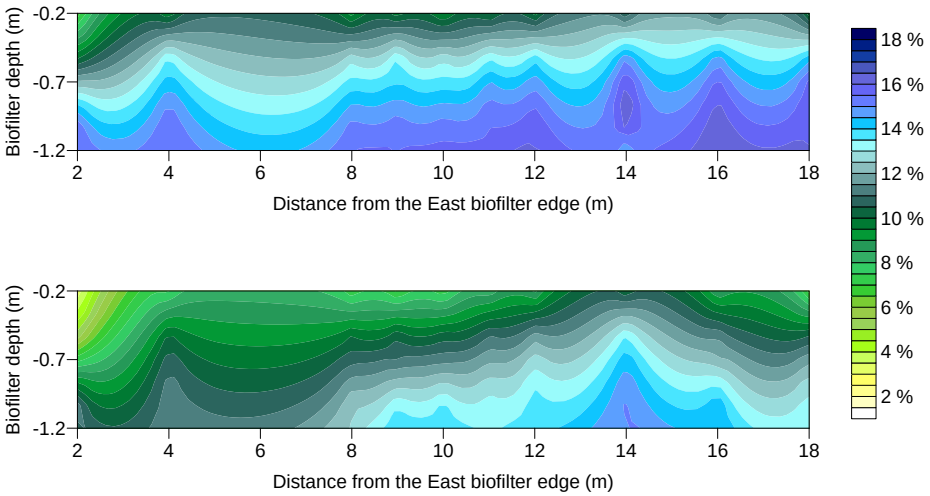

Figure 36: Northern section of the biofilter representing carbon dioxide distribution from the Eastern edge (left) to the biofilter center (right). Measurements were carried out on October 24th and November 14th.

OXYGEN IN BIOFILTER'S SOUTHERN AREA. The last gas monitored in the biofilter was oxygen. In the first period, before LFG gas flow opening, the distribution in the biofilter of this compound was non homogeneous as for CO_2. Hot spots were found and greater concentrations in the extremity rather than in the center have been observed, probably due to compost respiration (first graph in figure 35). After LFG was allowed to flow in, a layering of the concentrations occurred. The different concentrations between biofilter areas close and far to the LFG inlet point (biofilter center) are evident in the second graph of figure 35.

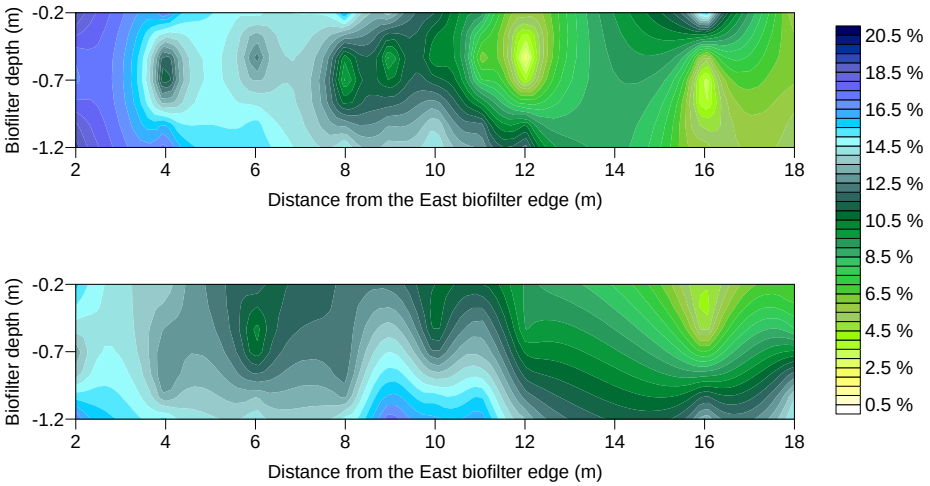

Figure 37: Southern section of the biofilter representing oxygen distribution from the Eastern edge (left) to the biofilter center (right). Measurements were carried out on August 8th and October 16th.

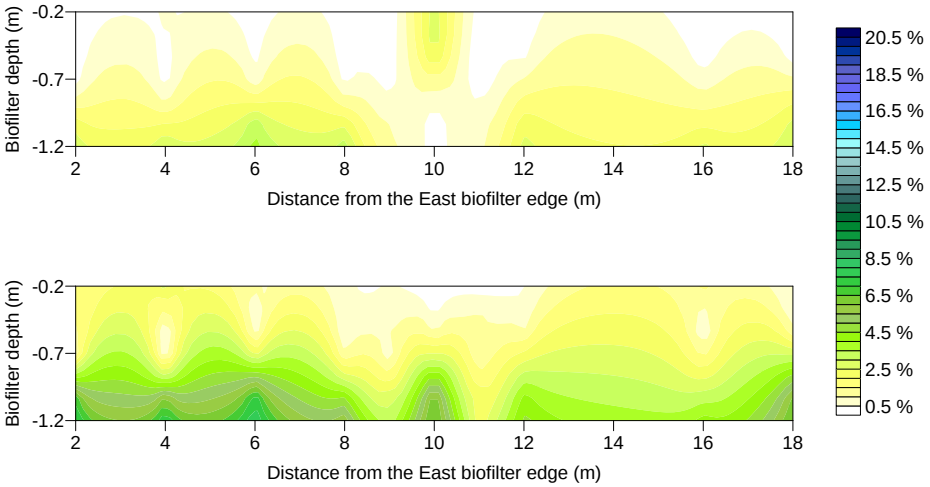

Figure 38: Southern section of the biofilter representing oxygen distribution from the Eastern edge (left) to the biofilter center (right). Measurements were carried out on October 24th and November 14th.

After the water lock closure, the concentration of oxygen in the soil decreased suddenly, reaching values between 0% and 2% (see first graph of figure 36). In the next weeks the level of oxygen reached a stable level around 2-4% (see the second graph of figure 36), with concentrations around 6% in the distribution layer (between -0.90 cm and -1.20cm). This sudden change in the oxygen distribution is another evidence of the oxidation activity carried out by methanotrophic bacteria. The concentration of O_2 was always higher that 0%, avoiding problems of methane generation in anaerobic conditions.

OXYGEN IN BIOFILTER'S NORTHERN AREA. The typical conformation with hot spots was also observed in the Northern part of the biofilter (see first graph of figure 37). Oxygen concentrations between 10 and 20% were recorded inside the biofilter substrate, with low concentrations in presence of a soil respiration activity. In the second period, after the LFG flow opening, the classic concentration layering was observed, with an homogenization of oxygen concentrations from 15 to 19% (see second graph in figure 37).

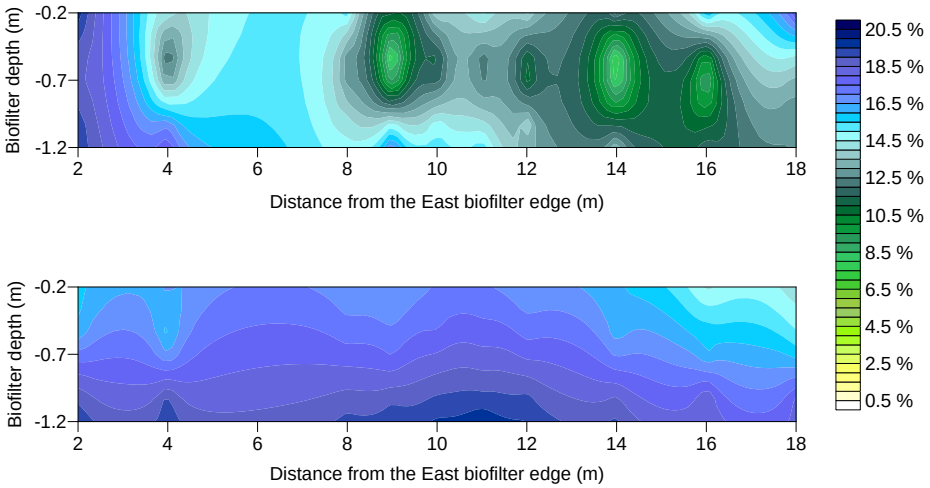

Figure 39: Northern section of the biofilter representing oxygen distribution from the Eastern edge (left) to the biofilter center (right). Measurements were carried out on August 8th and October 16th.

After water lock closure the same behavior of the southern part of the biofilter was observed; oxygen concentrations decreased suddenly but not in the same quantity of the Southern area of the biofilter. In fact, the average oxygen concentration observed in the biofilter after the stabilization was between 4 and 8%, far beyond the 2-3% of the South area (first graph in figure 38). From this observed conformation, it can be concluded that methane oxidation occurred also in the Northern part of the biofilter, but in a lower quantity than in the Southern areas. Methane has been oxidized, but however it ensures high oxygen concentrations far from anaerobic conditions. Moreover, interesting oxygen concentrations, which can be related to a consis-

tent methane oxidation activity, can only be observed in the area closer to the biofilter center, as O_2 concentration increases suddenly moving from the center to the edge (second graph in figure 38).

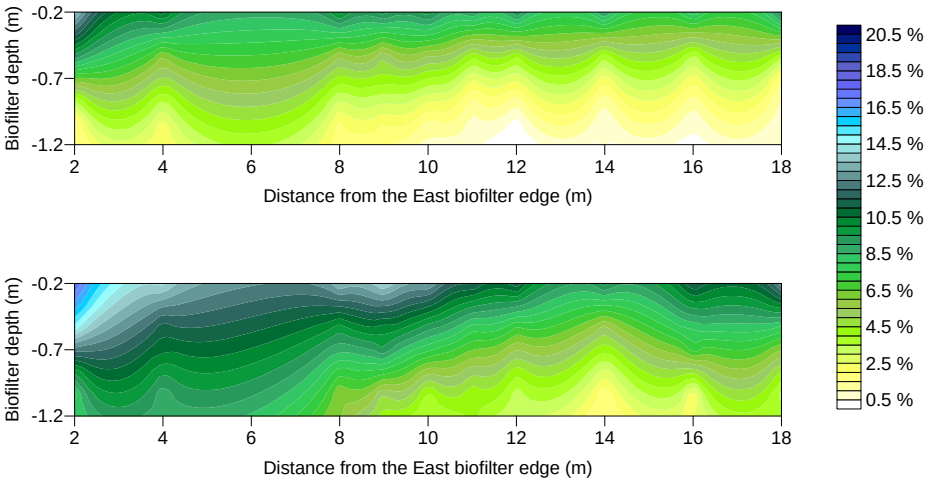

Figure 40: Northern section of the biofilter representing oxygen distribution from the Eastern edge (left) to the biofilter center (right). Measurements were carried out on October 24th and November 14th.

5.1.2 *Surface screening*

The results of the biofilter surface scanning are described in this chapter. Methane scanning has been carried out using a FID device, while for carbon dioxide detection the CARBOCAP® Sensor has been used. The final purposes of this analysis was to analyze the symmetry of the biofilter (from the point of view of LFG distribution and methane oxidation), to eventually identify the presence of hotspots.

METHANE SURFACE SCANNING USING FID DEVICE. CH_4 scanning was carried out on November 14th, November 28th and December 3rd. Methane concentrations measured on the biofilter's surface were always particularly low during all three scannings, ranging from a minimum of 1.2 ppmv to a maximum of 4 ppmv. The presence of a CH_4 emission hot spot has been identified in all the scanning made at AV Miljø biofilter. The hot spot is located in the South-East corner of the biofilter, with greater emissions than the average value measured for the rest of the biofilter. Measured emissions from the eye of the hot spot range from 4 ppmv to 10 ppmv, proving the presence of an non homogeneous soil distribution in this point. There are no other indications that suggest an irregular distribution of CH_4 in the biofilter due to inefficient distribution layer or differentially compacted soil. All measured values in each scanning demonstrate that the biofilter emission is practically homogeneous, with differences of 0.5 ppmv from the higher to the lower value measured. A superfi-

cial area, placed horizontally in the middle of the biofilter, shows for all the scanning the lower emission measured of the whole biofilter. It's complicated to ascribe this anomaly to the low penetration of methane or to an higher methane oxidation, considering that the difference between this area and the surroundings is about 0.2-0.6 ppmv. Methane oxidation carried out by methanotrophic bacteria seems to ensure a low methane emission in the whole biofilter, as showed in figure 39.

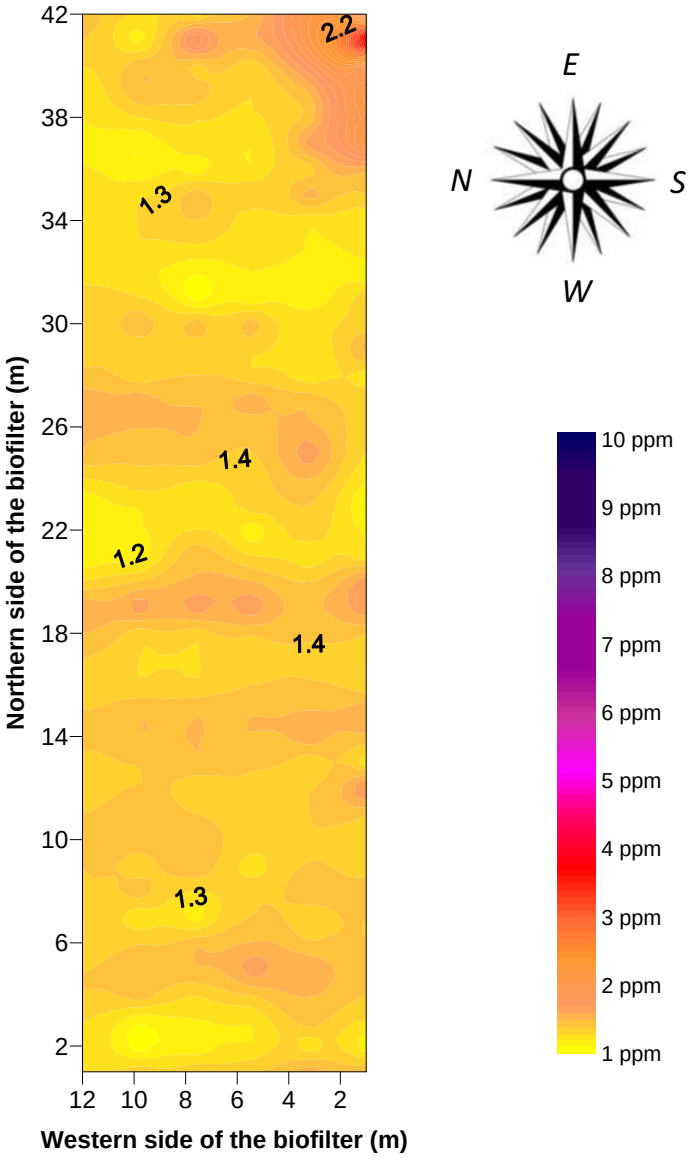

Figure 41: Biofilter scanning of surface methane concentrations, carried out on November 14th. The LFG inlet pipe and mixing chamber are placed on the right of the figure and in the center of the biofilter (around at 21 meters), where 1.2 ppmv concentration was measured.

Considering that the average atmospheric concentration of methane is generally 1.7 ppmv, concentrations measured during the first scanning (November 14th represented in figure 39) can indicate that part of the atmospheric methane has been removed from the atmosphere and oxidized inside the biofilter substrate by methanotrophic bacteria. This fact has already been reported in other studies (Stern et al., 2007) when negative fluxes of methane on compost soils have been measured. The latter consideration implies that a total oxidation of methane flowing from the bottom of the biofilter occurred. The FID scanning was used to locate a net of point measurement to evaluate the whole emissions of the biofilter, as suggested also in Huber-Humer et al. (2009).

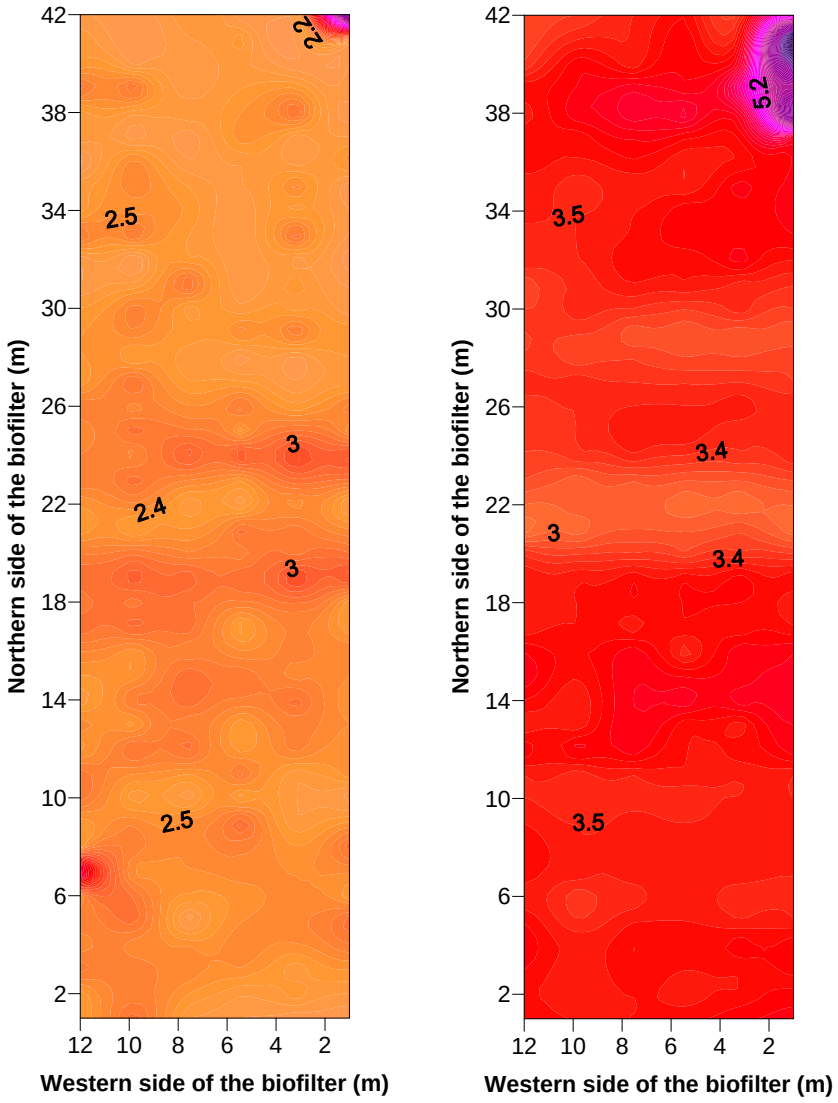

Figure 42: Biofilter scanning of surface methane concentrations, carried out on November 28th and December 3rd. The LFG inlet pipe to the biofilter is placed on the right of the figures, where lower values (2.4 and 3 ppmv respectively) were measured.

CO_2 SURFACE SCANNING USING CARBOCAP® SENSOR. CO_2 scanning was carried out on November 28th and December 3rd. Carbon dioxide background concentration in the atmosphere was measured to be around 390 ppmv, which is close to the scientifically acknowledged value of 394 ppmv (NOAA, 2013). Concentrations measured during the surface screening campaigns reported values between 395 ppmv and 450 ppmv, indicating a consistent CO_2 production in the biofilter substrate material. There are no hot spots constantly identified in the scanning procedure; higher emission points were detected during measurement campaigns, which changed location from time to time.

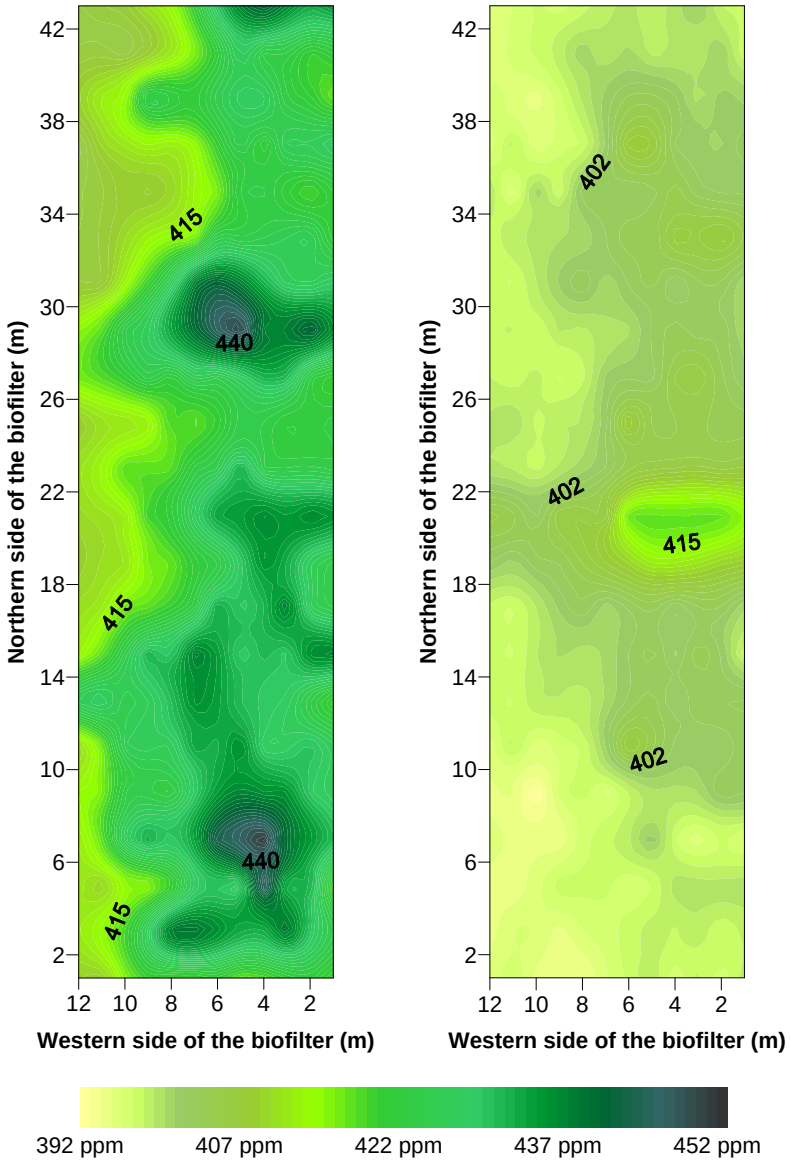

Figure 43: Biofilter scanning of surface carbon dioxide concentrations, carried out on November 28th and December 3rd. The LFG inlet pipe and mixing chamber are placed on the right of the graphs and in the center of the biofilter (around at 21 meters).

In both surface screenings an area with higher emission than the average value has been identified near the LFG inlet point. It's not possible to ascribe this CO_2 emission area to a single factor, as the cause could be a preferential pathway from the inlet flux or an enhanced compost respiration and methane oxidation.

There are evidences of a differential CO_2 emission from the South to the North part of the biofilter. In both screenings, the Southern area is emitting 4-7 % of CO_2 higher than the Northern area, in which emissions are slightly higher than the background level (395-400 ppmv). Considering an homogeneous distribution of compost quality and oxygen inflowing in the biofilter, is reasonable to suppose that CO_2 produced from soil respiration is almost constant in the whole biofilter. Then this differential emission of carbon dioxide has to be attributed to a greater activity of methanotrophic bacteria in the Southern area of the biofilter, which leads to a greater CH_4 consumption and CO_2 production.

5.1.3 *Flux chamber measurement campaigns*

From the two measurement campaigns carried out on November 18th and December 8th, concentrations of analyzed gases inside the flux chamber were recorded. For all the measured fluxes, the R^2 was found not only to be in the acceptable range (≥ 0.8) but even ≥ 0.9. The measured average R^2 for methane in both campaigns was 0.99, while for carbon dioxide was found to be 0.98. Also for the used tracer gas, HFC-134a, the average R^2 was found to be 0.97. No correlation was found between increasing concentrations inside the flux chamber and the R^2 factor.

From the theory it's know how to calculate surface fluxes using the flux chamber (see equation 2 in paragraph 3.3.1). Analyzing this equation it's evident that there is a linear correlation between the surface flux and the factor $\partial C/\partial t$. In fact, all the other variables are constant for the same measurement campaign (except the temperature which is slightly changing in time). The correlation between all the measured $\partial C/\partial t$ values (during the second campaign) can be observed in figure 42, 43.

In figure 42, three graphs are representing the behavior of measured gases in the Southern part of the biofilter. All the three graphs show the same general trend: the higher emission is localized in the S1 point, which is located in the farthest point from the biofilter inlet (practically near the biofilter edge). Emissions from points near the inlet, S10 and S8, are lower than S1 but practically equal to each other. In the end S4 shows the lower value recorded for all the gases. Trends measured for the gases, highlight the difference between S1 and the other sampling points. The average rate measured for CH_4 in S4, S8 and S10 is around 0.7 $l \cdot m^{-3} \cdot s^{-1}$, while is 0.13 $l \cdot m^{-3} \cdot s^{-1}$ in S1.

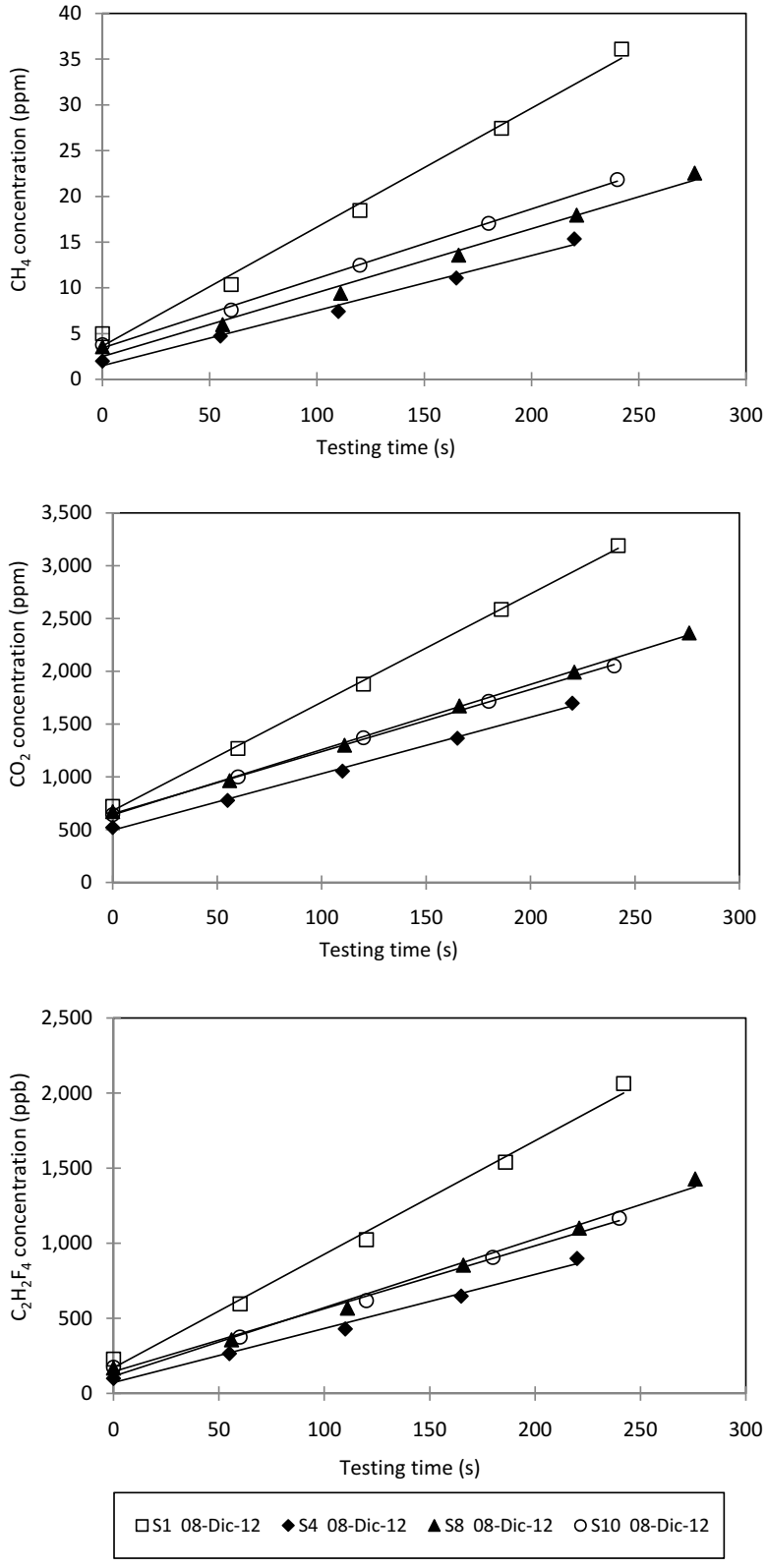

Figure 44: Concentrations of CH_4, CO_2 and $C_2H_2F_4$ (tracer gas) versus time, measured in the Southern part of the biofilter during flux chamber campaign on December 8th. The spatial distribution of the sampled points can be observed in figure 24, paragraph 4.7.

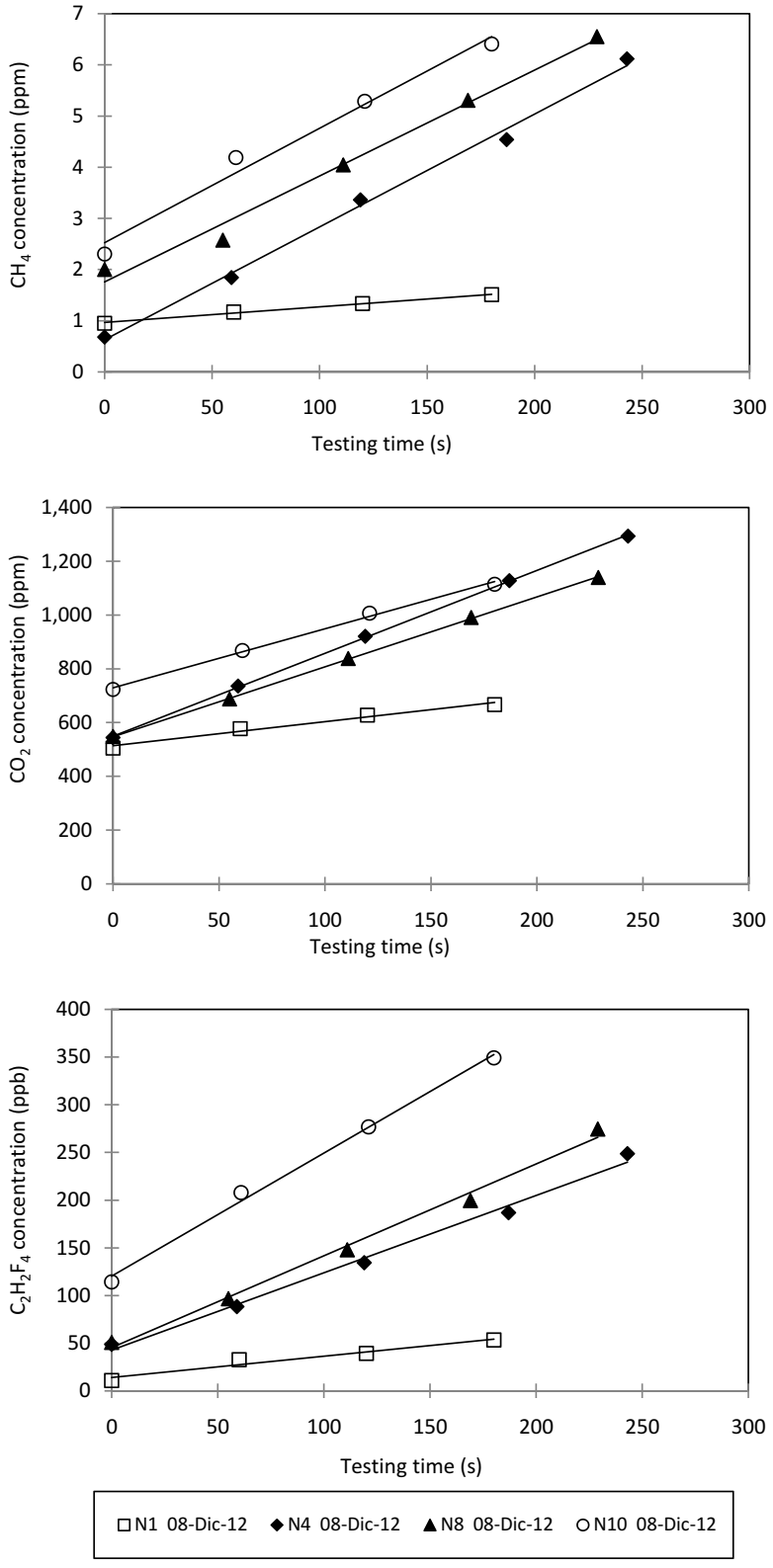

Figure 45: Concentrations of CH_4, CO_2 and $C_2H_2F_4$ (tracer gas) versus time, measured in the Northern part of the biofilter during flux chamber campaign on December 8th. The spatial distribution of the sampled points can be observed in figure 24, paragraph 4.7.

For CO_2 the average rate ranges from 6 to 7 $l \cdot m^{-3} \cdot s^{-1}$ for S4, S8 and S10, but for S1 it is 10.3 $l \cdot m^{-3} \cdot s^{-1}$ for S1. The same behavior can be observed for HFC-134a compound, with a 3.6-4.6 range for S4, S8 and S10 trends, instead of a 7.6 $l \cdot m^{-3} \cdot s^{-1}$ for S1 (see table 6). The presence of a greater emission of CH_4 in S1 cannot be explained by a lower methane oxidation activity, because in that case a lower CO_2 emission would be observed. This special conformation leads to the presence of a preferential pathway in the South-East part of the biofilter, which leads to higher concentration variations inside the flux chamber.

In figure 43, three graphs are representing the behavior of measured gases in the Northern part of the biofilter. The general trend represented by these graphs shows that in the Northern part of the biofilter, gases rates are almost equal to each other for points N4, N8 and N10. For methane all the rates are around 0.2 ±0.02 $l \cdot m^{-3} \cdot s^{-1}$ and for HFC-134a around 1 ±0.2 $l \cdot m^{-3} \cdot s^{-1}$(see table 6). The only exception concerns carbon dioxide because N10 (1.3 $l \cdot m^{-3} \cdot s^{-1}$) appears considerably lower than N4 and N8 (2.5 $l \cdot m^{-3} \cdot s^{-1}$). This, as the CH_4 rates are equals for N4, N8 and N10, can be caused by a lower respiration rate in the central part of the biofilter (N10) consequently to an higher presence of oxygen.

5.1.4 *Gas profiles*

The vertical distribution of methane, carbon dioxide and HFC-134a was tested in all the spots reported in table 6, in order to observe the dispersion of the different gases inside the soil. From this analysis, it's possible to observe and compare the distribution of an inert gas with the distribution of methane and carbon dioxide.

Graphs a) and b) in figure 44 illustrate the trends of analyzed gases in point S1, in the South-East corner of the biofilter. It can be observed that the tracer gas is diffusing homogeneously in the biofilter, with a slightly decreasing concentration from -1 m to 0.5 m. At the same time, CH_4 shows a considerably steeper decreasing rate, which brings methane concentration in the soil from almost 35,000 ppmv to almost 5,800 ppmv in the deepest 50 cm. The decreasing rate continues with an almost constant tracer gas concentration (from -0.5 m to -0.2 m), and methane decreases from 5,800 ppmv to 2,500 ppmv. Both gases then reach a superficial value really low, also due to atmospheric gas diffusion into the soil. On the contrary, while the inert gas is slightly decreasing, CO_2 concentration in the biofilter is highly increasing from almost 118,000 ppmv to 331,000 ppmv in the deepest 50 cm (from -1 m to -0.5 m) and slightly also in the following 30 cm (from 331,000 to almost 360,000 ppmv). From these considerations it's possible to conclude that:

Table 6: Rates ($l \cdot m^{-3} \cdot s^{-1}$), coefficients of determination R^2 for methane (CH_4), carbon dioxide (CO_2) and HFC-134a ($C_2H_2F_4$). Detected temperatures are also reported. All the parameters have been measured with the static flux chamber method during the two monitoring campaigns for all the points of interest. The spatial distribution of the sampled points can be observed in figures 23, 24, paragraph 4.7.

Parameter	*Testing day*	*S1*	*S4*	*S5*	*S8*	*S10*	*N1*	*N 4*	*N8*	*N10*
$\partial C/\partial t$ *for* CH_4	18-Nov-12	0.13	n.a.	0.02	n.a.	0.03	-0.001	n.a.	n.a.	-0.005
	08-Dec-12	0.13	0.06	n.a.	0.07	0.07	0.003	0.021	0.020	0.022
$\partial C/\partial t$ *for* CO_2	18-Nov-12	5.24	n.a.	6.75	n.a.	8.00	0.72	n.a.	n.a.	0.70
	08-Dec-12	10.26	5.85	n.a.	6.86	6.94	2.13	3.08	3.39	2.19
$\partial C/\partial t$ *for* $CO_{2,\star}$	18-Nov-12	4.05	n.a.	5.73	n.a.	6.75	0.49	n.a.	n.a.	0.76
	08-Dec-12	8.69	5.35	n.a.	6.17	5.89	1.20	2.56	2.59	1.13
$\partial C/\partial t$ *for* $C_2H_2F_4$	18-Nov-12	3.28	n.a.	2.56	n.a.	3.04	0.48	n.a.	n.a.	0.33
	08-Dec-12	7.56	3.60	n.a.	4.57	4.19	0.22	0.81	0.96	1.29
R^2 *for* CH_4	18-Nov-12	0.99	n.a.	0.99	n.a.	0.99	0.99	n.a.	n.a.	0.99
	08-Dec-12	0.99	0.99	n.a.	0.99	0.99	0.99	0.99	0.99	0.99
R^2 *for* CO_2	18-Nov-12	0.98	n.a.	0.92	n.a.	0.98	0.97	n.a.	n.a.	0.94
	08-Dec-12	0.99	0.99	n.a.	0.99	0.99	0.96	0.99	0.99	0.99
R^2 *for* $CO_{2,\star}$	18-Nov-12	0.96	n.a.	0.97	n.a.	0.94	0.94	n.a.	n.a.	0.96
	08-Dec-12	0.99	0.99	n.a.	0.99	0.99	0.97	0.97	0.99	0.99
R^2 *for* $C_2H_2F_4$	18-Nov-12	0.90	n.a.	0.99	n.a.	0.96	0.97	n.a.	n.a.	0.93
	08-Dec-12	0.99	0.99	n.a.	0.99	0.99	0.99	0.99	0.99	0.98
Temperature	18-Nov-12	283.26	n.a.	280.95	n.a.	281.16	282.52	n.a.	n.a.	282.52
	08-Dec-12	273.34	273.32	n.a.	273.31	273.0	272.94	273.32	273.40	273.76

$\star$ CO_2 rates and coefficients of determination measured with Vaisala CARBOCAP® sensor, installed inside the flux chamber. Al the other rates and coefficients have been measured with INNOVA 1412i. Temperature also have been detected by using Vaisala CARBOCAP® sensor.

n.a. Data not available, as the analysis has not been carried out in that campaign for this point.

- CH_4 decreases with a greater rate than the normal diffusion, represented by the tracer gas;
- carbon dioxide trend has rates not ascribable just to stabilized compost respiration.

It's reasonable to conclude that a consistent methanotrophic activity is acting in this area and methane has been largely oxidized from bacteria.

Graphs c) and d) in figure 44 illustrate the trend of analyzed gases in point N10, in the Northern central part of the biofilter. The inert gas (HFC-134a) shows a constant rate in the diffusion, with a constant decrease between -1 m to -0.75 m (from 93 ppmv to 75 ppmv) and between -0.75 m to -0.2 m (from 75 ppmv to 55 ppmv). Methane shows an higher decrease rate in the deepest interval (from 2,200 ppmv to 1,300 ppmv). In the shallowest part of the biofilter, methane shows the same behavior of the curve described by the tracer compound. In case of pure parallelism between the inert gas and one of the two compounds, it's easy to observe that gases are just decreasing their concentrations as effect of gas diffusion in the soil. In this case, no other phenomena are occurring and there is no methane oxidation. Analyzing the situation described by graphs c) and d) in figure 44, it's possible to conclude that a possible methane oxidation activity is happening in the deepest part of the biofilter, which vanishes in the shallowest portion of the biofilter (from -0.75 m to -0.2 m), where methane and tracer curves decreases homogeneously. This is also proved by carbon dioxide rate, which is always decreasing throughout the biofilter depth with almost the same rate of tracer gas.

Graphs e) and f) in figure 44 illustrate the trend of analyzed gases in point N1, in the North-East area of the biofilter. This is the farthest point to the biofilter LFG inlet and the most difficult point to be reached by the inflowing gases. The tracer gas diffuses inside the biofilter with a concentration of 75 ppmv at -1 m, decreasing to 59 ppmv at -0.75 m and in the end reaching 26 ppmv at -0.2 m. The same behavior can be observed for methane and carbon dioxide. CH_4 was measured to be around 1600 ppmv at -1 m, reaching 1400 ppmv at -0.75 m. In the end halves, as happened for the tracer gas, reaching 700 ppmv at -0.2 m. CO_2 was measured to decrease from 225,000 ppmv to 154,000 ppmv in the deepest 25 cm, then reaching 56,000 ppmv at -0.2 m. Observing graphs e) and f) is also evident how the three gases are diffusing parallel into the biofilter soil. From all the previous considerations, the homogenous decreasing of concentrations and parallelism between curves, it's possible to conclude that in this spot all the gases diffuse into the biofilter without be altered by other phenomena. This conclusion brings to the fact that probably there is not a relevant methane oxidation activity in this point.

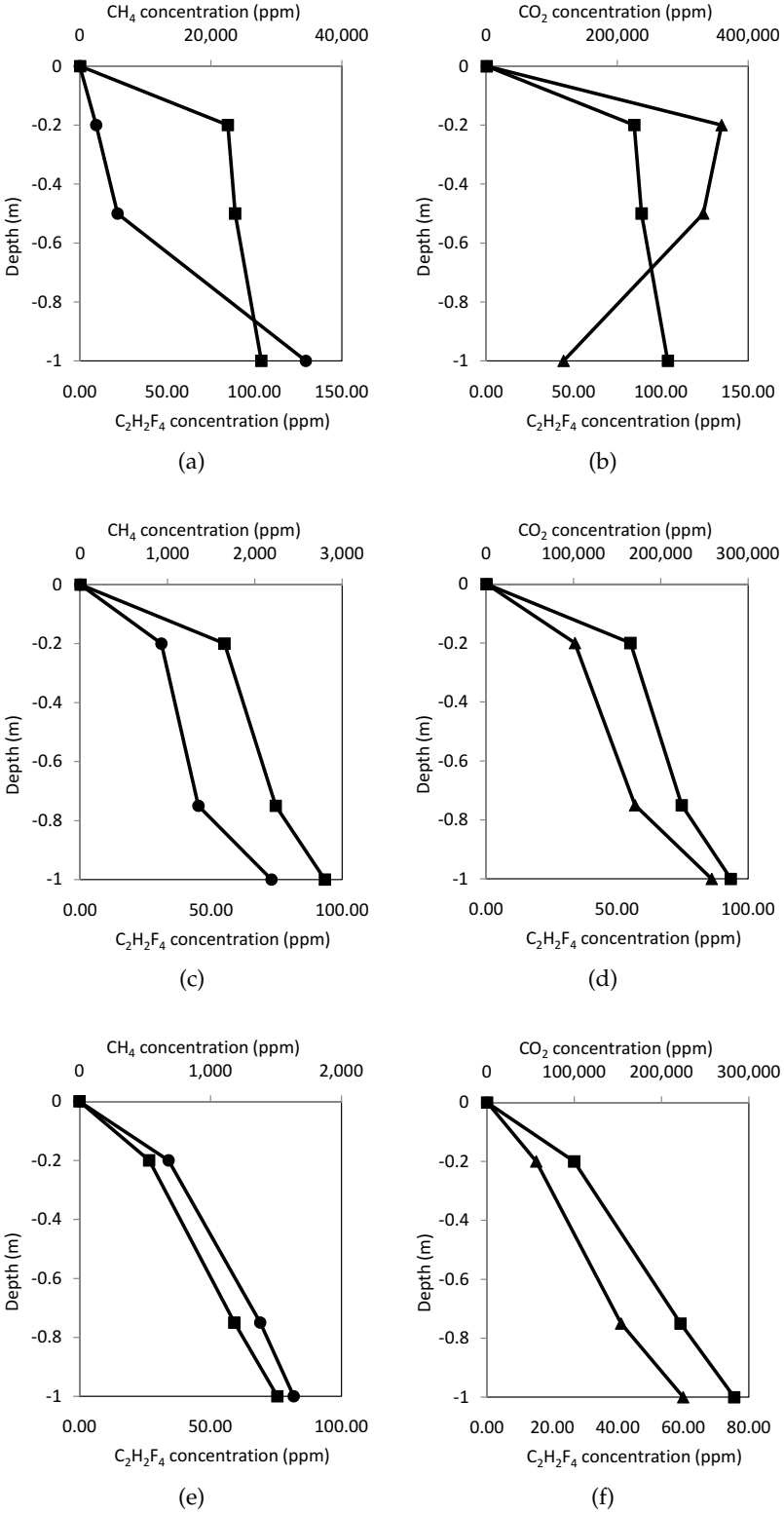

Figure 46: Representative gas profiles for methane (●), carbon dioxide (▲) and $C_2H_2F_4$ (■) measured in different points during December 8th campaign. Graphs a) and b) are referring to point S1, graphs c) and d) refer to point N10 and e) and f) to point N1. $C_2H_2F_4$ has been used as tracer gas. The spatial distribution of the sampled points can be observed in figure 24, paragraph 4.7.

These three behaviors represent the general behaviors observed in gas soil profiles in the biofilter. All the profiles measured in the South area of the biofilter (S1, S4, S5, S8, S10) correspond to the trend described by the first class and showed in graphs a) and b) in figure 44. In all these points an evident methanotrophic activity has been observed, considering the fluctuation of gas profiles. All the gas profiles measured in the Northern area (N1, N4, N8), except for N10, behave in the same way described by the third class and represented in graphs e) and f). In these points a low or non existent methane oxidation activity can be recognized. The second class, observed with point N10 and showed in graphs c) and d), describes a borderline behavior between the other two classes: a few methane oxidation just in the deepest part of the soil.

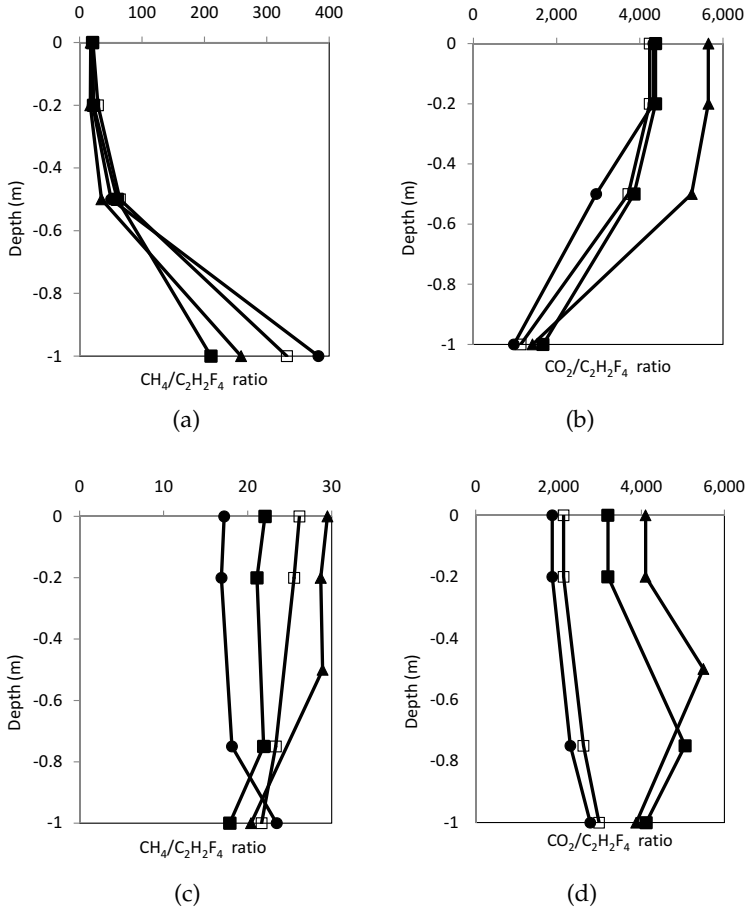

Figure 47: Profiles describing rates of the ratio between CH_4 or CO_2 concentrations and $C_2H_2F_4$ (used as tracer gas). Graph a) and b) are referred to Southern area, while c) and d) to Northern part. Concentrations were measured in different points during December 8th campaign, and refer to point S1-N1 (□), S4-N4 (▲), S8-N8 (■), S10-N10 (●).

All these conclusions can be supported analyzing graphs showed in figure 45. These graphs report the rate of the ratios between CH_4 and the tracer (and also between CO_2 and the tracer) for all the measured points.

Graphs a) and b) represent the concentration ratios in the Southern part of the biofilter. The $CH_4/C_2H_2F_4$ ratio is decreasing for all the points measured, with a steep decrease rate in the deeper part of the biofilter (between -1 m to 0.5 m). Equally, the $CO_2/C_2H_2F_4$ ratio is increasing throughout the biofilter depth, with a maximum rate in the deep soil. These considerations prove the presence of a consistent methanotrophic activity in the Southern area of the biofilter, which is localized between -1 m to -0.2 m.

Graphs c) and d) represent the concentration ratios in the Northern part of the biofilter. The $CH_4/C_2H_2F_4$ ratio is mainly constant or increasing for all the points throughout the biofilter depth, except for point N10 which shows an acceptable decrease between -1 m and -0.75 m. Also the $CO_2/C_2H_2F_4$ ratio shows a general constant or decreasing behavior for all the measured points. The only exceptions are N4 and N8, which show an increasing ratio in the deepest biofilter, but the real reason attributable to this fact is impossible to identify with certainty. Generally, the behavior of gas profiles for the North area of the biofilter demonstrates a low or inexistent methanotrophic activity, except in point N10.

5.1.5 *Surface flux chambers for total methane mass balance*

On January 25th a measurement campaign with the flux chamber method has been carried out to calculate fluxes of CH_4 and CO_2 from the biofilter. All the measured rates ($\partial C/\partial t$) had acceptable values of R^2.

The measured average R^2 for methane in both campaigns was 0.94, while for carbon dioxide was found to be 0.99. From theoretical backgrounds, it's known how to calculate surface fluxes using the flux chamber (see equation 2 in paragraph 3.3.1). Analyzing this equation it's evident that there is a linear correlation between the surface flux and the factor $\partial C/\partial t$, as all other variables are constant for the same measurement campaign (except the temperature which is slightly changing in time). In table 7 all the calculated gas rates are reported.

Methane rates are not homogeneously distributed on the biofilter surface, though the maximum rates from the Northern area and the Southern area of the biofilter are different.

Table 7: Calculated rates ($l \cdot m^{-3} \cdot s^{-1}$) for methane ($CH_4$) and carbon dioxide ($CO_2$). All the parameters have been measured with the static flux chamber method on January 25th, 2013. The spatial distribution of the sampled points can be observed in figure 26, paragraph 4.8.

Parameter	*Point*	*1*	*2*	*3*	*4*	*5*	*6*	*7*	*8*	*9*	10	*S-E corner*
$\partial C/\partial t$ *for* CH_4	*A*	n.a.	n.a.	0.000	n.a.	0 .000	n.a.	0.002	n.a.	0.001	n.a.	0.003
	B	0.003	0.000	0.004	0.003	0.004	0.012	0.004	0.002	0.008	0.000	0.005
	C	0.000	0.005	0.002	0.002	0.007	0.004	0.001	0.004	0.011	0.010	0.003
	D	0.002	0.009	0.003	0.011	0.002	0.007	0.004	0.005	0.006	0.007	0.003
	E	0.011	0.005	0.005	0.002	0.004	0.002	0.002	0.004	0.004	0.003	0.005
	F	0.004	0.004	0.005	0.000	0.002	0.001	0.003	0.002	0.000	0.000	0.002
$\partial C/\partial t$ *for* CO_2	*A*	n.a.	n.a.	4.19	n.a.	3.18	n.a.	3.69	n.a.	1.42	n.a.	8.17
	B	8.81	10.51	12.05	7.45	10.88	2.85	7.79	5.04	20.05	4.33	4.56
	C	2.81	6.38	6.99	9.70	28.98	4.02	7.32	2.37	16.79	12.94	2.99
	D	9.49	9.98	7.86	3.55	9.50	5.94	1.61	4.79	10.14	3.10	2.20
	E	2.79	3.55	5.66	5.73	3.37	1.16	4.21	1.82	3.27	1.48	1.88
	F	2.62	2.98	3.68	3.41	1.59	2.99	2.79	3.07	3.28	1.87	1.39

n.a. Data not available, as the analysis has not been carried out in that campaign for this point.

In the Northern area, rates range between 0 and 0.005 $l \cdot m^{-3} \cdot s^{-1}$, while in the Southern part they range between 0 and 0.012 $l \cdot m^{-3} \cdot s^{-1}$. The average rate is also different, as for North is about 0.003 $l \cdot m^{-3} \cdot s^{-1}$ and for South is 0.005 $l \cdot m^{-3} \cdot s^{-1}$.

Line A always shows low emission values, as it's placed on the Southern slope of the biofilter. Carbon dioxide rates strongly reflect the tendency of methane, with a net differentiation from South to North: the average emission rate in South is 8.9 $l \cdot m^{-3} \cdot s^{-1}$, considerably higher than the 2.9 $l \cdot m^{-3} \cdot s^{-1}$, average value for the Northern area.

Assuming that CO_2 is homogeneously generated in the biofilter by soil respiration, this difference in carbon dioxide emission has to be assigned to a differential methane oxidation greater in the South than in the North. Despite this considerably high CH_4 oxidation in the Southern area, the average emission of methane in the South part is equal or slightly greater than in the North part. From these last considerations it's evident that the CH_4 bottom flux and oxidation is higher in the Southern area than in the Northern area of the biofilter.

It's known that CH_4 emission and atmospheric pressure trend are strictly correlated (see chapter 4). For this reason, the atmospheric pressure has also been monitored during the measurement campaign and has been represented in figure 48. The monitoring procedure, started from the East side of the biofilter around 9 a.m., was concluded at 2 p.m. with the last measurements in the West part. From figure 48 is possible to underline how the atmospheric pressure has been constant from line 1 to line 8 (around 1018 hPa), with a sudden, but not really important, decrease in the last testing hour (from 1 p.m to 2 p.m.). In this last hour, line 9 and 10 was tested and CH_4 fluxes greater than the average was detected (see table 7). These greater fluxes in the Western area may have been influenced from the atmospheric pressure drop, resulting in a higher methane emission.

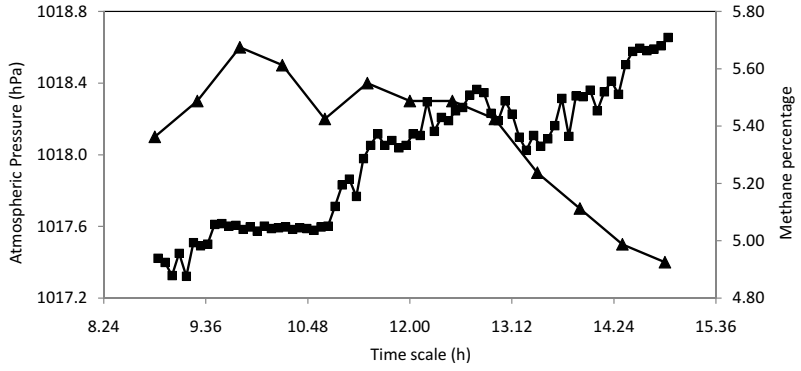

Figure 48: Measured methane percentage (■) in the inflowing LFG and atmospheric pressure trend (▲), during January 25th campaign.

5.2 RESULTS INTERPRETATION

5.2.1 *Carbon Mass Balance results*

Data from the flux chamber campaigns were elaborated and used to calculated superficial fluxes for all the measured gases. Equation (2) has been adopted, with a flux chamber volume of 0.015 m^3, a flux chamber area of 0.075 m^2, atmospheric pressure and temperatures measured during flux chamber campaigns. Using the theoretical method of carbon mass balance, described in paragraph 3.3.1, is also possible to calculate the theoretical flux of methane on the bottom of the biofilter. Carbon dioxide fluxes have been calculated using data from Vaisala CARBOCAP® and from Innova 1412i. These two fluxes, a maximum (usually the flux calculated with Innova 1412i) and a minimum (usually calculated with Vaisala CARBOCAP®) flux for every point, were then used to calculate a minimum and maximum methane flux from the bottom biofilter, and a minimum and maximum oxidation efficiency. All calculated surface and bottom fluxes from the measurement campaigns for all the analyzed points, are summarized in table 10.

In the end, it's possible to obtain the methane oxidation efficiency of the biofilter for the single spot, which can give an idea of the oxidation rate in this area of the biofilter. In table 8, the calculated methane oxidation efficiencies Methane Oxidation (MO) for the first measurement campaign have been reported. Oxidation efficiencies have been calculated, for the Southern part of the biofilter, to be between 84% (in the farthest point to LFG inlet) and 99%. Equally, methane oxidation efficiencies for the Norther area have been calculated. For this area, all the MO efficiencies ensue to be higher of 100%, as a consequence of negative surface fluxes measured.

Table 8: Surface fluxes, bottom fluxes and methane oxidation efficiencies from November 18th campaign, calculated with Carbon Mass Balance Approach. The spatial distribution of the sampled points can be observed in figure 23, paragraph 4.7.

	$J_{CH_4,surface}$ $(mol \cdot m^{-2} \cdot d^{-1})$	$J_{CH_4,bottom,max}$ $(mol \cdot m^{-2} \cdot d^{-1})$	$J_{CH_4,bottom,min}$ $(mol \cdot m^{-2} \cdot d^{-1})$	MO_{max} %	MO_{min} %
S1	0.09	0.79	0.61	87.7	84.2
S5	0.01	0.68	0.58	97.9	97.5
S10	0.02	2.02	1.71	98.7	98.5
N1	-0.0007	0.005	0.003	121.2	114.3
N10	-0.003	0.013	0.012	130.5	128.1

MO : Methane oxidation efficiency, expressed in percentage of methane oxidized on the total methane injected in the biofilter.

Two possible explanation can be attributed to this event. The first explanation is that a methanotrophic community is acting in this area and, due to the low presence of CH_4 in the biofilter, bacteria seize methane from the atmosphere creating a negative flux. The second reliable explanation is that the quantity of gas sampled every minute from the flux chamber is too much compared to the small quantity of CH_4 emitted from the biofilter surface in this area.

In table 9, fluxes and methane oxidation efficiencies are reported for the second measurement campaign. In this campaign no negative fluxes were recorded. However, it is possible to observe the difference between fluxes (surface and bottom) measured and calculated in the Southern and Northern part of the biofilter. Methane fluxes in the South area are one order of magnitude greater than those calculated in the Norther area, proving the difference between Southern and Northern emissions. Calculated MO efficiencies in the South area are between 93% and 96%, more or less in the same range found in the previous campaign. Regarding the Northern area, only point N1 (near to LFG inlet) shows an acceptable oxidation efficiency (between 65 and 80%), while all the other spots show negative percentage values. The presence of these negative values derives from a calculated bottom flux of CH_4, which is lower than the methane surface flux. This happens when, observing equation (3), the concentration of CH_4 measured in the bottom biofilter is too low related to CO_2 concentration in the same place. Also in this case, as in the previous campaign, the problem is strictly related to the low concentration of CH_4 in the Norther area of the biofilter.

Table 9: Surface fluxes, bottom fluxes and methane oxidation efficiencies from December 8th campaign, calculated with Carbon Mass Balance Approach. The spatial distribution of the sampled points can be observed in figure 24, paragraph 4.7.

	$J_{CH_4,surface}$ $(mol \cdot m^{-2} \cdot d^{-1})$	$J_{CH_4,bottom,max}$ $(mol \cdot m^{-2} \cdot d^{-1})$	$J_{CH_4,bottom,min}$ $(mol \cdot m^{-2} \cdot d^{-1})$	MO_{max} %	MO_{min} %
S1	0.10	1.81	1.53	94.4	93.4
S4	0.04	0.70	0.64	93.4	92.8
S8	0.05	0.59	0.53	91.1	90.1
S10	0.05	1.52	1.30	96.2	95.5
N1	0.002	0.011	0.006	80.5	65.4
N4	0.016	0.012	0.010	-29.2	-55.3
N8	0.015	0.011	0.008	-35.5	-76.5
N10	0.017	0.014	0.007	-18.1	-126.8

MO : Methane oxidation efficiency, expressed in percentage of methane oxidized on the total methane injected in the biofilter.

5.2.2 *Tracer Mass Balance results*

The Tracer Mass balance approach has been also adopted to calculate the theoretical methane oxidation efficiency of the biofilter in different spots. Knowing the inlet flux of tracer gas and CH_4, and measuring the biofilter surface flux of these two compounds, it's possible to calculate the methane oxidation with the method described in paragraph 3.3.2. The results of the tracer mass balance approach are summarized in table 11.

Methane oxidation, calculated for all the points, has an average efficiency of 98%, with only one point (S1) who shows an oxidation efficiency of 92%. Oxidation performances are greater than 100% in the Northern area (as calculated in the first measurement campaign) due to negative surface fluxes of methane. Those fluxes, reported also in table 8, are probably altering the final results. It's anyway possible to assign a proper oxidation efficiency also to the Northern area, considering results from the second monitoring campaign (December 8th, 2012).

Table 11: Molar flux ratios (-) and methane oxidation efficiencies (%), at different spots, calculated with the Tracer Mass Balance Approach. The spatial distribution of the sampled points can be observed in figures 23, 24, paragraph 4.7.

	$J_{CH_4}/J_{C_2H_2F_4,inlet}$		$J_{CH_4}/J_{C_2H_2F_4,surface}$		MO_{tracer}	
	18-Nov-12	08-Dec-12	18-Nov-12	08-Dec-12	18-Nov-12	08-Dec-12
S1	476.5	1,349.8	39.6	17.1	91.6	98.7
S4	n.a.	1,349.8	n.a.	16.6	n.a.	98.7
S5	476.5	n.a.	7.4	n.a.	98.4	n.a.
S8	n.a.	1,349.8	n.a.	15.1	n.a.	98.8
S10	476.5	1,349.8	10.8	17.9	97.7	98.6
N1	476.5	1,349.8	-2.1	17.9	100.4	98.6
N4	n.a.	1,349.8	n.a.	28.4	n.a.	97.9
N8	n.a.	1,349.8	n.a.	20.8	n.a.	98.4
N10	476.5	1,349.8	-15.1	17.1	103.1	98.7

n.a. Data not available, as the analysis has not been carried out in that campaign for this point.

Table 10: Surface and bottom fluxes calculated with the Carbon Mass Balance Approach. Calculations have been carried out for all the available points and all the sampled gases, analyzed during two different monitoring campaigns (November 18th and December 8th). The spatial distribution of the sampled points can be observed in figures 23, 24, paragraph 4.7.

Parameter	*Unit*	*Testing day*	*S1*	*S4*	*S5*	*S8*	*S10*	*N1*	*N4*	*N8*	*N10*
$J_{CH_4,surface}$	$(g \cdot m^{-2} \cdot d^{-1})$	18-Nov-12	1.54	n.a.	0.22	n.a.	0.39	-0.01	n.a.	n.a.	-0.05
		08-Dec-12	1.60	0.73	n.a.	0.85	0.92	0.03	0.25	0.24	0.27
$J_{CO_2,surface,max}$	$(g \cdot m^{-2} \cdot d^{-1})$	18-Nov-12	171.46	n.a.	222.77	n.a.	263.96	23.71	n.a.	n.a.	22.98
		08-Dec-12	347.77	198.30	n.a.	232.55	235.50	72.30	104.40	114.81	74.18
$J_{CO_2,surface,min}$	$(g \cdot m^{-2} \cdot d^{-1})$	18-Nov-12	132.47	n.a.	188.83	n.a.	222.67	16.03	n.a.	n.a.	24.99
		08-Dec-12	294.55	181.35	n.a.	209.16	199.87	40.73	86.78	87.97	38.27
$J_{C_2H_2F_4,surface}$	$(g \cdot m^{-2} \cdot d^{-1})$	18-Nov-12	0.24	n.a.	0.19	n.a.	0.23	0.03	n.a.	n.a.	0.02
		08-Dec-12	0.59	0.28	n.a.	0.35	0.32	0.01	0.06	0.07	0.10
$J_{CH_4,surface}$	$(mol \cdot m^{-2} \cdot d^{-1})$	18-Nov-12	0.09	n.a.	0.01	n.a.	0.02	-0.0007	n.a.	n.a.	-0.003
		08-Dec-12	0.10	0.04	n.a.	0.05	0.05	0.002	0.016	0.015	0.017
$J_{CO_2,surface,max}$	$(mol \cdot m^{-2} \cdot d^{-1})$	18-Nov-12	3.89	n.a.	5.06	n.a.	5.99	0.53	n.a.	n.a.	0.52
		08-Dec-12	7.90	4.50	n.a.	5.28	5.35	1.64	2.37	2.60	1.68
$J_{CO_2,surface,min}$	$(mol \cdot m^{-2} \cdot d^{-1})$	18-Nov-12	3.01	n.a.	4.29	n.a.	5.06	0.36	n.a.	n.a.	0.56
		08-Dec-12	6.69	4.12	n.a.	4.75	4.54	0.92	1.97	1.99	0.86
$J_{C_2H_2F_4,surface}$	$(mol \cdot m^{-2} \cdot d^{-1})$	18-Nov-12	0.002	n.a.	0.001	n.a.	0.002	0.0003	n.a.	n.a.	0.0002
		08-Dec-12	0.005	0.003	n.a.	0.003	0.003	0.0002	0.0006	0.0007	0.0009
$J_{CH_4,bottom,max}$	$(mol \cdot m^{-2} \cdot d^{-1})$	18-Nov-12	0.79	n.a.	0.68	n.a.	2.02	0.005	n.a.	n.a.	0.013
		08-Dec-12	1.81	0.70	n.a.	0.59	1.52	0.011	0.012	0.011	0.014
$J_{CH_4,bottom,min}$	$(mol \cdot m^{-2} \cdot d^{-1})$	18-Nov-12	0.61	n.a.	0.58	n.a.	1.71	0.003	n.a.	n.a.	0.012
		08-Dec-12	1.53	0.64	n.a.	0.53	1.30	0.006	0.010	0.008	0.007

n.a. Data not available, as the analysis has not been carried out in that campaign for this point.

5.2.3 *Biofilter's total emission and efficiency*

CH_4 and CO_2 fluxes from 60 points homogeneously distributed on the biofilter surface have been calculated. A summary of calculated fluxes for these two gases is presented in table 13. Graphs in figure 49 represent the spatial distribution of methane and carbon dioxide fluxes, obtained using Kriging interpolation.

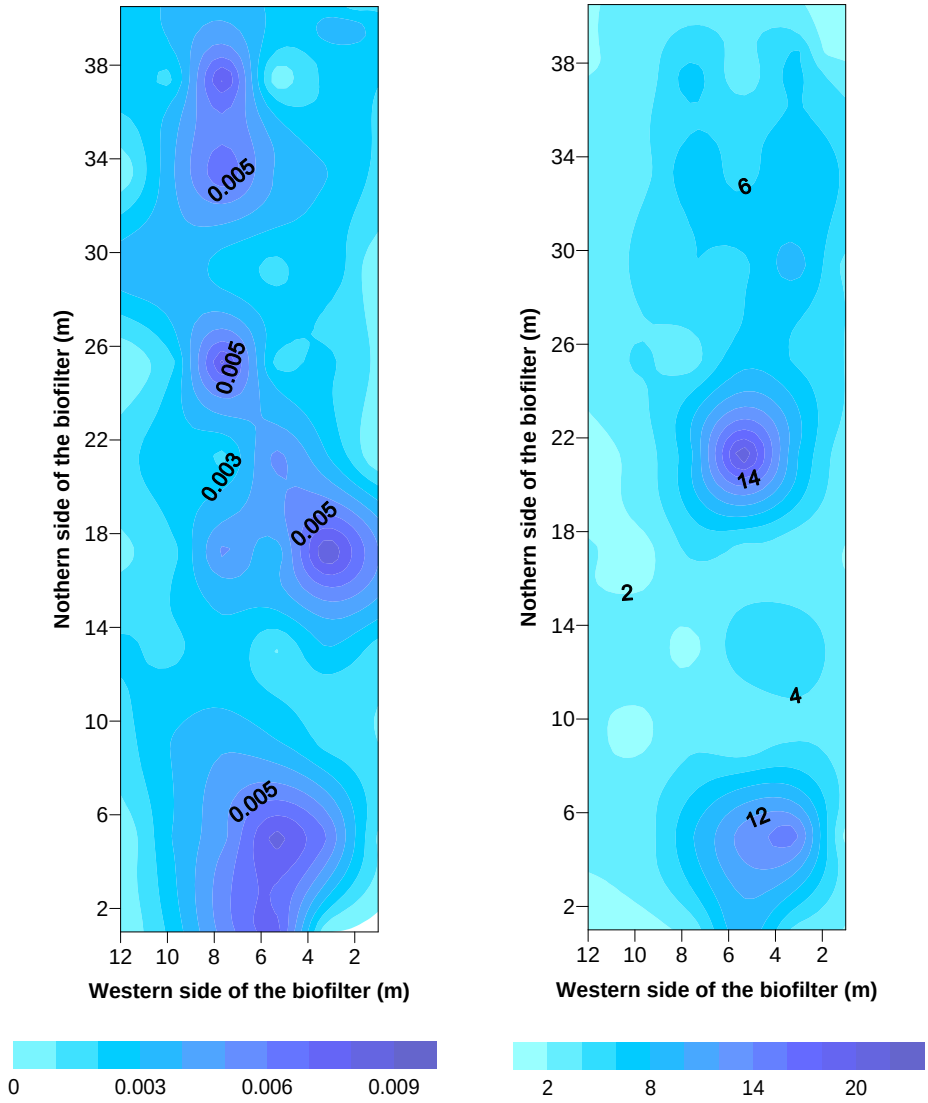

Figure 49: The surface spatial distribution of methane (graph on the left) and carbon dioxide (graph on the right) fluxes is represented, with fluxes expressed in $mol \cdot m^{-2} \cdot d^{-1}$. Data were collected on January 25th campaign, using the static flux chamber method. The LFG inlet pipe and mixing chamber are placed on the right of the graphs and in the center of the biofilter (around at 21 meters).

The distribution of methane emissions doesn't appear to be homogeneous, though higher emissions localized at the biofilter western and Eastern extremities and 4 meters from the biofilter center have

been observed (in the graph at 21 meters circa). Carbon dioxide distribution is represented in the second graph. Observing CO_2 spatial distribution, it's clear how carbon dioxide has a greater emission in the Southern part of the biofilter than in the Northern, with two peaks in the center and in the Western area. The presence of a consistent CH_4 oxidation activity is proved by the distribution of these two gases in the Southern part of the biofilter.

In the Eastern part (from 40 m to 26 m) methane emission from the biofilter is almost homogeneous. Greater emissions of CO_2 have been measured in the Southern area, which underline the greater methane oxidation activity. In the central part (from 26 m to 14 m) methane emission shows two peaks with a decrease in correspondence to the biofilter inlet. At the same time, a peak CO_2 emission in the South area proves a relevant methane oxidation activity. In the Western part (from 14 m to 2 m) a low methane emission in the South part is correlated with a relevant CO_2 emission (4 $mol \cdot m^{-2} \cdot d^{-1}$). At the Western extremity, a high emission area of CH_4 in the Southern part, in correspondence to a great emission of CO_2 , also prove the presence of a substantial methanotrophic activity. This greater flux area detected in the Western side of the biofilter, could have been created by the atmospheric pressure drop occurred during the sampling of this sector (as showed in paragraph 5.1.5).

The final aim of this analysis was also to assess the biofilter total oxidation performance and efficiency in order to prove the reliability of this technology. For this purpose, a molar balance of CH_4 and CO_2 in the inlet and in the outlet needs to be carried out. Using Surfer 8, the spatial distribution of gas fluxes has been used to calculate the area with different emission values. For CO_2 , 22 areas have been calculated, related to 22 different molar fluxes. The same was done for CH_4, with 9 emission areas calculated. The correlated flux, in $mol \cdot m^{-2} \cdot d^{-1}$, was then multiplied with the emission area and the daily molar flux calculated. In the end, from the total summation of all the daily fluxes, the whole biofilter emission was found. The inlet fluxes has been calculated by multiply the gas concentration in the inlet and the measured daily flux of LFG.

Table 12: Methane oxidation efficiency and performance of AV Miljø biofilter, measured on January 25th, 2013.

	J_{inlet} ($mol \cdot d^{-1}$)	$J_{surface}$ ($mol \cdot d^{-1}$)	$MO_{efficiency}$ %	$MO_{performance}$ ($g \cdot m^{-2} \cdot d^{-1}$)
CH_4	577.5	1.6	99.7	18.3
CO_2	510.1	2,083.9	-	-

Table 13: Calculated surface fluxes ($mol \cdot m^{-2} \cdot d^{-1}$) for methane ($CH_4$) and carbon dioxide ($CO_2$) based on measurements carried on January 25th, 2013. The spatial distribution of sampled points can be observed in figure 26, paragraph 4.8.

Parameter	*Point*	*1*	*2*	*3*	*4*	*5*	*6*	*7*	*8*	*9*	*10*	*S-E corner*
$J_{surface}$ *for* CH_4	*A*	n.a.	n.a.	0.000	n.a.	0.000	n.a.	0.0015	n.a.	0.0007	n.a.	0.0023
	B	0.0023	0.0030	0.0030	0.0023	0.0030	0.0092	0.0030	0.0015	0.0061	0.000	0.0038
	C	0.000	0.0038	0.0015	0.0015	0.0053	0.0030	0.0007	0.0030	0.0084	0.0077	0.0023
	D	0.0084	0.0069	0.0023	0.0084	0.0015	0.0053	0.0030	0.0038	0.0046	0.0053	0.0023
	E	0.0015	0.0038	0.0038	0.0015	0.0030	0.0015	0.0015	0.0030	0.0030	0.0023	0.0038
	F	0.0030	0.000	0.0038	0.000	0.0015	0.0007	0.0023	0.0015	0.000	0.000	0.0015
$J_{surface}$ *for* CO_2	*A*	n.a.	n.a.	3.231	n.a.	2.452	n.a.	2.846	n.a.	1.095	n.a.	6.301
	B	6.795	8.106	9.294	5.746	8.392	2.198	6.008	3.887	15.465	3.339	3.517
	C	2.167	4.921	5.391	7.482	22.353	3.100	5.646	1.828	12.950	9.981	2.306
	D	7.320	7.698	6.062	2.738	7.327	4.581	1.241	3.694	7.821	2.391	1.696
	E	2.152	2.738	4.365	4.419	2.599	0.894	3.247	1.403	2.522	1.141	1.450
	F	2.020	2.298	2.838	2.630	1.226	2.306	2.152	2.368	2.530	1.442	1.072

n.a. Data not available, as the analysis has not been carried out in that campaign for this point.

The calculated efficiency of the biofilter (99.7 % of methane oxidized) shows the effectiveness of the pilot plant installed at AV Miljø landfill. This result is also supported by the high carbon dioxide emission (2,080 $mol \cdot d^{-1}$), compared to the inlet flux (510 $mol \cdot d^{-1}$). CO_2 is probably produced from bacteria respiration and from methanotrophic activity inside the biofilter.

To calculate the quantity of carbon dioxide produced by bacteria respiration, data from laboratory experiences carried out at DTU by Master Student Jan De Schoenmaeker have been used. These data, reported in another Master Thesis, define the respiration rate of the compost used as substrate at AV Miljø biofilter. The results obtained, expressed in $\mu gCO_2 \cdot gDM^{-1} \cdot h^{-1}$, have been associated with soil temperatures measured during the monitoring campaign carried out on January 25th. Compost bulk density of the soil was reasonably assumed to be 505 $kgDM \cdot m^{-3}$ (Pedersen et al., 2011). Data and results are reported in table 14.

Table 14: Respiration rates and generated Carbon Dioxide for every compost layer. Respiration rates have been calculated by Master Student Jan De Schoenmaeker while temperatures have been measured on January 25th, 2013.

Soil depth	Temperature (°C)	Respiration Rate ($\mu gCO_2 \cdot gDM^{-1} \cdot h^{-1}$)	CO_2 generated ($gCO_2 \cdot d^{-1}$)	CO_2 generated ($molCO_2 \cdot d^{-1}$)
0 m - 0.2 m	6	5	6,060	137.7
0.2 m - 0.4 m	15	6	5,817	132.2
0.4 m - 0.6 m	27	5	4,848	110.2
0.6 m - 0.8 m	35	16	15,513	352.6
0.8 m - 0.95 m	40	25	18,180	413.2

The total calculated respiration from AV Miljø biofilter is 1145 $molCO_2 \cdot d^{-1}$.

6 DISCUSSION

6.1 METHANE OXIDATION LAYER DISPLACEMENT

Temperatures have been monitored at AV Miljø biofilter at different depths (-0.2 m, -0.5 m, -0,9 m) and the temperature trend in time of the biofilter is represented in figure 50. Generally, the seasonal variation of the outdoor temperature affects the underground soil temperature, with decreasing magnitude as the soil goes deep. Regarding AV Miljø biofilter, outdoor temperature variation can influence the shallowest zone of the biofilter as well as the deepest zone. The shallowest zone is directly affected by heat exchange with the atmospheric temperature, while the deepest zone is affected by LFG temperature. LFG is collected in boxes placed on the top of the leachate wells and then pumped at the bottom of the biofilter. During the storing time in these boxes, a thermal exchange with the outdoor air occurs, cooling LFG and the deepest layer of the biofilter. This phenomenon has also been reported in Dever et al. (2011). The most stable layer of the biofilter is between -0.4 m and -0.6 m, as illustrated in figure 50.

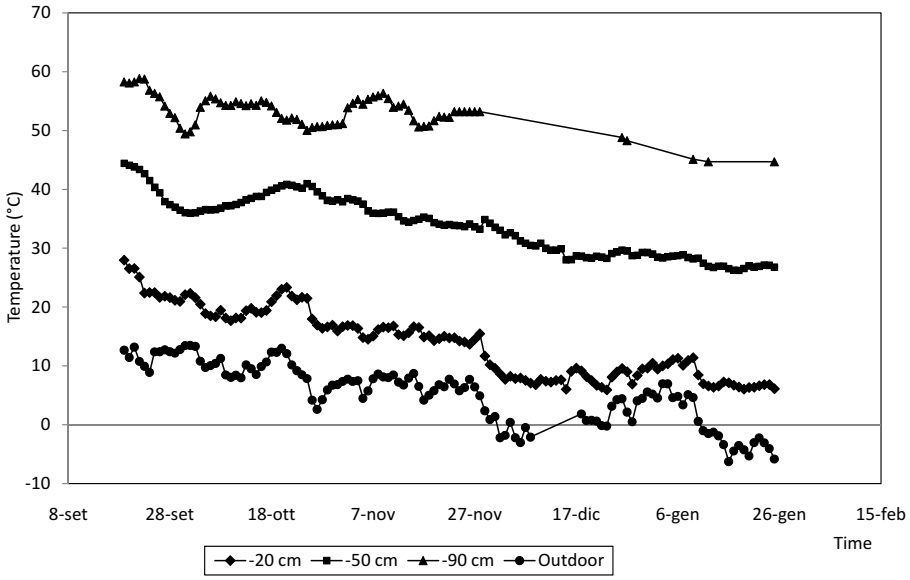

Figure 50: Temperature trends in time at different depths in the biofilter compost substrate. Temperature data have been monitored continuously during the whole period between September 2012 and January 2013.

From theoretical backgrounds, it's known that the optimal temperature for bacteria growth is between 25°C and 40°C. During the two flux chamber campaigns carried out on November 18th and December 8th, biofilter's temperature has been monitored and profiles are reported in figure 51. The optimal depth for methanotrophic bacteria activity, was found to be different from one campaign to the other. During the first campaign, the optimal temperature range was recorded between -30 cm and -60 cm, while in the second campaign was found between -50 cm and -70 cm. This shifting of the optimal methane oxidation layer is due to the cooling of the atmospheric air, which affects the biofilter temperature.

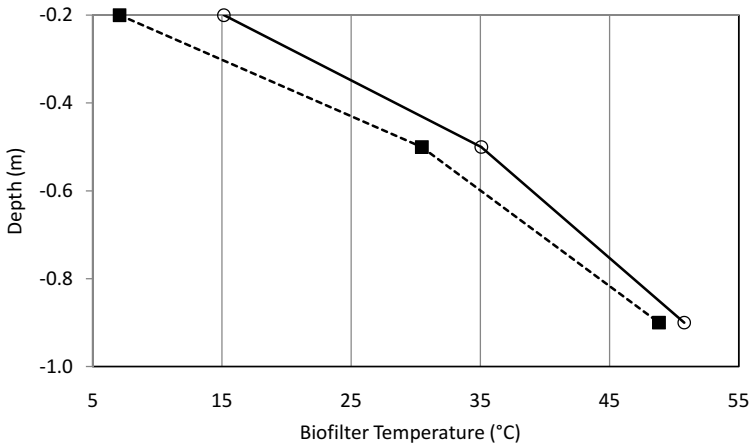

Figure 51: Temperature trend in the biofilter substrate at different depths. Profiles represent the temperature behavior during the two flux chamber campaigns, carried out on November 18th (◯) and on December 8th (■).

With the cooling of the superficial layer of the biofilter, the optimal conditions for bacteria growth change and the methane oxidation efficiency decreases (Roncato and Cabral, 2012). It's reasonable to assume that the active methanotrophic layer shifts deep in the soil, were the optimal conditions for bacteria growth are provided. There are several studies which report that, during the cold season, the methane oxidation of the biofilter drops suddenly and reaches also 0% of oxidation efficiency (Stern et al., 2007). This is probably attributed to the deep displacement of the methane oxidation layer, at depths in which the atmospheric oxygen is not able to penetrate. If the methanotrophic layer shifts at depths deeper than -50 cm, bacteria have an optimal temperature environment but they don't have enough oxygen to transform CH_4 in CO_2. This fact leads to the nullification of methane oxidation activity.

A relevant difference needs to be highlighted between most of the previous studies and AV Miljø biofilter pilot plant. In most of the previous studies, O_2 was supplied to the biofilter only through the diffusion of the atmospheric air via the biofilter substrate. AV Miljø biofilter, receives LFG mixed with atmospheric air directly to the biofilter bottom; this supply, with the support of the atmospheric air diffusion from biofilter's surface, ensures a proper oxygen supply to the biofilter. The main effect of this technical characteristic is that, in case of methanotrophic layer displacement, bacteria are always supplied by a constant flux of oxygen at every depth, as showed in figures 38 and 40. The shifting of the methanotrophic active layer has been proved during the two measurement campaigns of November 18th and December 8th, as reported in figure 52.

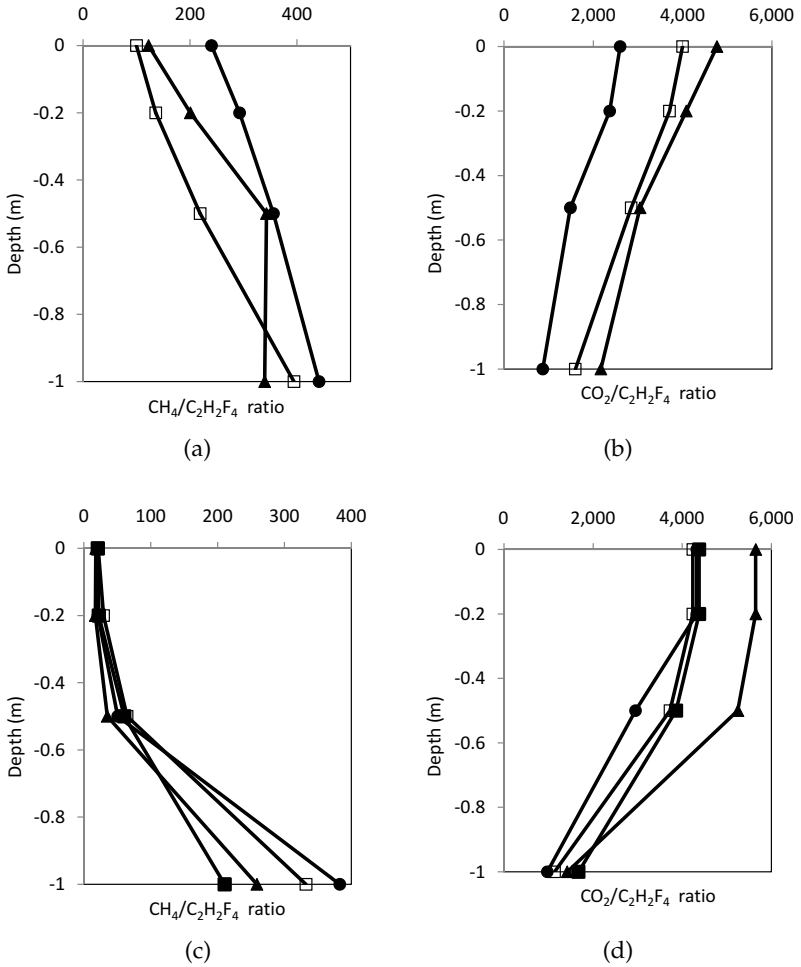

Figure 52: Profiles describing rates of the ratio between CH_4 or CO_2 concentrations and $C_2H_2F_4$ (used as tracer gas). Concentrations were measured in different points during November 18th (a and b) and December 8th (c and d) campaigns, and refer to points S1 (□), S5 (▲), S8 (■) and S10 (●). The spatial distribution of the sampled points can be observed in figure 23, 24, paragraph 4.7.

Due to the equal distribution of O_2 at every depth, methanotrophic oxidation was always found to be active. However, observing figure 52, it's evident how CH_4 oxidation has been localized at different depths from one measurement to the other. In the first campaign (graphs a and b, figure 52), methane oxidation was evenly distributed in the whole biofilter depth, sometimes with almost 0% oxidation in the deepest layer (spot S5 between -50 cm and -90 cm). In the second measurement campaigns (graphs c and d, figure 52), due to the temperature drop inside the biofilter, methanotrophic activity was mainly localized in the layer between -50 cm and -90 cm. This last layer, as previously explained, was characterized by the presence of the optimal temperature for CH_4 oxidation activity.

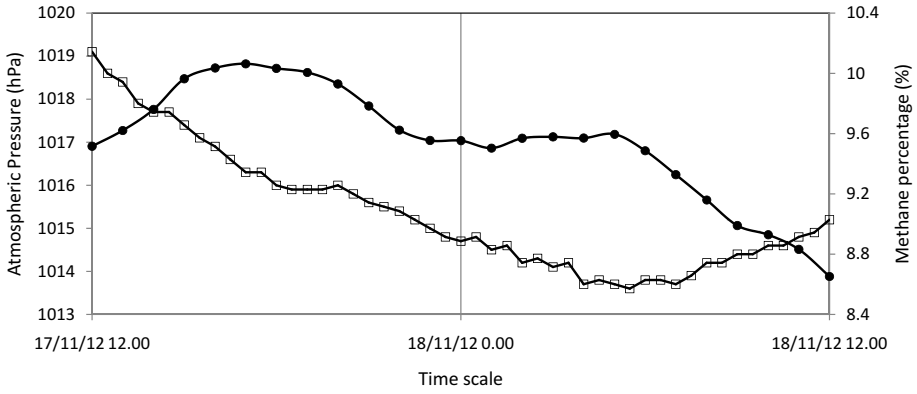

(a)

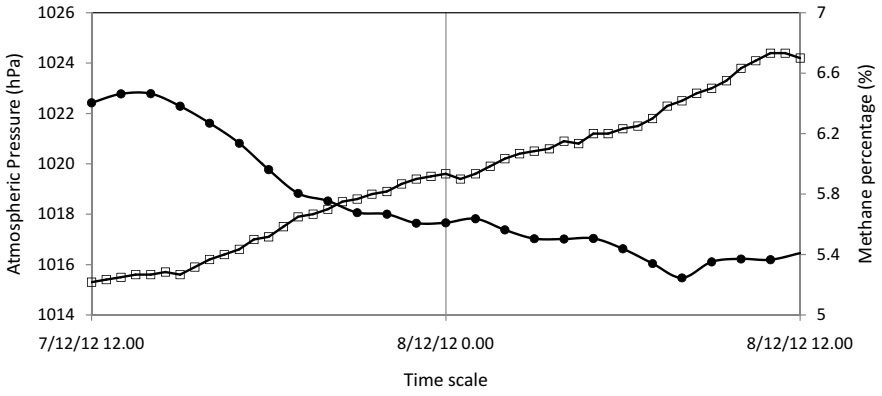

(b)

Figure 53: Methane measured in the biofilter inlet (•) and atmospheric pressure (□) trends, during the two flux chamber campaigns carried out on November 18th (a) and December 8th (b). Atmospheric pressure is expressed in hPa, while injected methane in percentage concentration.

Probably, the deepening of the optimal temperature layer, is not the only reason of the different conformation observed in figure 52. The different atmospheric pressure trend is also involved in this phenomenon. In figure 53, it's possible to observe the atmospheric pressure trend registered during the two campaigns and the CH_4 concentration in the inflow LFG. From theory, it's known that a decreasing atmospheric pressure trend can promote CH_4 emission and, conversely, an increasing pressure trend can reduce CH_4 flux from the soil. During the first campaign (November 18th in graph a, figure 53) atmospheric pressure showed a decreasing trend, allowing methane to diffuse in the biofilter volume. Contrary to that, in the second measurement campaign atmospheric pressure confined CH_4 in the deepest layer of the biofilter due to its increasing trend.

There are no certain evidence that these two factors (temperature and atmospheric pressure mutation) really influenced the conformation of methane distribution and of the methanotrophic active layer in the biofilter. Despite this uncertainty, derived from the few measurement campaigns carried out during this project, this analysis seems to provide a reliable explanation to all the behaviors observed at AV Miljø biofilter.

In any case, the special design of the biofilter, which provides the injection of LFG mixed with atmospheric air, endows this pilot plant of a remarkable versatility. This feature allows the biofilter to react to external factors (temperature and pressure changes) and restore the optimal setting to achieve always a maximum CH_4 oxidation performance.

6.2 CARBON AND TRACER MASS BALANCE RELIABILITY

The biofilter CH_4 oxidation efficiency has been tested with two different approaches, the Carbon Mass Balance (paragraph 3.3.1) and the Tracer Mass Balance (paragraph 3.3.2). The difference between these two methods deals mainly about three issues: the used methodology, results and applicability. Concerning the first point, methodology, the two approaches require both similar and different measurements. The common measurement which needs to be carried out is the CH_4 and CO_2 surface flux, used for the Carbon Approach in equation (8) and for Tracer Approach in equation (9).

$$a)\ J_{CH_4,in} = (J_{CO_2,out} + J_{CH_4,out}) \cdot \frac{C_{CH_4,in}}{C_{CH_4,in} + C_{CO_2,in}} \tag{8}$$

$$b)\ MO = \frac{\left(J_{CH_4}/J_{C_2H_2F_4}\right)_{inlet} - \left(J_{CH_4}/J_{C_2H_2F_4}\right)_{surface}}{\left(J_{CH_4}/J_{C_2H_2F_4}\right)_{inlet}} \tag{9}$$

Equally, different parameters also need to be measured in order for these approaches to be applied: for the Carbon based approach, the determination of the inflow concentration of methane and carbon dioxide is fundamental. Contrarily, to apply the tracer based approach, the measurement of the inflow flux of these two gases is basic. The field application of these methods will be afterwards described in the applicability paragraph. In any case, it's easily understandable that oxidation efficiencies obtained using the tracer method, are more reliable than results obtained with the Carbon based approach. In fact, the Tracer approach is simply based on field measurements and all the parameters involved in the CH_4 oxidation efficiency calculation are obtained on the field. Contrarily, the Carbon based approach relies on the calculation of the inflow flux through equation 8. The application of this equation, considering also the approximation that CO_2 production from bacteria respiration is negligible, certainly adds an uncertainty factor compared to the Tracer Mass Balance. To sum up, from a methodology point of view the Tracer Mass Balance Approach is definitely more reliable than Carbon Mass Balance.

Regarding the second point, which is the results, the Tracer approach appears to be more accurate than the Carbon one. In figure 54, CH_4 oxidation efficiencies calculated with the two methods are presented for field measurements carried out on December 8th. Graph a) presents measurements done in the Southern area of the biofilter, in which high fluxes (0.01-0.1 $mol \cdot m^{-2} \cdot d^{-1}$) have been recorded. In this graph it's possible to highlight how the difference between results obtained with the two methods is not very significant. An interesting difference between these two approaches can be observed when lower fluxes (0.001-0.01 $mol \cdot m^{-2} \cdot d^{-1}$) of methane are detected, as in the Northern part of the biofilter. Graph b) in figure 54 describes this comparison. CH_4 oxidation efficiencies obtained with the Tracer Mass Balance (represented in black) show a high efficiency rate, as for the Southern area. On the contrary, the oxidation efficiencies calculated with the Carbon Mass Balance show low or negative percentage values. The main cause of this negative efficiencies, as explained in paragraph 5.2.1, derives from the calculation of methane bottom flux with equation 8. In fact, when the CH_4 bottom concentration value was very low, the concentrations ratio expressed in equation 8 turns out to be several orders of magnitude lower than 1. This is also due to the assumption that no CO_2 is produced in soil respiration activities. Then the final value of methane bottom flux is lower than the surface flux, producing the paradox of negative methane oxidation efficiencies. Moreover concerning results, it's evident how efficiencies obtained with the Tracer Mass Balance Approach are more reliable than results obtained with the Carbon Mass Balance Approach, especially in presence of low methane concentrations and fluxes.

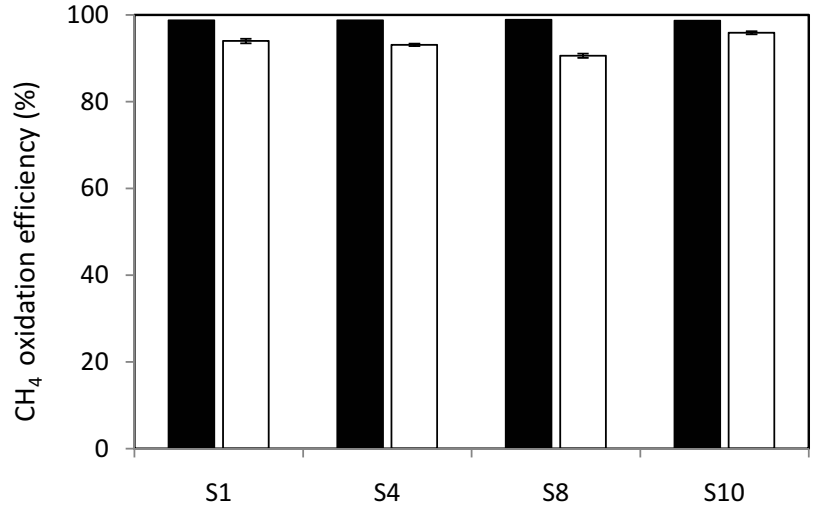

(a)

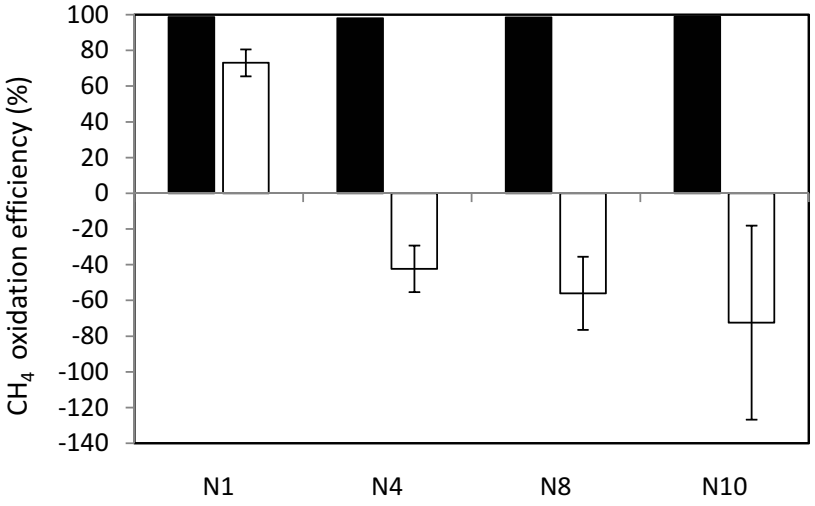

(b)

Figure 54: Methane oxidation efficiencies from field measurements carried out on December 8th, 2012. Efficiencies have been calculated with two different approaches, the Tracer Mass Balance (■) and the Carbon Mass Balance (□). The spatial distribution of the sampled points (graph a) for South and graph b for North can be observed in figure 24, paragraph 4.7.

The last discussion point is related to the applicability of these two approaches. The Carbon approach is based on the measurement of methane and carbon dioxide concentrations at the bottom of the active oxidation layer, while the Tracer approach is based on the measurement of bottom fluxes. This is probably the main applicability difference between the two methods and the main reason of the different use. The Carbon based method can simply be used in measurement

campaigns carried out on biofilters and biocovers, as in both types of plant is possible to implement technologies to measure the bottom concentrations of CH_4 and CO_2. On the other hand, the Tracer based approach shows greater issues in the field application. The main problem is related with the calculation of methane, carbon dioxide and tracer bottom fluxes. In fact, while for biofilters it's possible to sample LFG in the inlet pipe (as done in this study), for biocovers the practical measurement of these parameters represents a complicated issue. The injection of tracer gas on the bottom of the methane oxidation layer can be done only with biofilters, as it's not feasible to obtain a constant flux and homogeneous distribution of tracer gas through the biocover body. Additional disadvantages of the Tracer Mass Balance approach are the purchasing of the tracer gas (which is generally expensive) and the frequent use of greenhouse gases (GHG) as tracers.

6.3 BIOFILTER EFFICIENCY IN NORTHERN AND SOUTHERN AREA

Results obtained from all measurement campaigns carried out at AV Miljø biofilter, suggest the substantial presence of a methanotrophic active community. In particular, gas concentrations and methane oxidation activity show a different configuration from the Southern part of the biofilter to the Northern. There are several evidence of this fact.

The first evidence is related to the MLPGS (Multi Level Probes for Gas Sampling) profiles of CH_4, CO_2 and O_2 presented in paragraph 5.1.1. The standard configuration of these gases in the biofilter is showed in figure 55, from monitoring activities performed on November 14th, 2012. LFG percentage concentrations have been measured also in the biofilter inlet on November 14th. Methane concentration was recorded to be 6.8 %, Carbon Dioxide 7.3 % and Oxygen concentration 10%. Graphs b) and c) show CO_2 and O_2 concentrations and appear to be complementary. In the Southern biofilter area carbon dioxide average concentration was found to be between 13 % and 15 %, while in the Northern part the average concentration ranged between 10 % and 12 %. Considering Oxygen, the average Southern concentration was 2 %, unlike in the Northern part in which the average value fluctuated from 6 % to 10 %. Graphs b) and c) provide detailed explanation regarding the biofilter phenomenology about methane oxidation. Methane in the Southern distribution system (4-5 %) shows concentrations close to those detected in the inlet (6.8 %), reaching values close to 0 % in the upper biofilter. At the same time CO_2 increases of 5-7 % in the structural material and O_2 decreases of 8 %. Contrary to that, methane in Northern distribution system (0.1 %) shows concentrations well away from the inlet (6.8 %), reaching non detectable values in the substrate material. Moreover, the lower CO_2 concentration and the higher O_2 (almost close to 10 % measured

in the inlet), substantiate the absence of a considerable CH_4 oxidation activity.

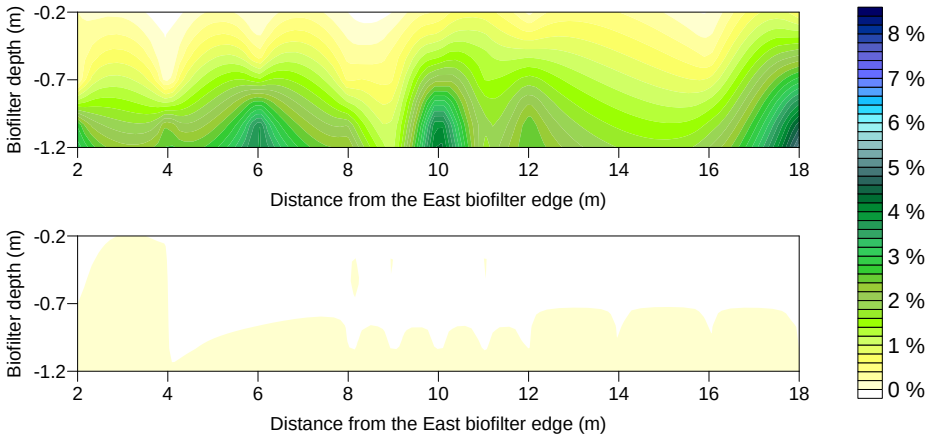

(a)

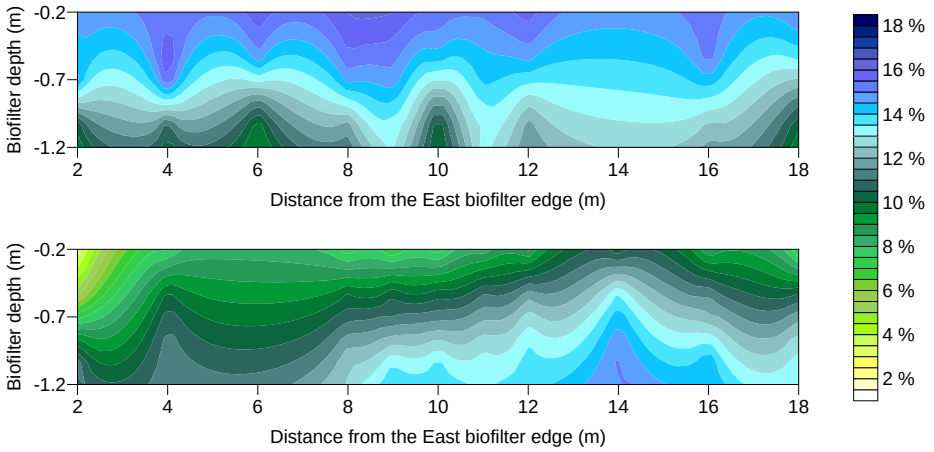

(b)

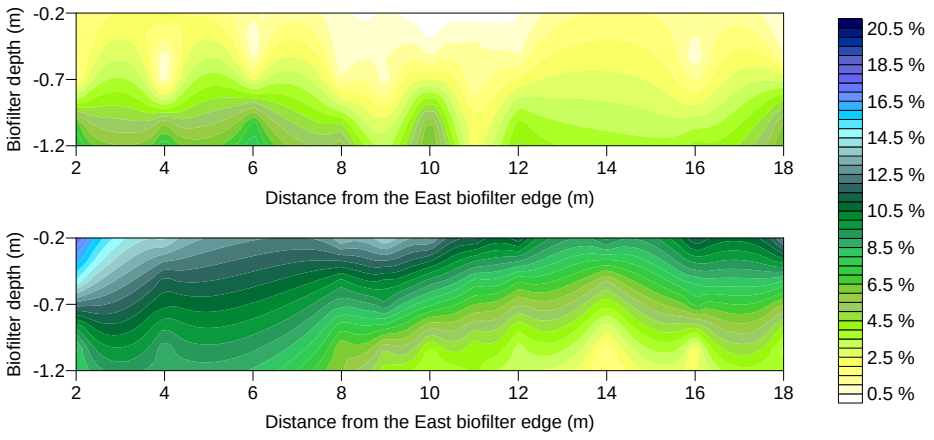

(c)

Figure 55: Biofilter profiles obtained from LFG measurements carried out with MLPGS on November 14th. Graphs a, b and c respectively represent the distribution inside the biofilter of CH_4 , CO_2 and O_2 in the Southern and in the Northern part.

The second piece of evidence relies on biofilter scannings, which have been carried out both qualitatively and quantitatively. The qualitative scanning of the biofilter has been done for CH_4 (using FID device) and for CO_2 with Carbocap sensor and has shown an accurate picture of the emissions distribution. Methane qualitative emission was found to be almost homogeneous for the whole biofilter surface, while CO_2 emission showed a notable difference between the Southern and the Northern part. The quantitative biofilter scanning (made with flux chambers) has also shown the same tendency. A non substantial difference has been detected between CH_4 average flux in Southern and in Northern areas (respectively 0.0033 $mol \cdot m^{-2} \cdot d^{-1}$ for South and 0.0018 $mol \cdot m^{-2} \cdot d^{-1}$ for North). On the contrary, a greater difference was detected in CO_2 fluxes, with an average flux in the Southern area of 6.91 $mol \cdot m^{-2} \cdot d^{-1}$ and in the Northern area of 2.25 $mol \cdot m^{-2} \cdot d^{-1}$. It can be concluded that the small amount of CH_4 which reaches the Northern part of the biofilter is oxidized, resulting in carbon dioxide and low methane emissions. At the same time, in the Southern part a great quantity of methane reaches the biofilter substrate and is oxidized, producing low methane emissions and CO_2 fluxes greater than those in the North part.

The third evidence of the substantial difference between Northern and Southern biofilter activity, relies on gas profiles presented in paragraph 5.1.4. In figure 56, the rates of the ratio between methane and the tracer gas are reported, both for South (graph a) and for North (graph b). From graph a) it's evident that the ratio decreases suddenly in the substrate material, reaching values close to zero.

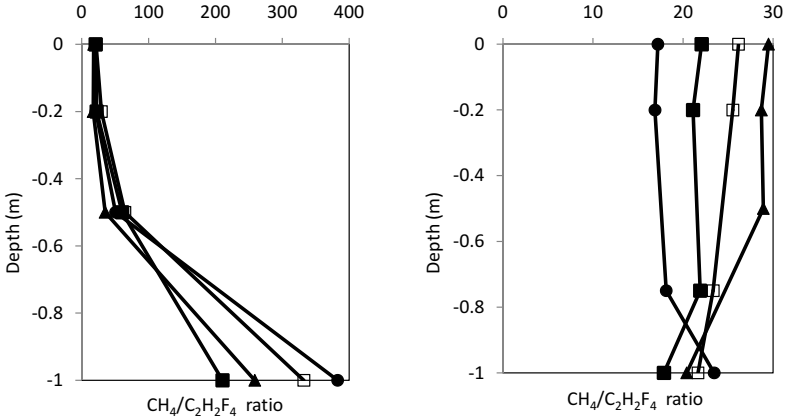

(a) (b)

Figure 56: Profiles describing rates of the ratio between CH_4 concentrations and $C_2H_2F_4$ (used as tracer gas). Graph a) is referred to Southern area and b) to Northern part. Concentrations were measured in different points during December 8th campaign, and refer to points S1-N1 (□), S4-N4 (▲), S8-N8 (■), S10-N10 (●). The spatial distribution can be observed in figure 24, paragraph 4.7.

While the tracer gas is only subjected to the diffusion effect, methane is reduced both from diffusion and methanotrophic bacteria activity. This sudden decrease leads to the ratio decrease, which is an indicator of methane oxidation. Contrarily, observing graph b) it's evident that the ratio between CH_4 and the tracer gas remains almost constant throughout the biofilter volume. This indicates that the only factor affecting methane reduction in the soil is diffusion. Since diffusion the only factor involved in methane and tracer gas reduction into the biofilter substrate, there are no reasons to uphold the presence of a methanotrophic activity in the Northern part.

These evidence prove the substantial difference from the Southern area to the Northern area of the biofilter. The main reason for this difference has to be attributed to the different methane concentration, with a evident deficiency of CH_4 in the Northern volume. The cause for this lack of CH_4 in the Northern part can be ascribed to different factors:

- the partial inefficiency of the LFG distribution layer, unable to distribute homogeneously methane in the farthest volume of the biofilter. A great part of methane entering in the biofilter is distributed in the Southern part, rendering the Northern part almost useless;
- the presence on the gravel distribution layer of a methanotrophic biofilm, which is able to oxidize methane before it reaches the upper compost layer. The presence of a methanotrophic biofilm has been reported in other studies as well (Huber-Humer, 2004) and could have an influence on the observed phenomena;

Figure 57: Gravel sample taken from LFG distribution system of the pilot biofilter implemented in Huber-Humer (2004) in 2004.

- the presence of a lower pressure in the Southern part of the biofilter, which creates a suction flux and prevents LFG diffusion in the whole volume. Methane oxidation reaction ($CH_4 + 2O_2 \longrightarrow CO_2 + 2H_2O$) provides the consumption of 3 gas moles

with the production of only 1 gas mole (produced water is adsorbed by the soil or integrated in the water phase). The reduction of generated volume in the soil pores by methanotrophic activity, creates a pressure lack and the consequent suction phenomena. Therefore, the intense methanotrophic activity in the Southern biofilter part could be the reason for the low LFG diffusion in the Northern volume.

In order to try to understand the main reasons of this partial inefficiency, it's important to compare previous studies with observations obtained from this analysis. Table 15 summarizes the main biofilter characteristics of the previous field biofilter studies.

Table 15: Main design characteristics from previous biofilter field studies.

Reference	*Distribution layer height* (m)	*Biofilter Area* (m^2)	*Average inflow* ($\frac{gCH_4}{d}$)	*Average specific inflow* ($\frac{gCH_4}{d \cdot m^2}$)
Cabral et al. (2010)	0.4	26.8	6,700	250
Dever et al. (2011)	0.5	9	2,200	240
Gebert and Grongroft (2006)	0.1 - 0.3	6 - 9	6,700	1,114
Philopoulos et al. (2008)	0.8	9.2	370	40
Roncato and Cabral (2012)	0.9	26.8	15,500	580
This study	0.3 - 0.5	504	10,000	20

From the analysis of table 15 it's extracted that, while the average total inflow of AV Miljø biofilter has an average value comparable to previous studies, the biofilter dimension is several times greater. Consequently, the specific biofilter inflow is 2-50 times lower than the ones reported in all the previous studies. Methane inflow reported in this study can be compared with precedent studies on biocovers, as in Stern et al. (2007) which measured fluxes of 12 $g \cdot m^{-2} \cdot d^{-1}$. The main reason for this uneven distribution can then be attributed also to the excessive biofilter size. Adopting the optimal gravel distribution layer used for this biofilter pilot plant, the maximal allowable width for a biofilter could be set around 5 meters.

6.4 BIOFILTER METHANE OXIDATION PERFORMANCES

In paragraph 5.2.3, the average total biofilter performance has been estimated to be around 18 $g \cdot m^{-2} \cdot d^{-1}$. This specific methane oxidation performance appears to be very low compared to the average oxidations obtained in the previous studies carried out on biofilters.

In fact, the average oxidation performances reported in literature are usually between 30 and 400 $g \cdot m^{-2} \cdot d^{-1}$, which is 1.5-22 times the oxidation efficiency achieved in AV Miljø biofilter. Previous studies performances are reported in table 16.

In order to investigate problems related to this low performance, the punctual analysis of biofilter's performances has to be carried out. Oxidations obtained from the two static flux chamber campaigns are reported in table 17. From the comparison of calculated methane oxidation performances in the Southern and in the Northern part of the biofilter, interesting conclusions can be achieved. In fact, the biofilter shows average oxidation performances between 3 and 35 times greater in the South than in the North.

Table 16: Methane oxidation performances achieved in previous studies, carried out on pilot plant biofilters.

Reference	*System*	*Average performance* ($\frac{gCH_4}{d \cdot m^2}$)	*Maximal performance* ($\frac{gCH_4}{d \cdot m^2}$)
Dever et al. (2011)	Biofilter	96 - 175	600
Gebert and Grongroft (2006)	Biofilter	-	1,280
Philopoulos et al. (2008)	Biofilter	28.4 - 36.4	-
Roncato and Cabral (2012)	Biofilter	352	576
Streese and Stegmann (2003)	Biofilter	424	875
Wilshusen et al. (2004)	Column biofilter	100	400

The average CH_4 oxidation also proves this trend, with an average of 10 $g \cdot m^{-2} \cdot d^{-1}$ in the North and 50 $g \cdot m^{-2} \cdot d^{-1}$ in the South. This differential performance is probably the main reason of the low total biofilter oxidation capacity (18 $g \cdot m^{-2} \cdot d^{-1}$). The methane oxidized flux of 50 $g \cdot m^{-2} \cdot d^{-1}$ in the Southern area is absolutely remarkable and comparable to previous studies. Moreover, the biofilter efficiency has been tested to be able to reach greater oxidation efficiencies, with a maximum of 124 $g \cdot m^{-2} \cdot d^{-1}$ in case of a considerable methane flux. These observations lead to the conclusion that a potential biofilter efficiency is really high, but the scarceness of injected methane quantities prevents the biofilter from reaching considerable average performances.

The Northern part of the biofilter shows low efficiencies because it's not properly fed, while the Southern part shows acceptable oxidation performances, which may be increased by reducing the biofilter area. An average performance of the biofilter around 50 $g \cdot m^{-2} \cdot d^{-1}$ could be easily achieved , without applying a intensive flux.

Table 17: Punctual oxidation performances of the biofilter calculated with the Tracer Mass Balance Approach.

	Date	$J_{CH_4,oxidized}$ $(mol \cdot m^{-2} \cdot d^{-1})$	$J_{CH_4,oxidized}$ $(g \cdot m^{-2} \cdot d^{-1})$
S1	18-Nov-2012	1.16	17.03
	8-Dec-2012	7.86	124.18
S4	18-Nov-2012	n.a.	n.a.
	8-Dec-2012	3.74	59.16
S5	18-Nov-2012	0.91	14.42
	8-Dec-2012	n.a.	n.a.
S8	18-Nov-2012	n.a.	n.a.
	8-Dec-2012	4.75	75.19
S10	18-Nov-2012	1.08	16.95
	8-Dec-2012	4.36	68.86
N1	18-Nov-2012	0.16	2.72
	8-Dec-2012	0.23	3.66
N4	18-Nov-2012	n.a.	n.a.
	8-Dec-2012	0.84	13.21
N8	18-Nov-2012	n.a.	n.a.
	8-Dec-2012	1.00	15.77
N10	18-Nov-2012	0.11	1.93
	8-Dec-2012	1.33	21.16

n.a. Data not available, as the analysis has not been carried out in that campaign for this point.

In several previous biofilter studies, an intensive methane flux has been applied (400-1,200 $g \cdot m^{-2} \cdot d^{-1}$) in order to evaluate the maximum biofilter efficiency, while the purpose of this study is finding the best setting for this technology. The application of an intensive flux of methane to a biofilter is able to optimize spaces and costs, but may not guarantee the long term life of the plant. The formation of EPS has been reported in several studies with an high rate of methane applied. Haubrichs and Widmann (2006) reported a decrease of methane oxidation efficiency in a biofilter column test after 230 days with a methane inlet of 670 $g \cdot m^{-2} \cdot d^{-1}$. Wilshusen et al. (2004) observed a decrease of oxidation performances in a biofilter column after 100 days from 400 to 100 $g \cdot m^{-2} \cdot d^{-1}$. In both studies, the formation of EPS has been observed with the decrease of CH_4 oxidation. The real mechanisms of EPS formation are still undefined, but several hypotheses have been proposed. One of the most plausible hy-

potheses has been presented in Huber-Humer (2004), who attributed the formation of EPS to the overload of carbon (Scheutz et al., 2009).

Moreover, an intensive flux of methane in the AV Miljø biofilter could modify the balanced distribution of oxygen measured in the Southern part of the biofilter (2-3%). The excessive consumption of O_2 due to a higher methanotrophic activity could create anaerobic zones in the biofilter body, neutralizing the biofilter flexibility of reacting to external factors (i.e. temperature and atmospheric pressure variation, as described in 6.1.). The reduction of methane oxidation efficiency with the increasing loading rate has also been proved in Dever et al. (2011), due to the reduced presence of O_2 in the biofilter's volume.

In the end, a total Mass Balance can be carried out using results described in paragraph 5.2.3. The total Carbon injected in the biofilter during the measurement campaign carried out on January 25th was 1,087 $molC \cdot d^{-1}$. The measured surface emission was calculated to be 2,086 $molC \cdot d^{-1}$. Considering that the carbon generated by bacteria respiration in the soil has been calculated to be 1,145 $molC \cdot d^{-1}$, the total carbon generated or injected in the biofilter is 2,232 $molC \cdot d^{-1}$, while the emitted carbon is 2,086 $molC \cdot d^{-1}$. The negligible difference between the obtained values, considering the variability of parameters, proves the measurements reliability.

7

CONCLUSIONS

The conclusions of this study are then presented. The purpose of this chapter is to summarize the achieved results and introduce the possible future studies which could be carried out on this topic, then described in chapter 8.

The reliability of the Tracer Mass Balance Approach has been evaluated in this study. This method, used to calculate the methane oxidation performances of a methanotrophic based technology, showed its strength and consistency giving results similar to the consolidated Carbon Mass Balance Approach. Moreover, the Tracer Approach demonstrated to be more reliable than the Carbon Mass Balance Approach regarding the methodology and results, especially when surface methane fluxes are low. From the point of view of the applicability, the Tracer Approach shows its limits. The underground injection of a tracer gas and the calculation of the underground flux of methane are only applicable to biofilter technologies, while for biocovers the most feasible Mass Balance is still The Carbon based Approach.

Preliminary scannings using FID device and Carbocap sensor have proved to be a interesting and reliable tool to evaluate the surface distribution of CH_4 and CO_2 emissions. The homogeneous methane surface emissions detected with the FID device and the different South-North emission of CO_2 detected with Carbocap sensor, have been confirmed with the following measurements. This analysis can be considered a fundamental preliminary step to plan more accurate measurements campaigns, as the static flux chamber monitoring.

The LFG distribution in the biofilter has been proved to be optimal in the whole biofilter length. The presence of methane emission hot spots, identified with the FID device, has not been confirmed with the flux chamber method. Conversely, the flux chamber method showed the optimal and homogeneous distribution of CH_4 surface emissions, which range between 0 and 0.16 $g \cdot m^{-2} \cdot d^{-1}$. A permanent problem with LFG distribution has been proved in the father volume from biofilter inlet. Several hypothesis to explain this inhomogeneity have been proposed (negative $\triangle P$ due to methane oxidation, methanotrophic biofilm in distribution layer, inefficiency of LFG distribution pipes), but the real cause has not been assessed. Generally, the distribution system of AV Miljø biofilter can be judged to be effective and the compost compaction optimal to guarantee an homogeneous distribution of injected LFG.

The biofilter implemented at AV Miljø landfill showed a considerable methane oxidation efficiency (99.7 %). The methanotrophic per-

formance obtained in the Southern part of the biofilter (50 $g \cdot m^{-2} \cdot d^{-1}$) during the winter season (January 25th) demonstrates the substantial strength of the pilot plant. This demonstrates that the biofilter is able to obtain high performances also with the most unfavorable environmental conditions. The homogeneous distribution of O_2 in the whole volume and the great substrate thermal insulation, guarantee its flexibility. The O_2 presence at every depth allows the methanotrophic layer displacement (due to temperature and atmospheric pressure changes), preserving the methane oxidation activity. At the same time, the low temperature variation of the substrate guarantees the optimal environmental conditions for methanotrophic bacteria. The main factors affecting biofilter temperature are the injected LFG heat, the compost insulation capacity, the heat generated from methanotrophic bacteria and from compost respiration.

The biofilter designing is fundamental for a proper functioning. The increase of the specific methane load ($g \cdot m^{-2} \cdot d^{-1}$) reduces construction costs of the biofilter, but it also reduce the plant lifetime (due to EPS formation) and the oxidation efficiency (due to O_2 scarceness). Therefore, the right compromise has to be achieved between costs and biofilter duration. AV Miljø biofilter could be optimized by removing the Northern part and reshaping the remaining volume. Consequently, the biofilter volume could be reduced by half and the average methane oxidation of 50 $g \cdot m^{-2} \cdot d^{-1}$ may be acceptable as average performance. The current and the reshaped pilot plant are represented in figures 58, 59, 60.

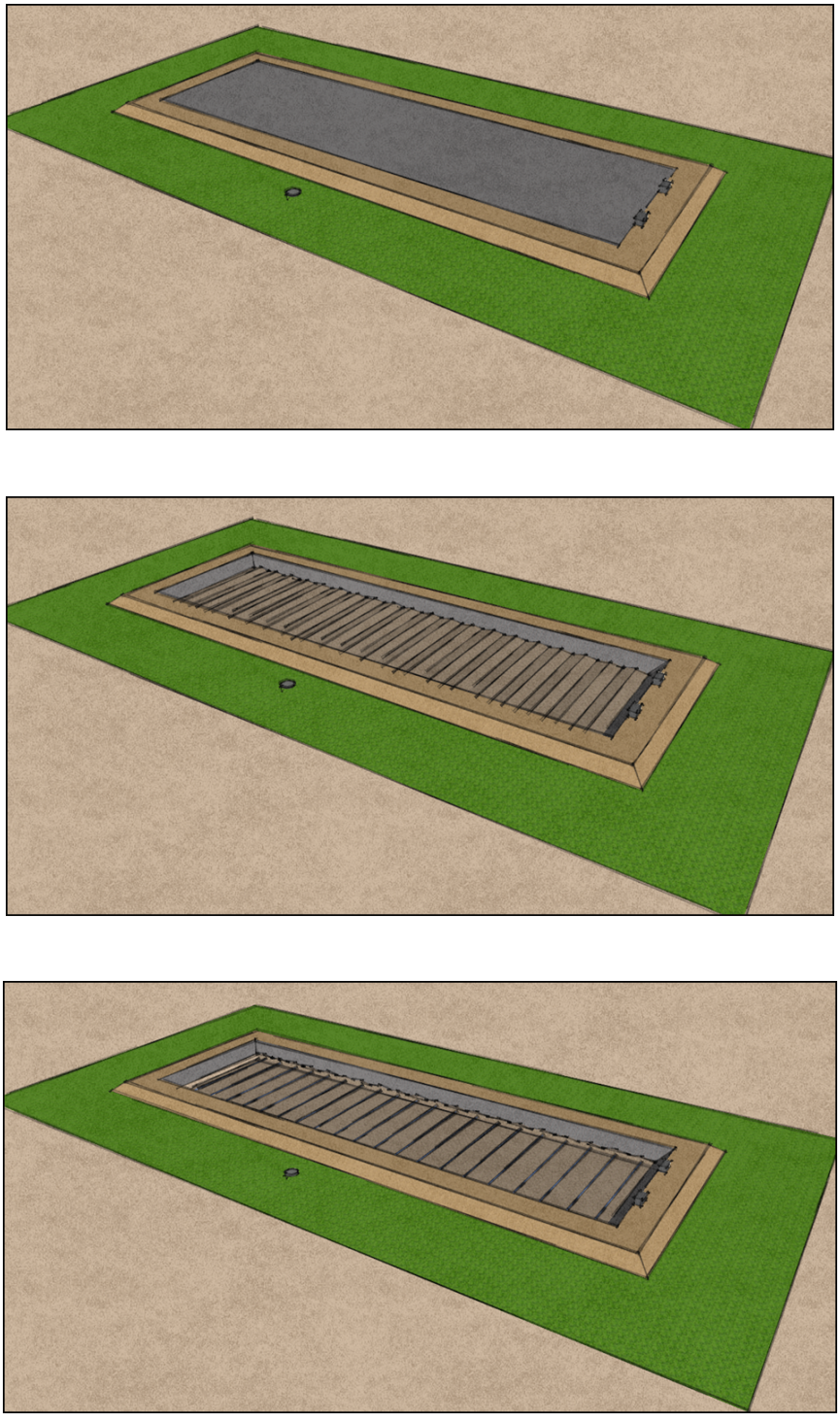

Figure 58: Renderings of the biofilter currently implemented at AV Miljø landfill. In the first picture the aerial view is illustrated, while in the second and third picture show the gravel distribution layer and the distribution pipes.

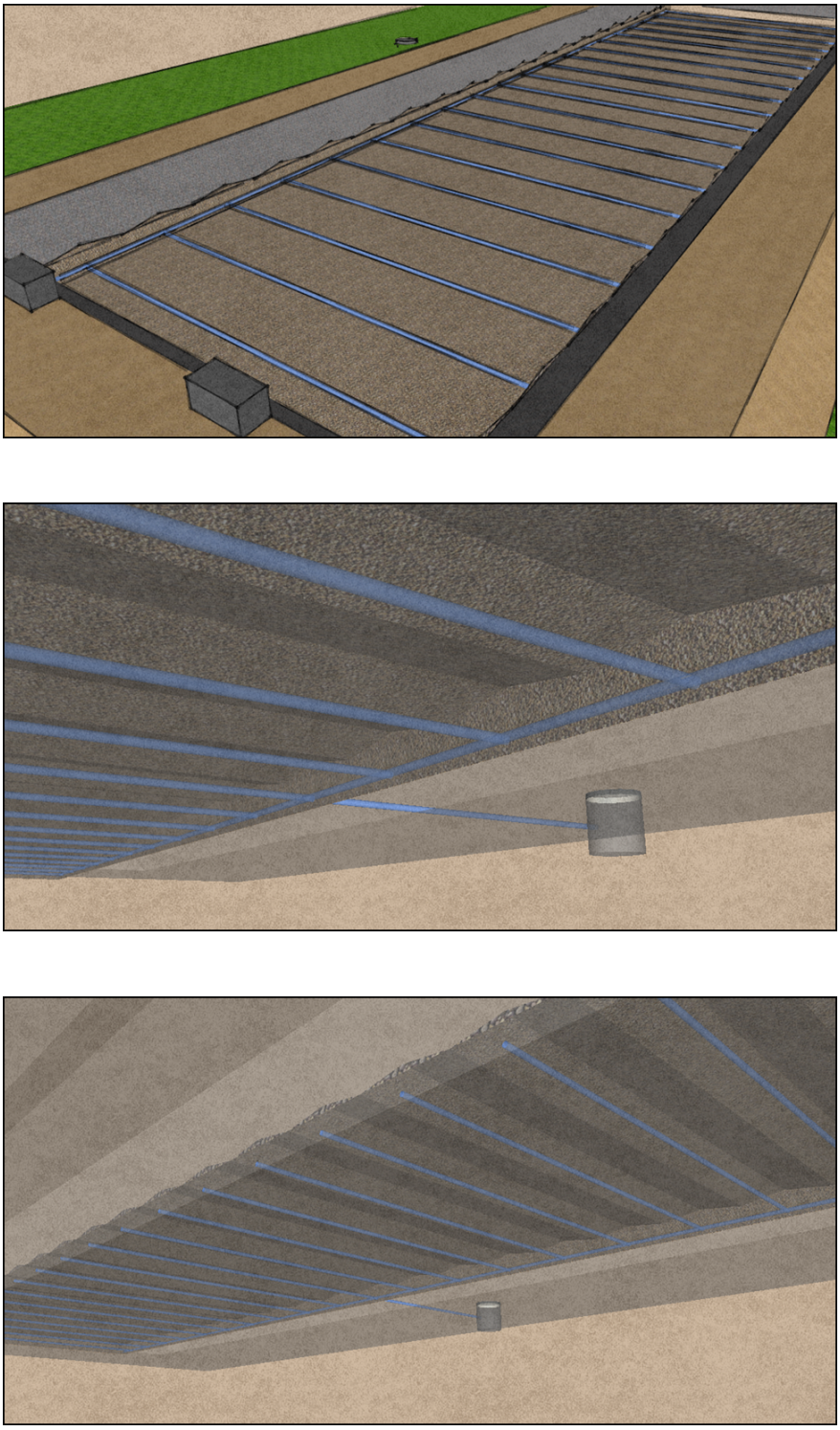

Figure 59: Renderings of the biofilter currently implemented at AV Miljø landfill. In the first picture the aerial view shows the LFG distribution pipes. The second and third picture illustrate the biofilter distribution system, with the pipes embedded in the gravel layer and the mixing chamber.

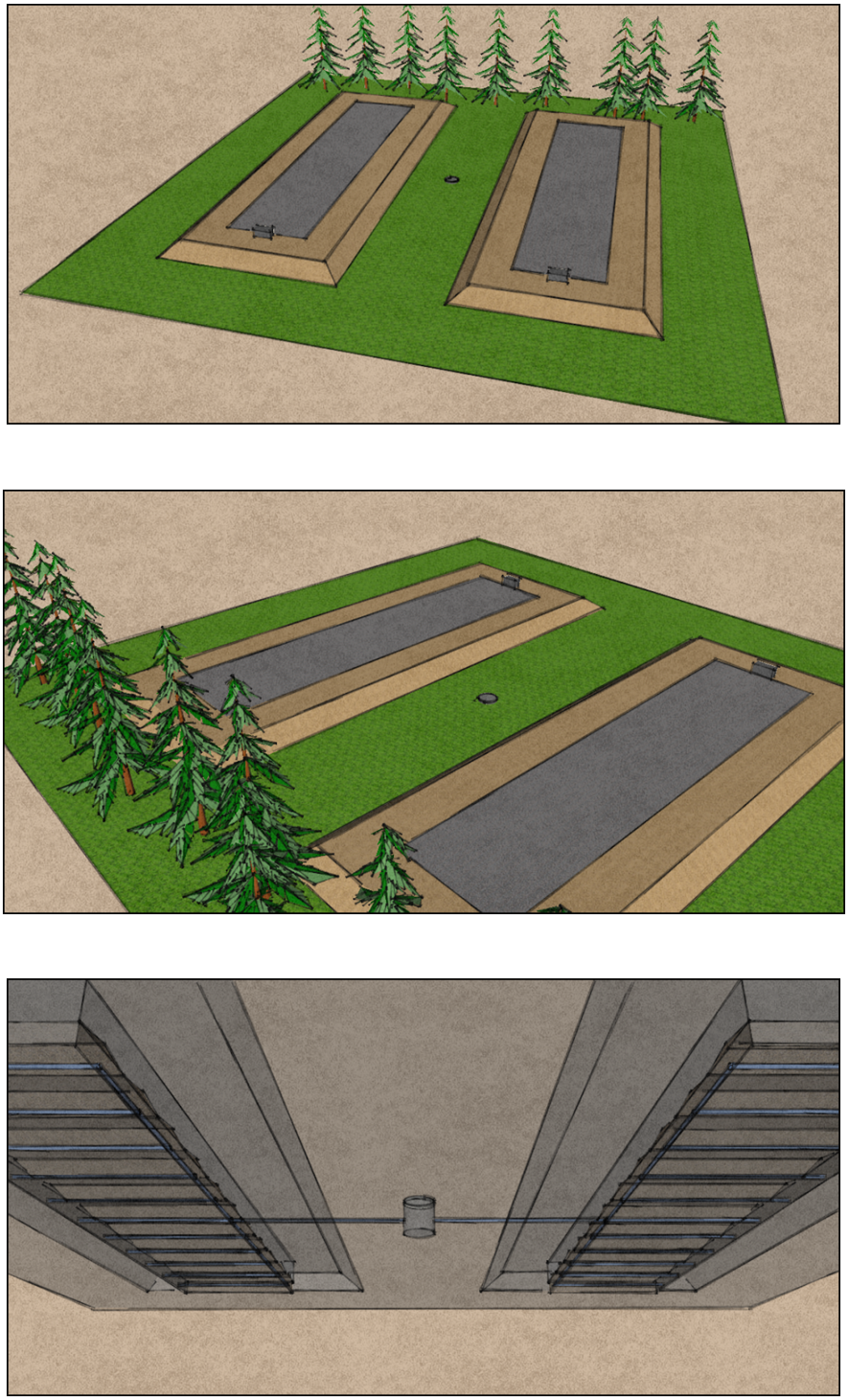

Figure 60: Renderings of the reshaped AV Miljø biofilter. The Northern volume of the original biofilter has been removed and the remaining volume divided in two biofilters. The mixing chamber, placed in the middle, allows to close the LFG inlet of one of the two biofilter during maintenance operations.

8

FUTURE PERSPECTIVES

Future researches at AV Miljø biofilter could focus on the main aspects highlighted in this study. The biofilter strengths need to be confirmed, measuring methane oxidation performances throughout the year. Moreover, further analysis could focus on the main causes of the underlined deficiencies, as the differential distribution of LFG in the biofilter. Particularly the following analysis are suggested:

- Increase the biofilter load by injecting CH_4 in the mixing chamber from an external source. The injection of an additional quantity of methane is useful to understand if the LFG distribution issue in the biofilter are due to distribution layer quality or to the low load. Moreover, this analysis allows to calculate if the biofilter can achieve higher oxidation performances;

- Test the pressure throughout the biofilter depth, to identify the presence of a $\triangle P$ generated by methanotrophic activity in the biofilter. This test is required to understand if this phenomena can be the reason of the LFG scarceness in the Northern biofilter volume;

- Carry out more static flux chamber campaigns, measuring the whole biofilter oxidation performance. The aim of these campaigns is to confirm the previous results obtained in this study and calculate the methane oxidation performances throughout the year. The surface spatial distribution of CH_4 and CO_2 could be investigated;

- Perform an additional static flux chamber campaign of the whole biofilter, injecting the HFC-134a tracer in the mixing chamber. The purpose of this analysis is to obtain a surface spatial distribution of CH_4, CO_2 and tracer which can provide a better idea of the distribution layer and biofilter efficiency;

- Test the methane flux in the South-East corner to confirm or deny the presence of the emission hot spot locate with the FID device.

A

APPENDIX

A.1 LFG FLUX TO BIOFILTER

In order to guaratee a constant flux of LFG to the pilot plant from the landfill, pumps were installed at AV Miljø biofilter. Characteristics of pumps are descibed in detail in chapter 3. The accumulated LFG flow has been recorded for every pump regularly, at least every week, from June to December. The accumulated LFG flow is represented in figure 6.1. It's possible to observe that pumps operated steadily during the whole monitoring period (from September to December). In the previous period, energy supplies problems occured at AV Miljø biofilter, causing the instability of pumps flow. This fact is evident in the period between September 15th and September 30th, in which pumps stopped to operate properly and LFG supply to the biofilter was interrupted. The average flows for every leachate well were calculated. The average flow from leachate well 1 and well 3 are almost comparable and are approximately 52 m^3/d and 48 m^3/d respectively. The LFG flow from leachate well 2 is generally higher than the other two, due to the different operating pump, and is estimated to be around 82 m^3/d.

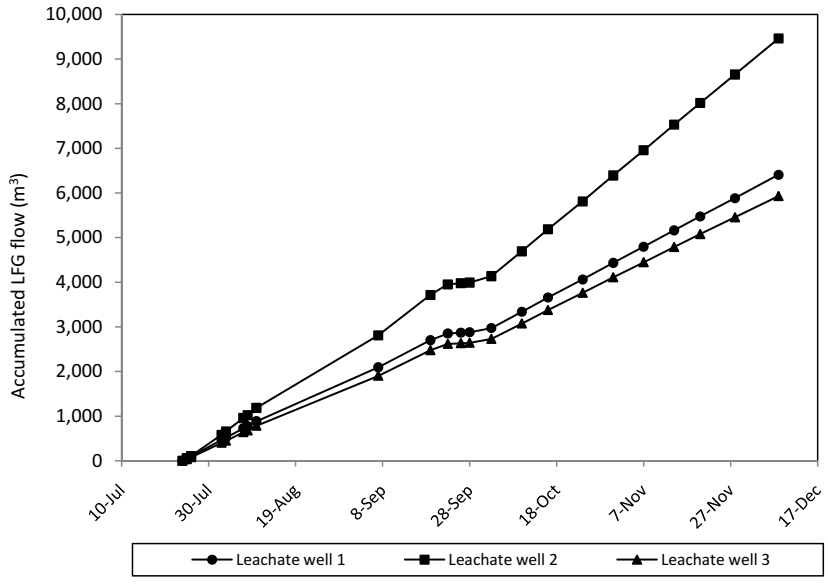

(a)

Figure 61: Accumulated landfill gas flow injected into AV Miljø biofilter from landfill leachate wells. Flows are reported in the period betwen June and December 2012.

A.2 MLPGS PROFILES OF THE BIOFILTER

A.2.1 *Methane in biofilter's southern area*

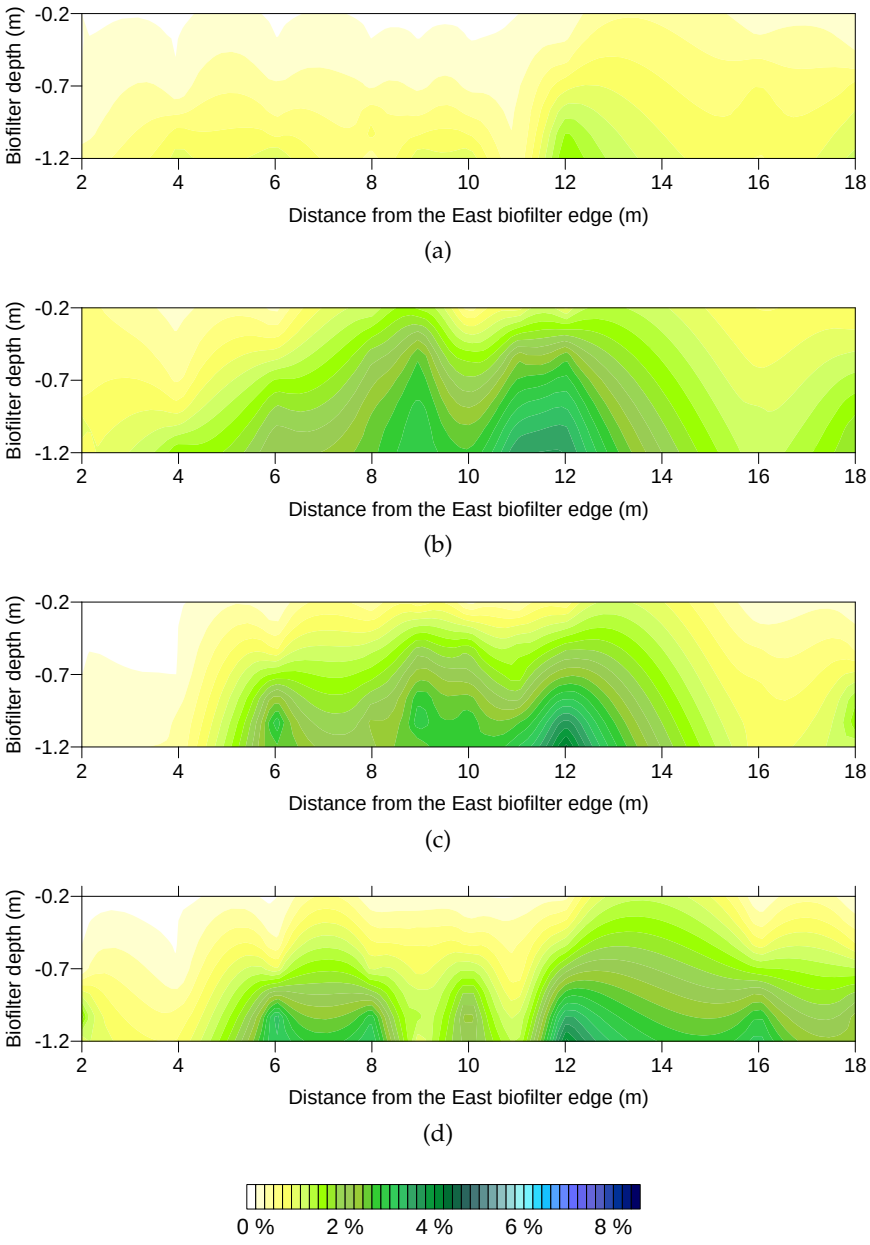

Figure 62: Southern sections of the biofilter representing methane distribution from the Eastern edge (left) to the biofilter center (right). Measurements were carried out on September 26th (a), October 3rd (b), October 10th (c) and October 16th (d), 2012.

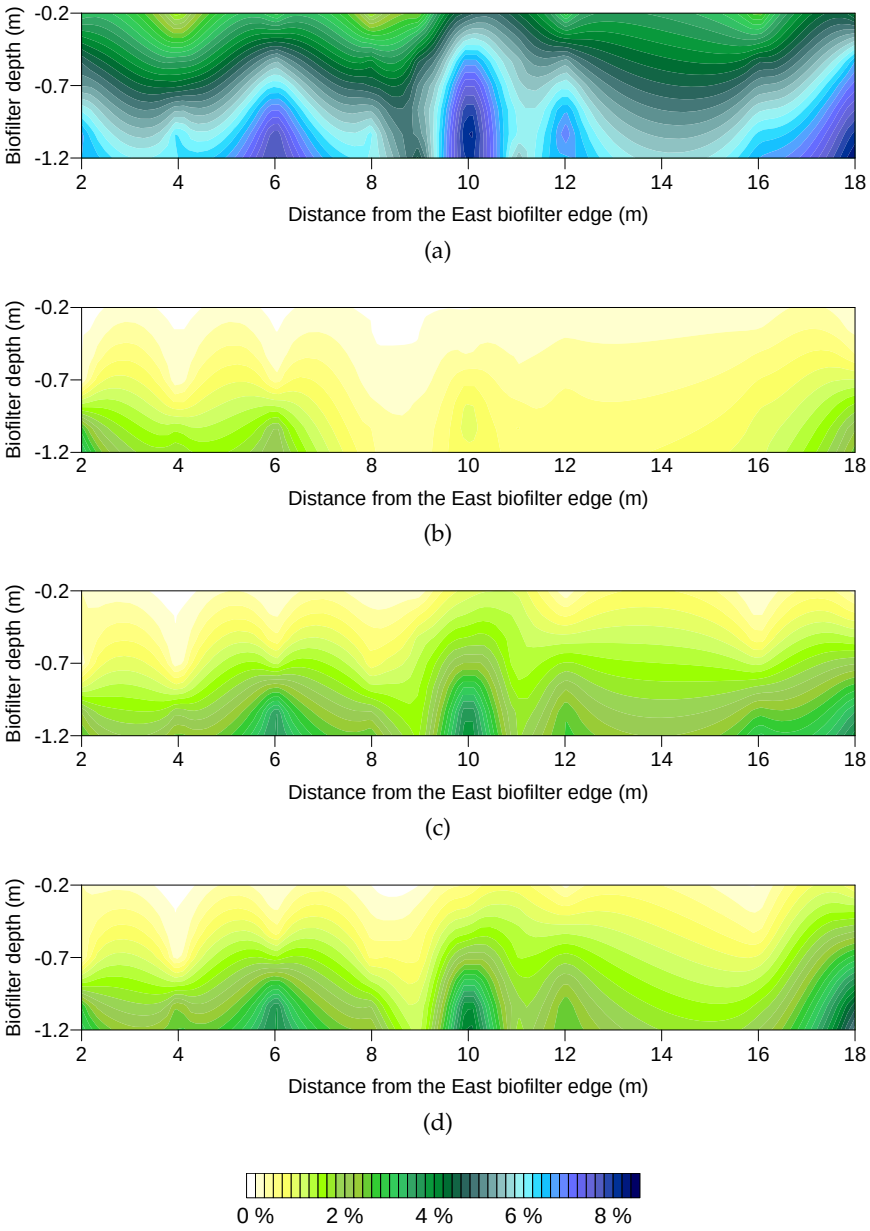

Figure 63: Southern sections of the biofilter representing methane distribution from the Eastern edge (left) to the biofilter center (right). Measurements were carried out on October 24th (a), October 31st (b), November 7th (c) and November 14th (d), 2012.

A.2.2 *Methane in biofilter's northern area*

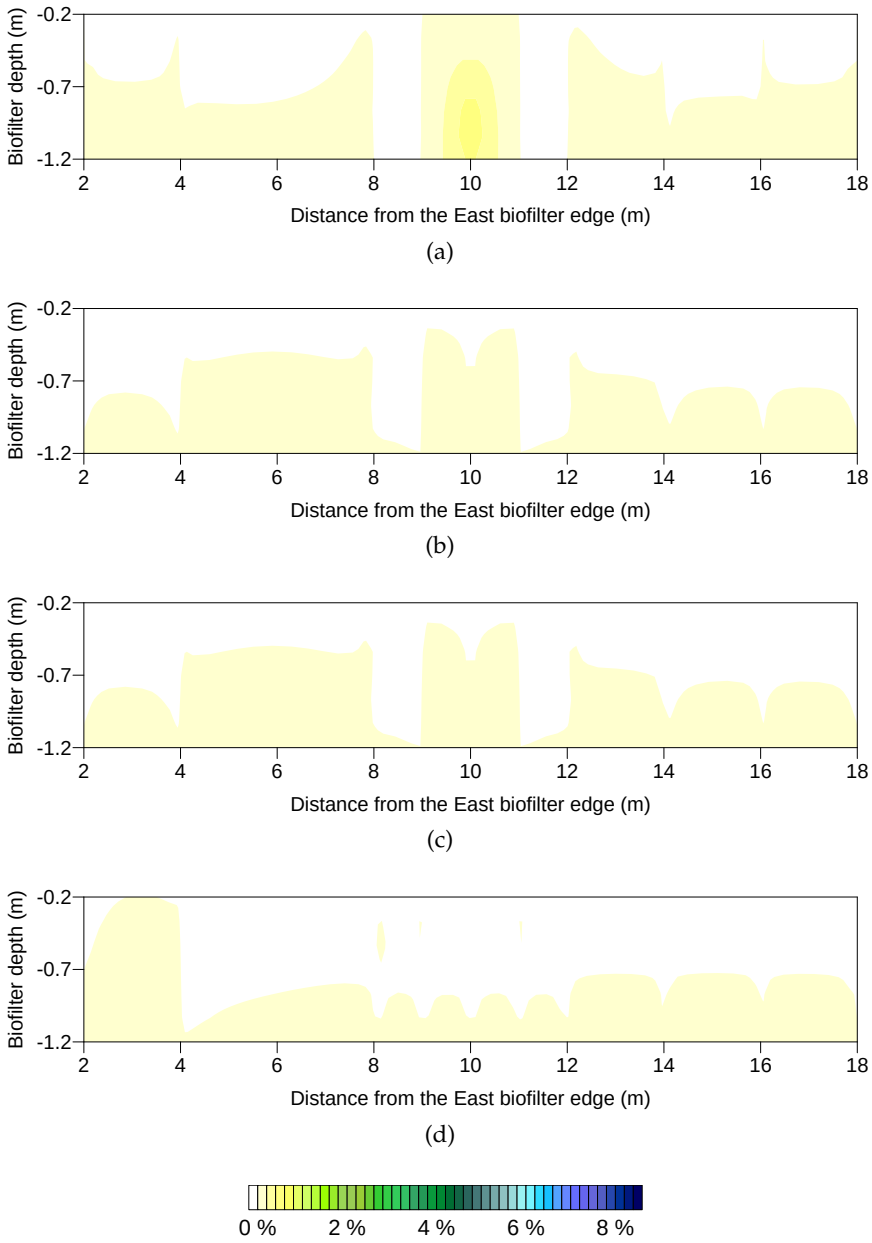

Figure 64: Northern sections of the biofilter representing methane distribution from the Eastern edge (left) to the biofilter center (right). Measurements were carried out on September 26th (a), October 3rd (b), October 10th (c) and October 16th (d), 2012.

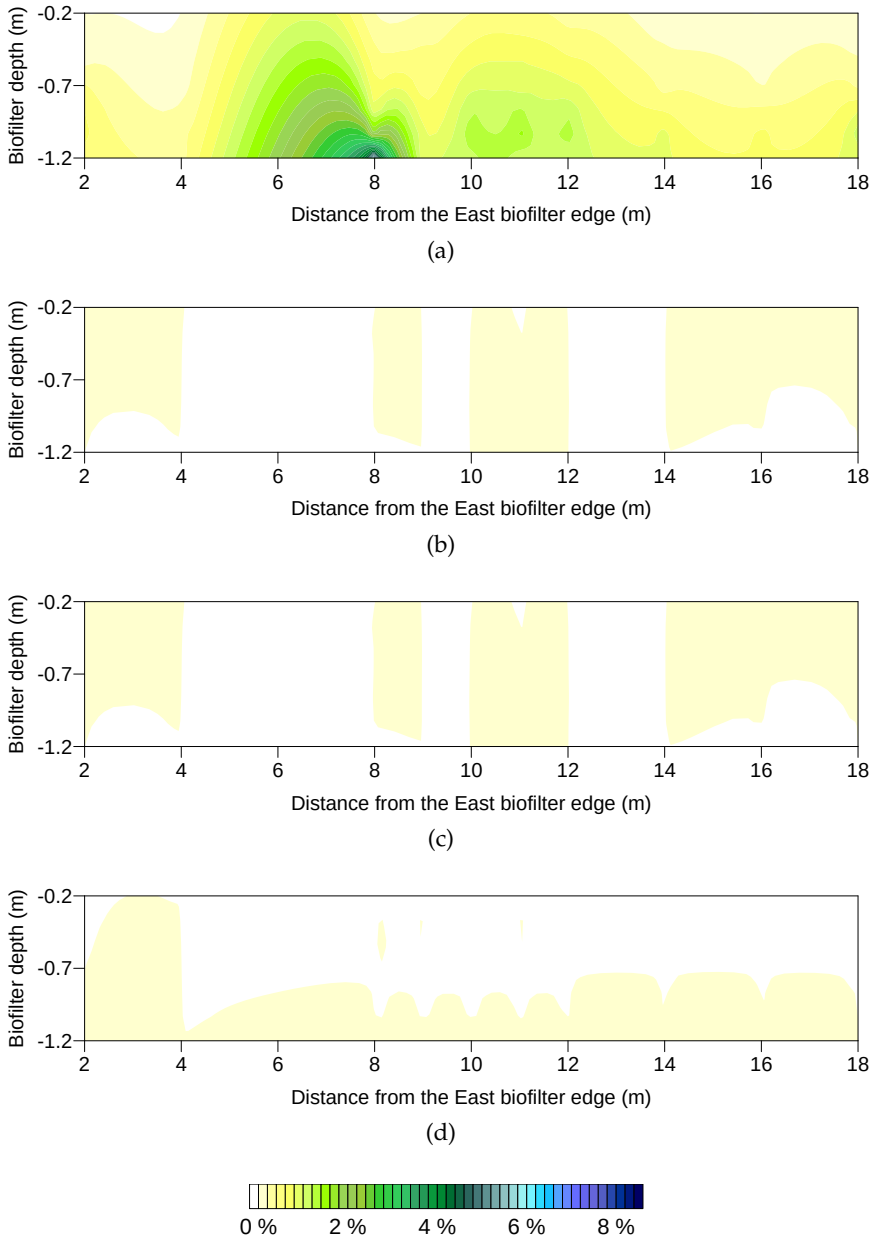

Figure 65: Northern sections of the biofilter representing methane distribution from the Eastern edge (left) to the biofilter center (right). Measurements were carried out on October 24th (a), October 31st (b), November 7th (c) and November 14th (d), 2012.

A.2.3 *Carbon dioxide in biofilter's southern area*

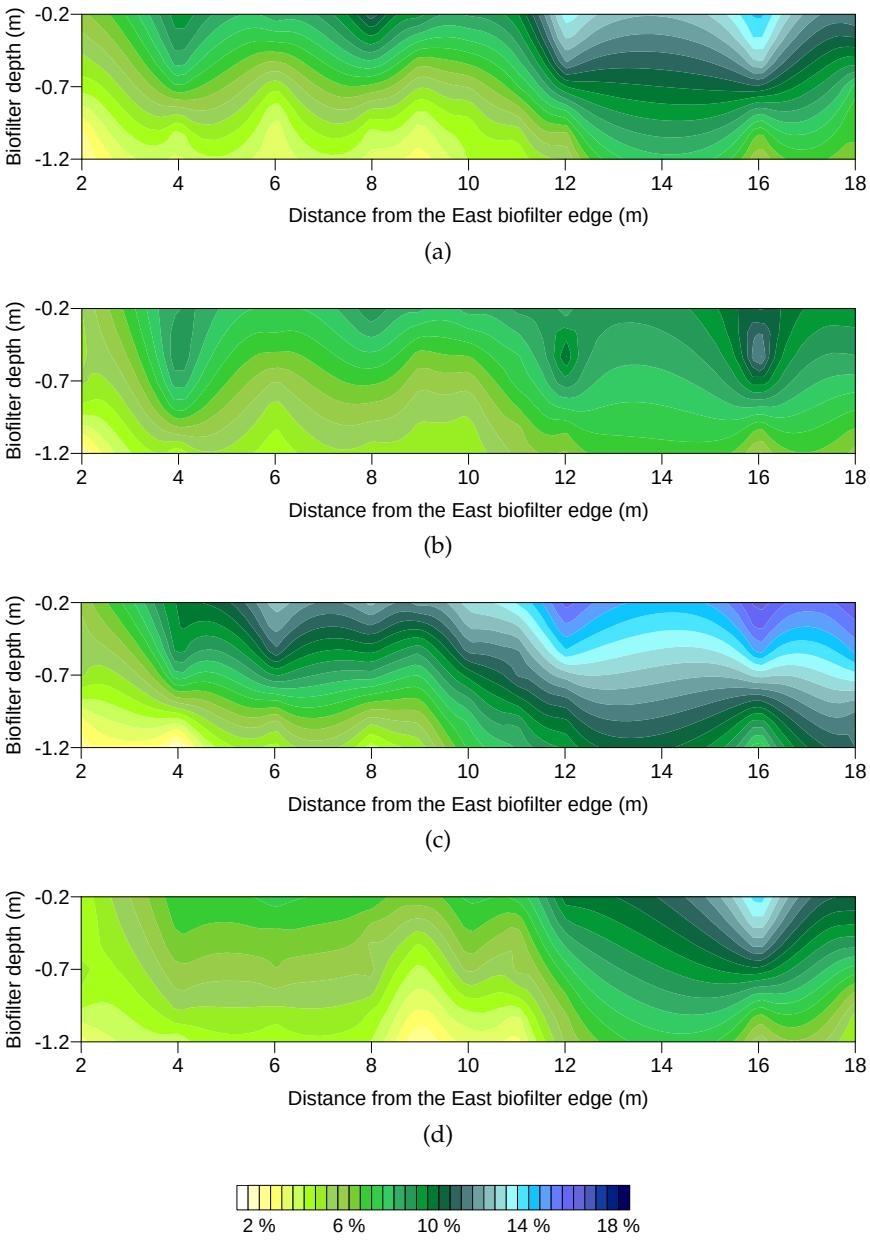

Figure 66: Southern sections of the biofilter representing carbon dioxide distribution from the Eastern edge (left) to the biofilter center (right). Measurements were carried out on September 26th (a), October 3rd (b), October 10th (c) and October 16th (d), 2012.

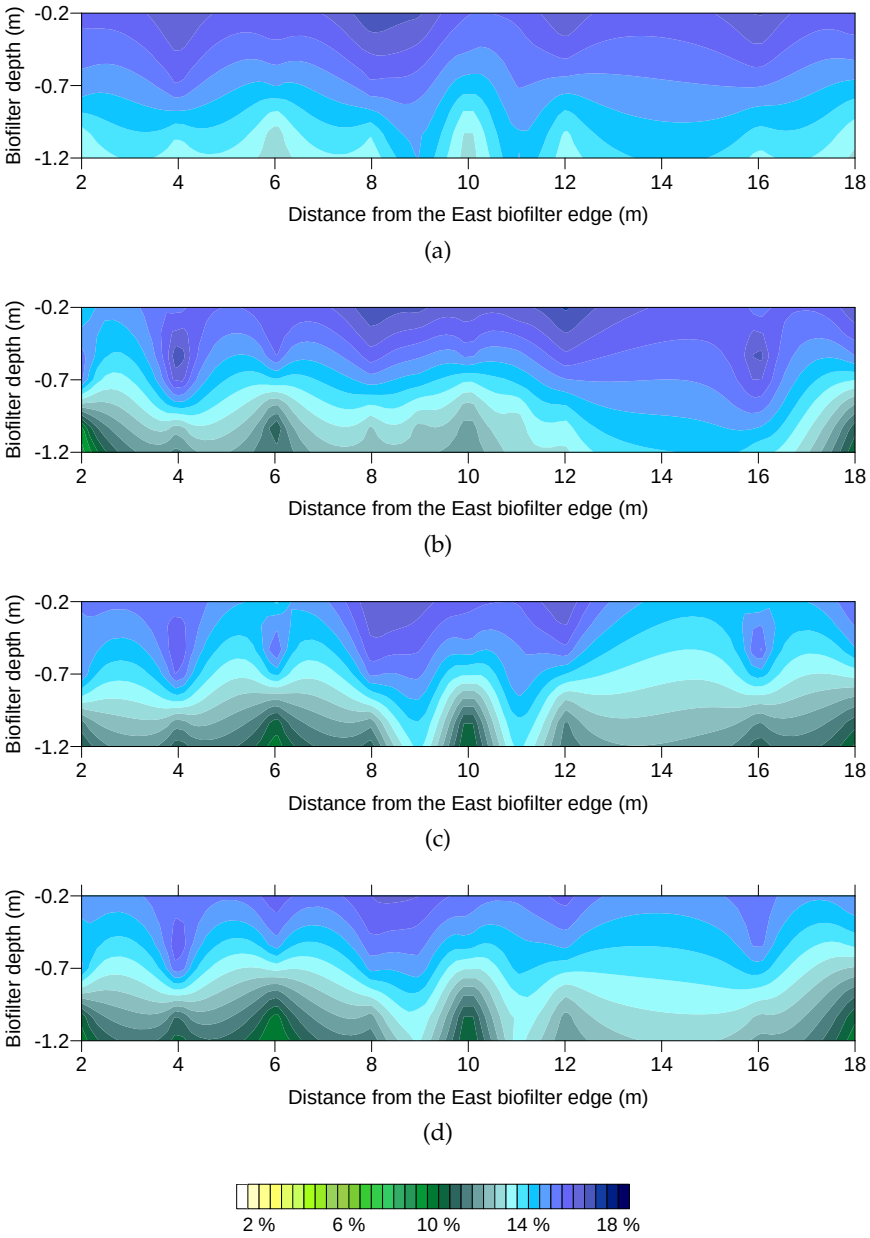

Figure 67: Southern sections of the biofilter representing carbon dioxide distribution from the Eastern edge (left) to the biofilter center (right). Measurements were carried out on October 24th (a), October 31st (b), November 7th (c) and November 14th (d), 2012.

A.2.4 *Carbon dioxidein biofilter's northern area*

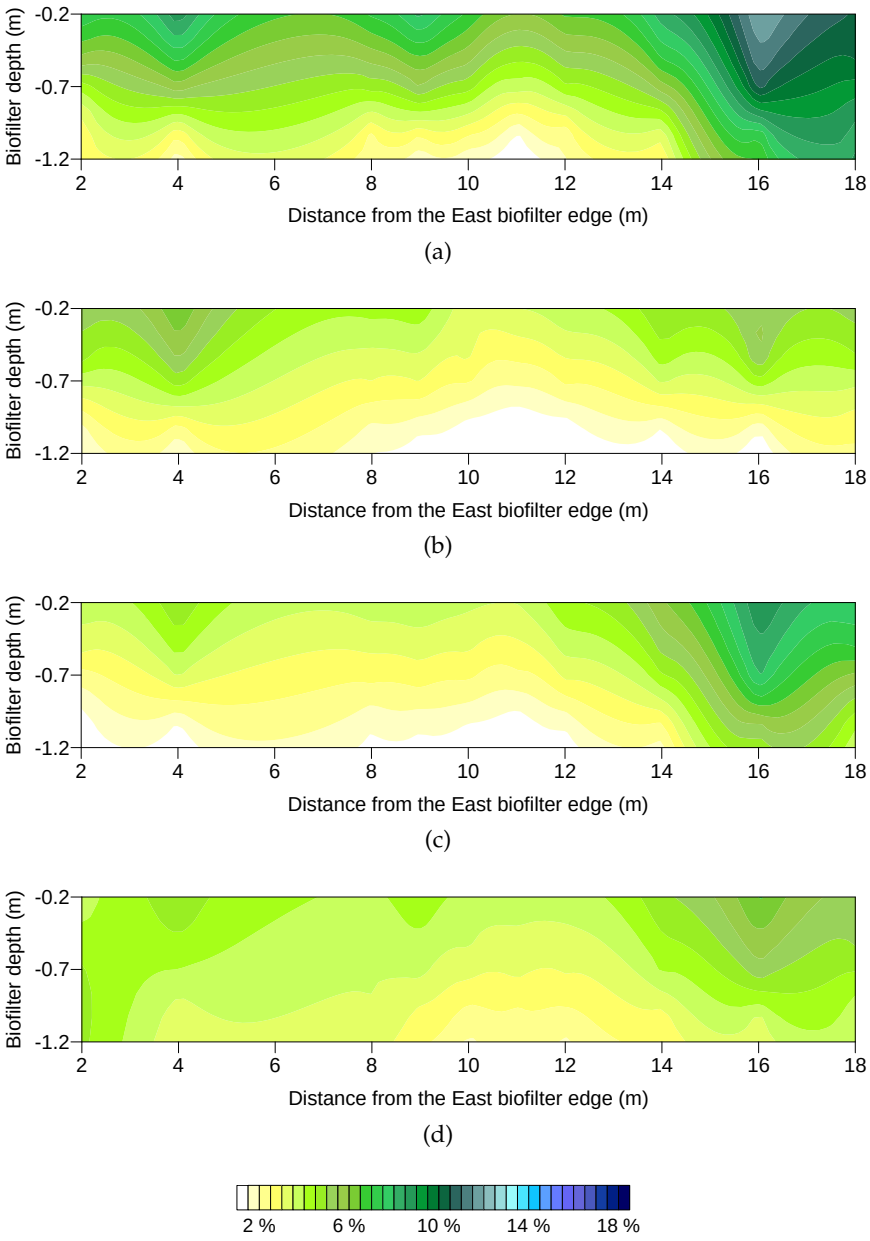

Figure 68: Northern sections of the biofilter representing carbon dioxide distribution from the Eastern edge (left) to the biofilter center (right). Measurements were carried out on September 26th (a), October 3rd (b), October 10th (c) and October 16th (d), 2012.

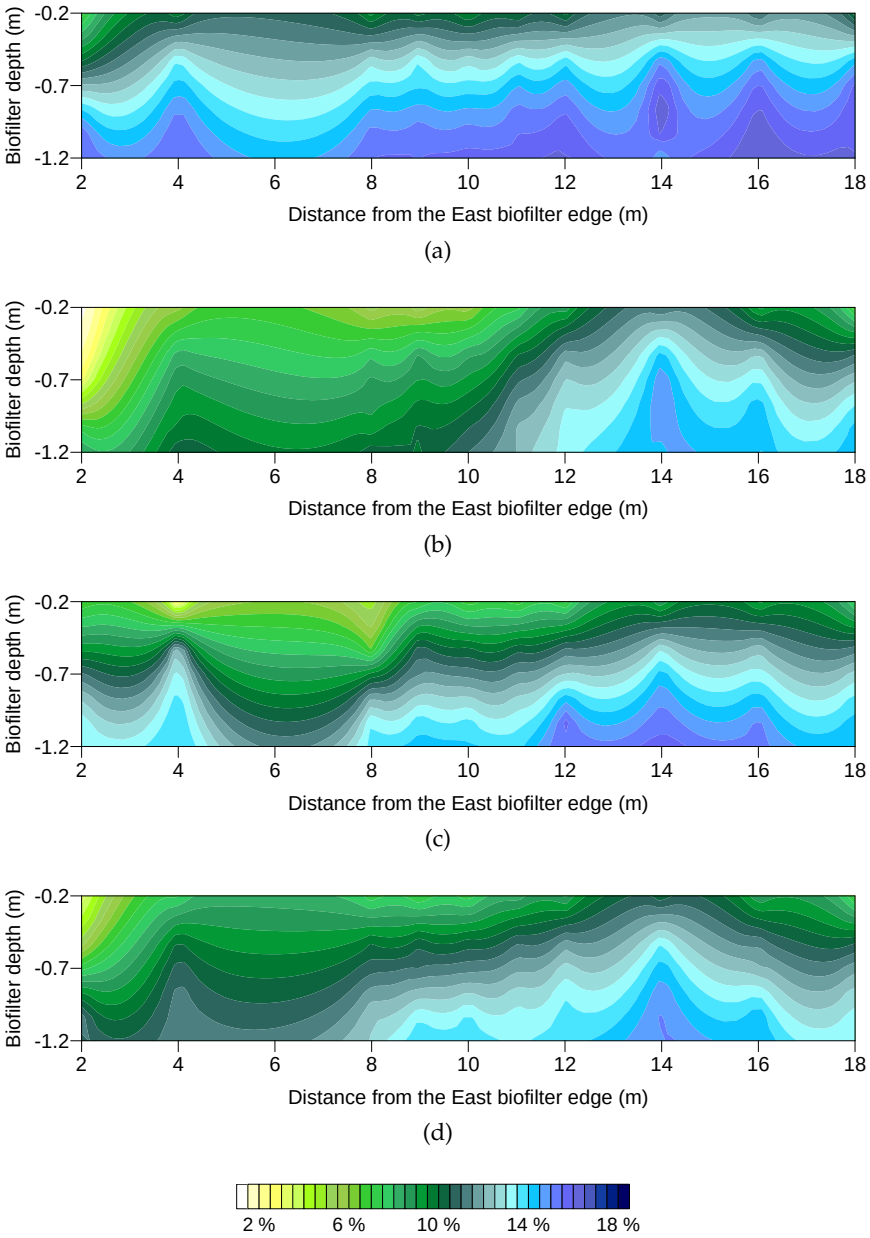

Figure 69: Northern sections of the biofilter representing carbon dioxide distribution from the Eastern edge (left) to the biofilter center (right). Measurements were carried out on October 24th (a), October 31st (b), November 7th (c) and November 14th (d), 2012.

A.2.5 *Oxygen in biofilter's southern area*

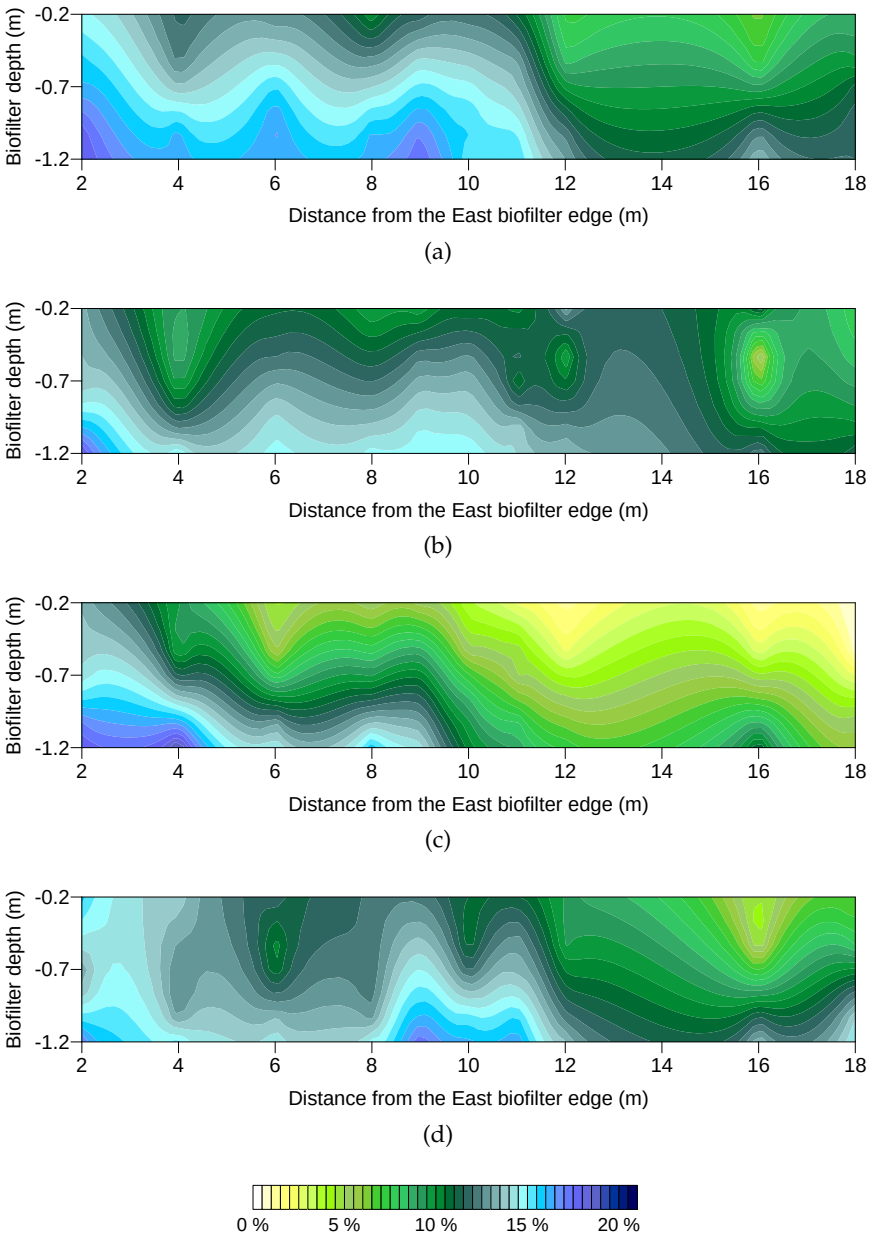

Figure 70: Southern sections of the biofilter representing oxygen distribution from the Eastern edge (left) to the biofilter center (right). Measurements were carried out on September 26th (a), October 3rd (b), October 10th (c) and October 16th (d), 2012.

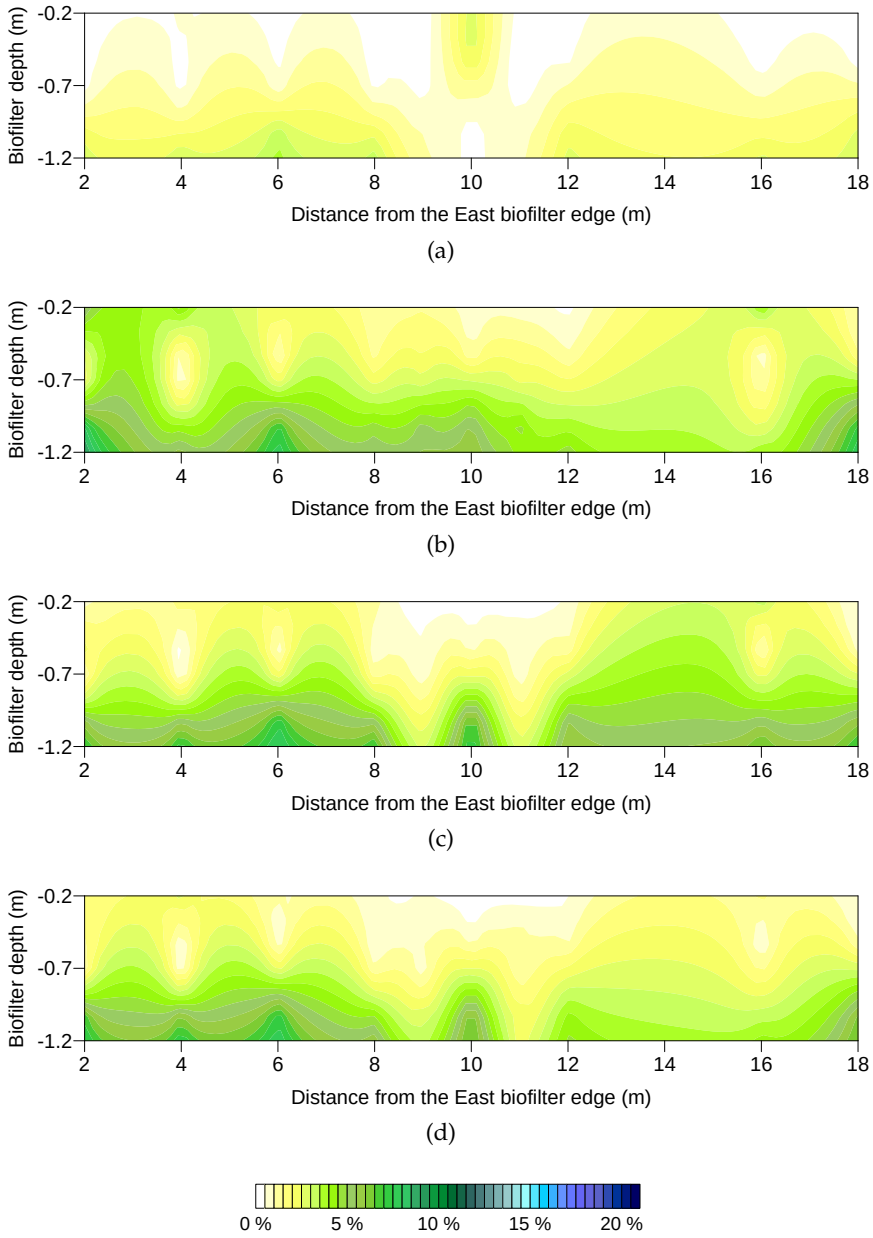

Figure 71: Southern sections of the biofilter representing oxygen distribution from the Eastern edge (left) to the biofilter center (right). Measurements were carried out on October 24th (a), October 31st (b), November 7th (c) and November 14th (d), 2012.

A.2.6 *Oxygen in biofilter's northern area*

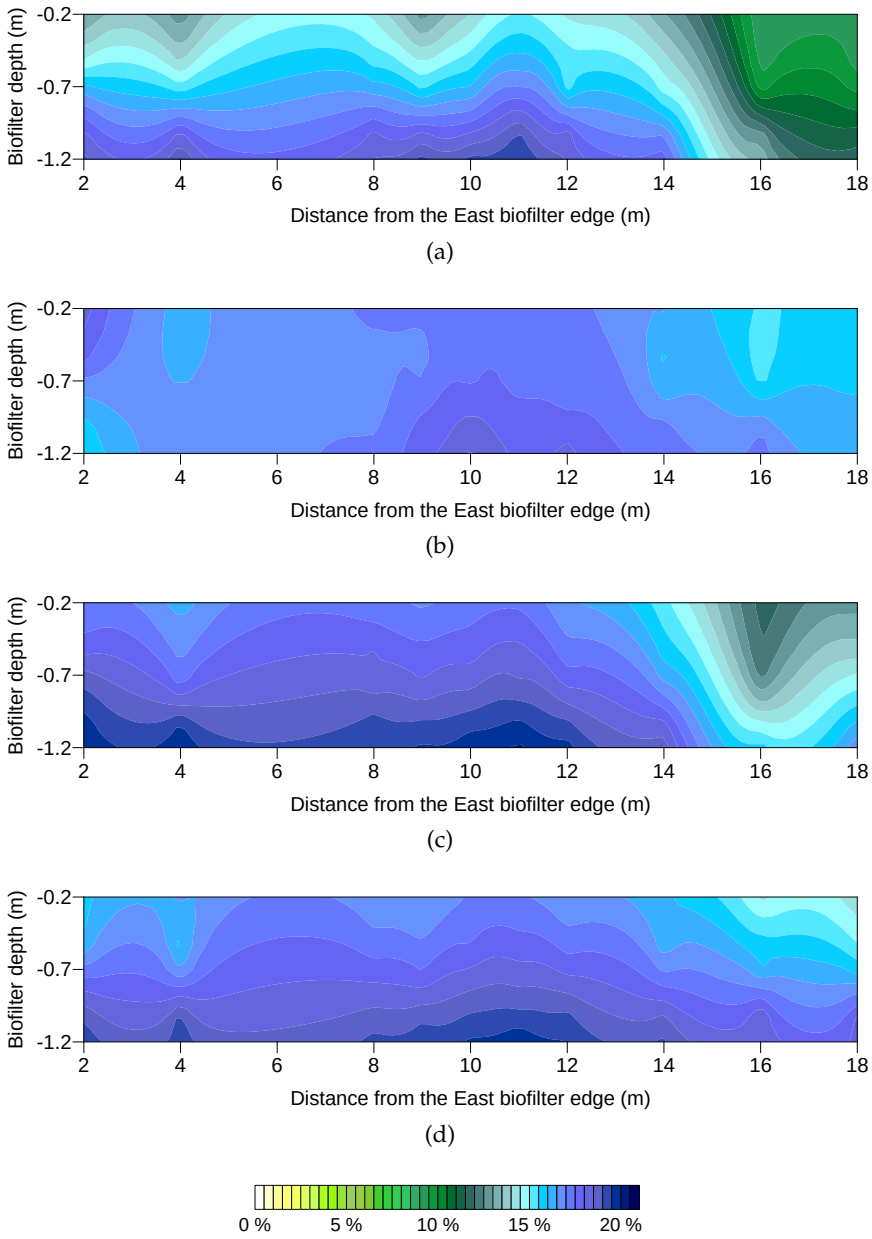

Figure 72: Northern sections of the biofilter representing oxygen distribution from the Eastern edge (left) to the biofilter center (right). Measurements were carried out on September 26th (a), October 3rd (b), October 10th (c) and October 16th (d), 2012.

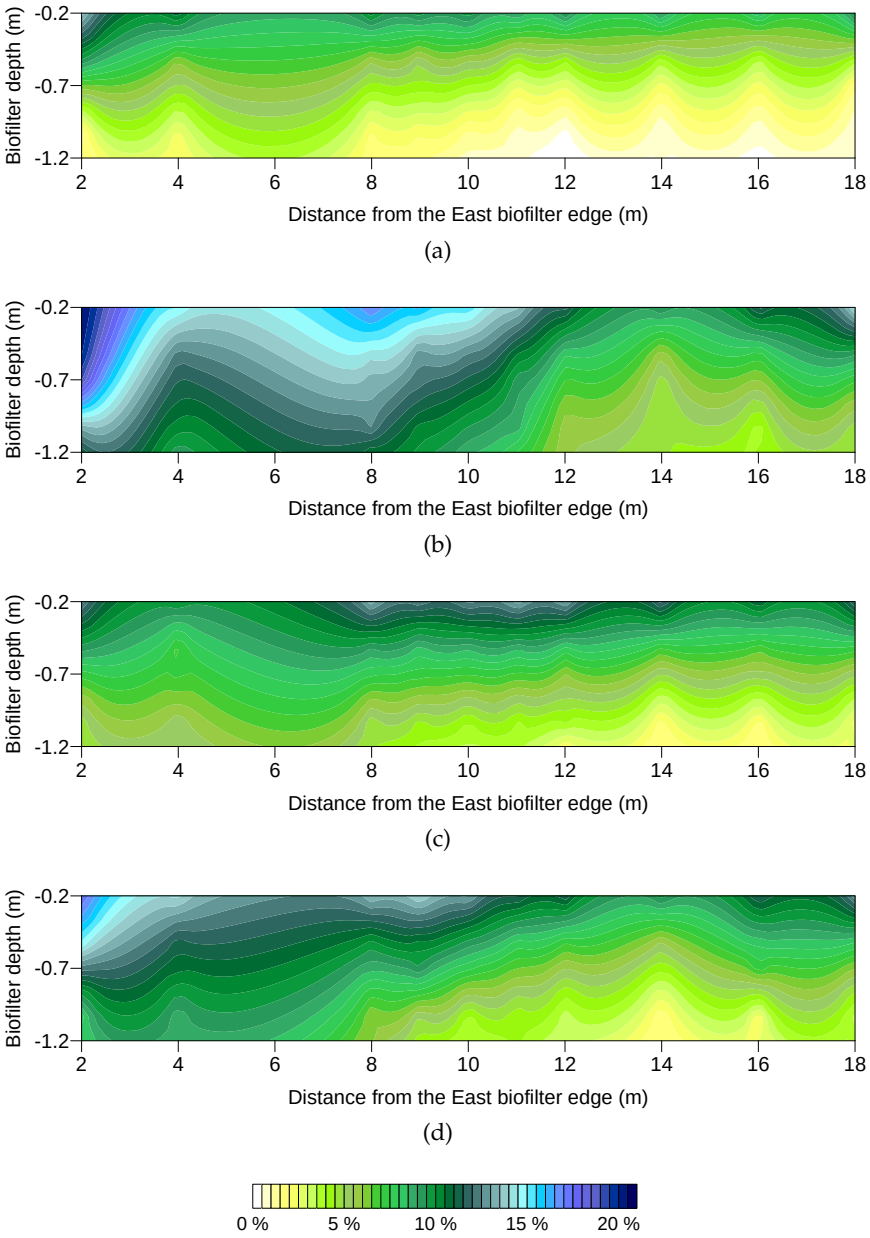

Figure 73: Northern sections of the biofilter representing oxygen distribution from the Eastern edge (left) to the biofilter center (right). Measurements were carried out on October 24th (a), October 31st (b), November 7th (c) and November 14th (d), 2012.

A.3 FLUX CHAMBER MEASUREMENTS

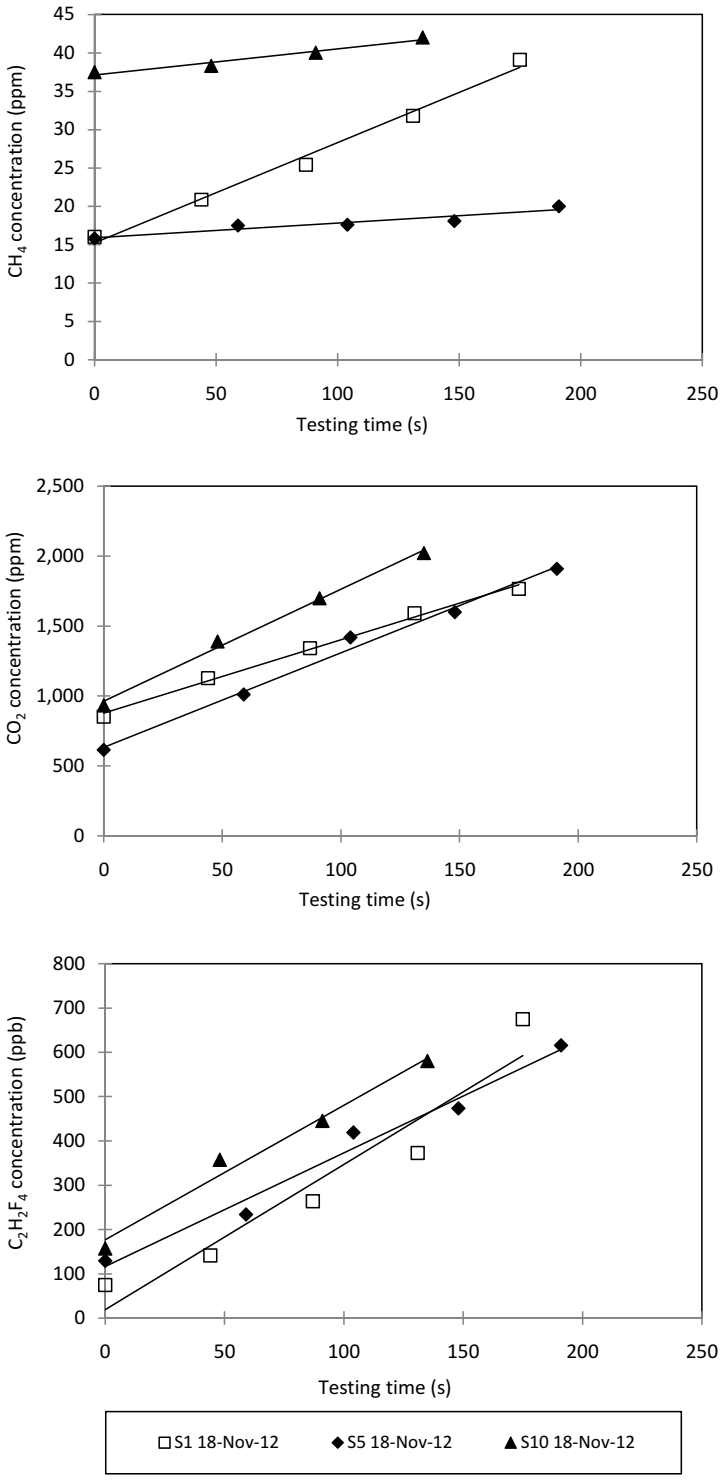

Figure 74: Concentrations of CH_4, CO_2 and $C_2H_2F_4$ (tracer gas) versus time measured in the Southern part of the biofilter during flux chamber campaign on November 18th. The spatial distribution of the sampled points can be observed in figure 23, paragraph 4.7.

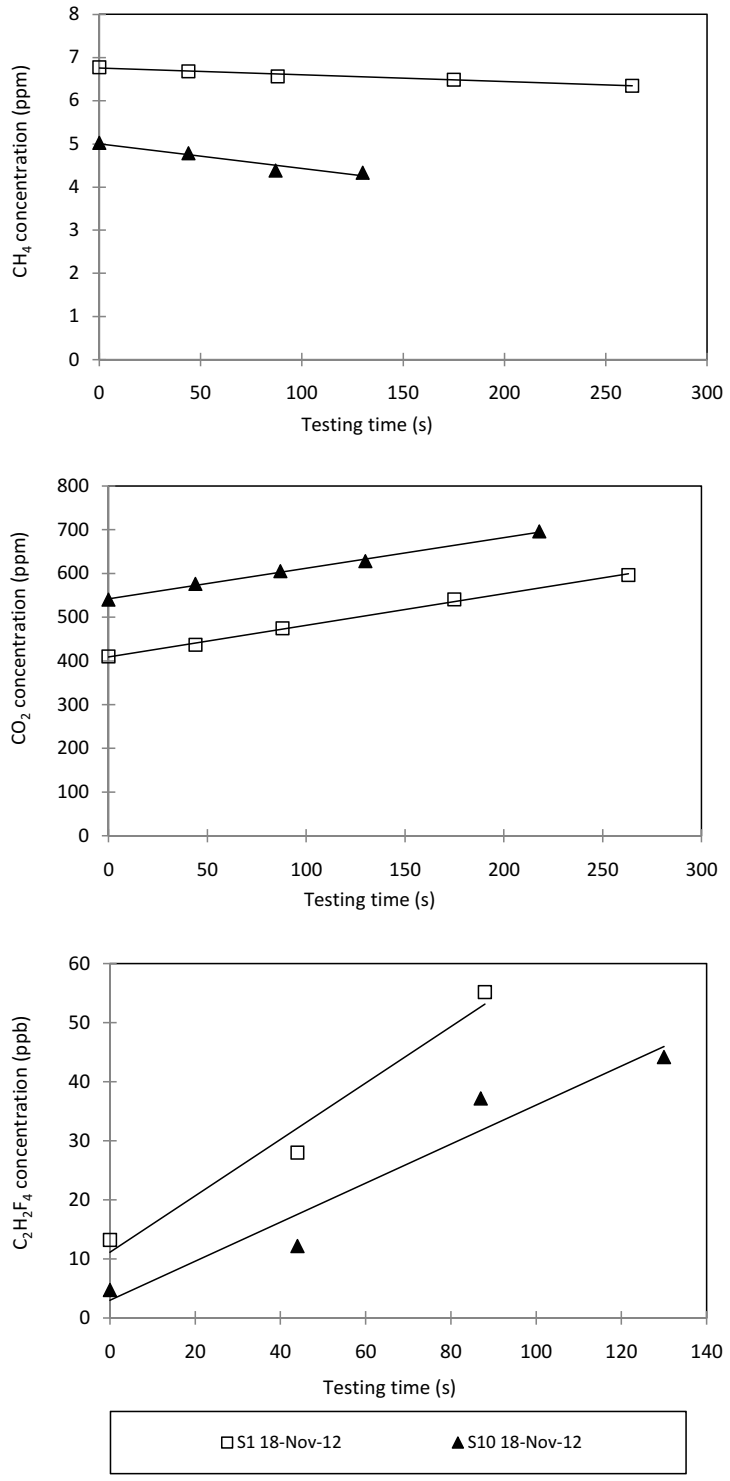

Figure 75: Concentrations of CH_4, CO_2 and $C_2H_2F_4$ (tracer gas) versus time measured in the Northern part of the biofilter during flux chamber campaign on November 18th. The spatial distribution of the sampled points can be observed in figure 23, paragraph 4.7.

A.4 GAS PROFILES OF THE BIOFILTER

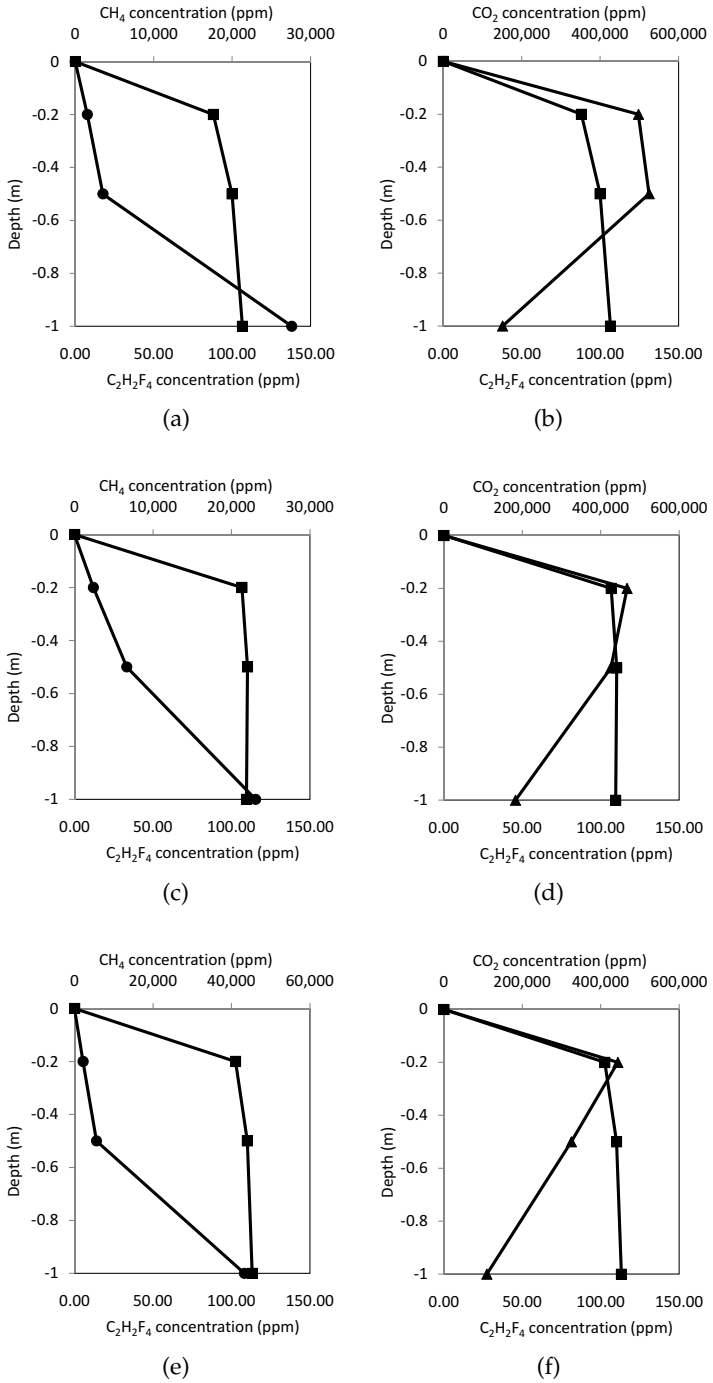

Figure 76: Representative gas profiles for methane (●), carbon dioxide (▲) and tracer (■) measured in different points during December 8th campaign. Graphs a) and b) are referring to point S4, graphs c) and d) are referring to point S8 and e) and f) to point S10. The spatial distribution of the sampled points can be observed in figure 24, paragraph 4.7.

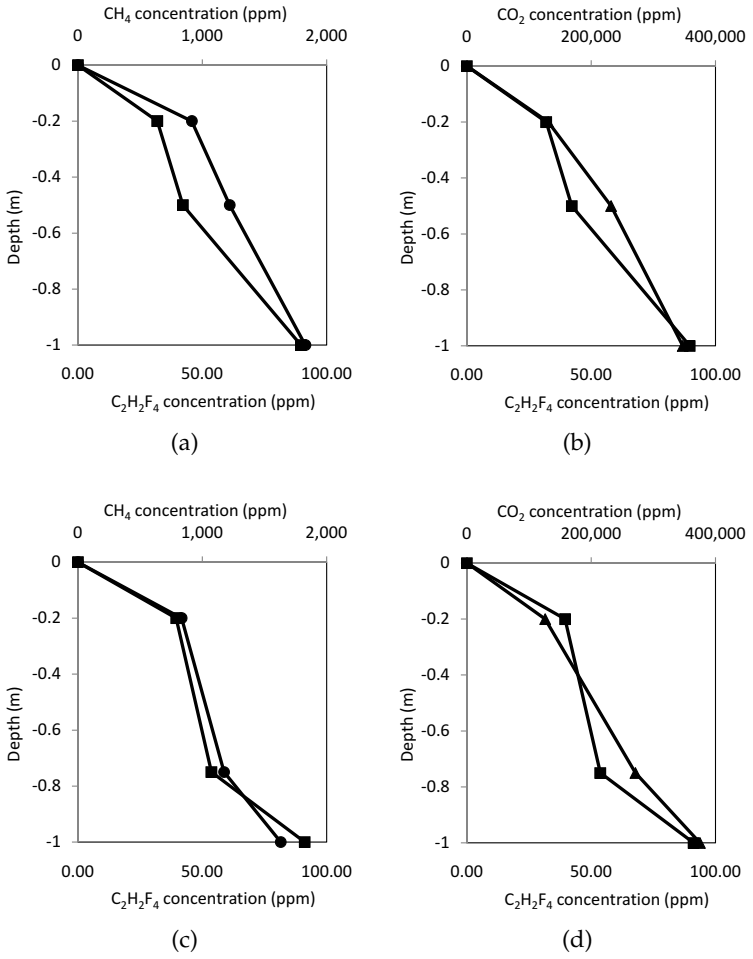

Figure 77: Representative gas profiles for methane (•), carbon dioxide (▲) and tracer (■) measured in different points during December 8th campaign. Graphs a) and b) are referring to point N4 and graphs c) and d) are referring to point N8. $C_2H_2F_4$ has been used as tracer gas. The spatial distribution of the sampled points can be observed in figure 24, paragraph 4.7.

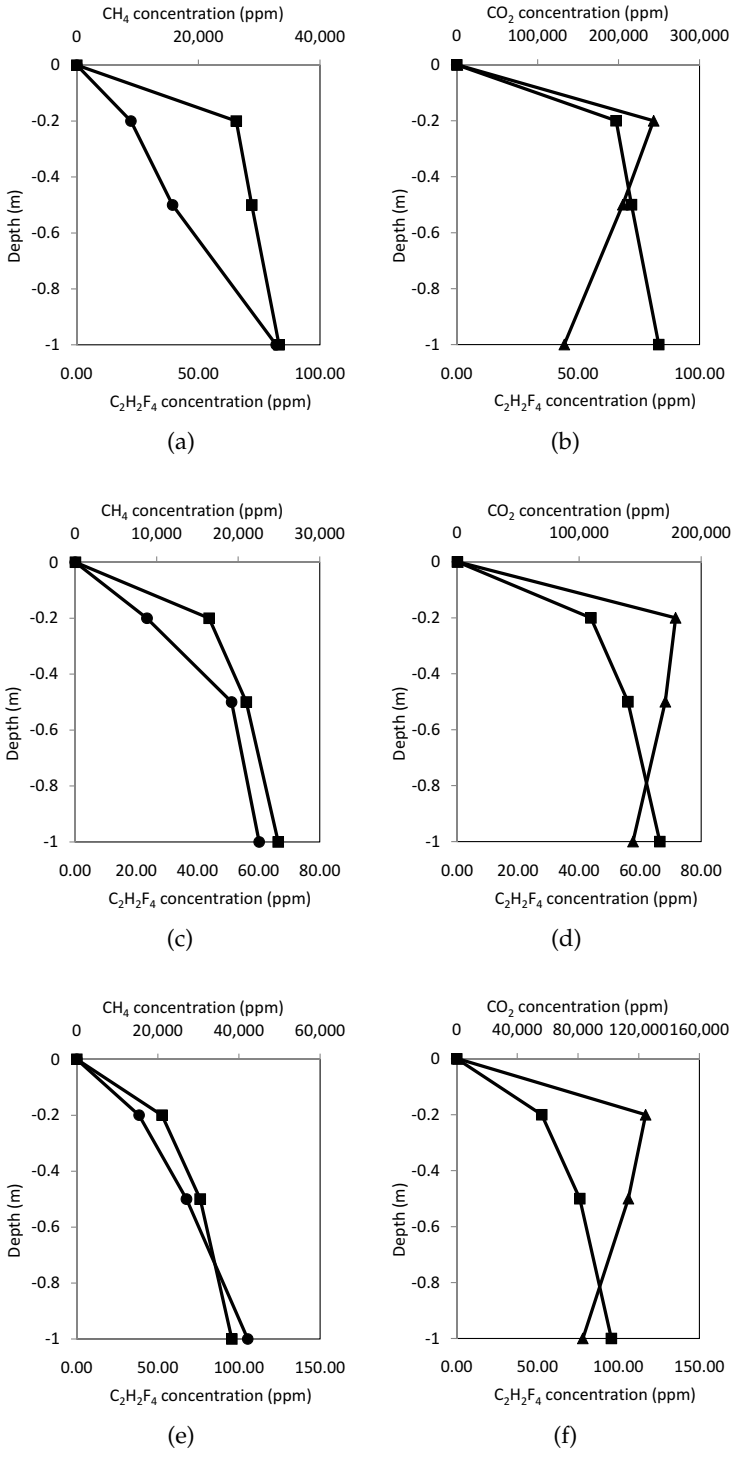

Figure 78: Representative gas profiles for methane (●), carbon dioxide (▲) and tracer (■) measured in different points during November 18th campaign. Graphs a) and b) are referring to point S1, graphs c) and d) are referring to point S5 and e) and f) to point S10. $C_2H_2F_4$ has been used as tracer gas. The spatial distribution of the sampled points can be observed in figure 23, paragraph 4.7.

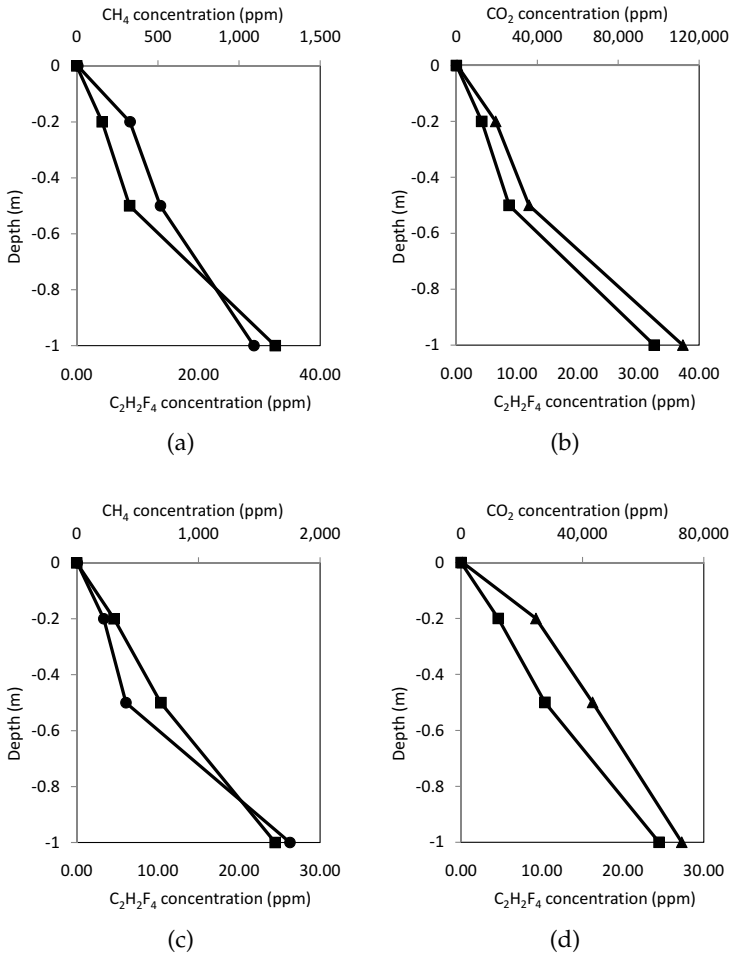

Figure 79: Representative gas profiles for methane (•), carbon dioxide (▲) and tracer (■) measured in different points during November 18th campaign. Graphs a) and b) are referring to point N1 and graphs c) and d) are referring to point N10. $C_2H_2F_4$ has been used as tracer gas. The spatial distribution of the sampled points can be observed in figure 23, paragraph 4.7.

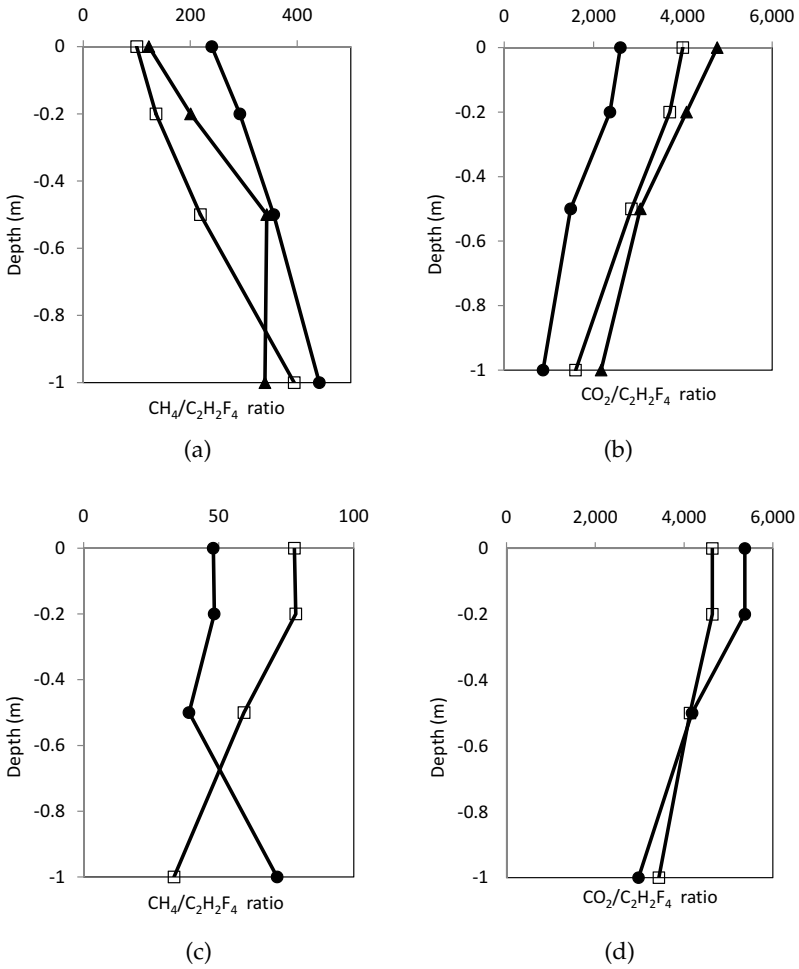

Figure 80: Profiles describing rates of the ratio between CH_4 or CO_2 concentrations and the tracer gas. Concentrations were measured in different points during November 18th campaign, and are referring to point S1-N1 (□), S5 (▲), S10-N10 (•). $C_2H_2F_4$ has been used as tracer gas. The spatial distribution of the sampled points can be observed in figure 23, paragraph 4.7.

BIBLIOGRAPHY

AVMiljø, 2011. Årsrapport 2011. COWI, AV Miljø, <http://www.av.dk/>, –. (Cited on pages xix, 22, and 23.)

Bogner, J., Pipatti, R., Hashimoto, S., Diaz, C., Mareckova, K., Diaz, L., Kjeldsen, P., Monni, S., Faaij, A., Gao, Q., Zhang, T., Ahmed, M. A., Sutamihardja, R. T. M., Gregory, R., FEB 2008. Mitigation of global greenhouse gas emissions from waste: conclusions and strategies from the Intergovernmental Panel on Climate Change (IPCC) Fourth Assessment Report. Working Group III (Mitigation). WASTE MANAGEMENT & RESEARCH 26 (1), 11–32. (Cited on pages 1, 3, 5, and 8.)

Borjesson, G., Danielsson, Svensson, B. H., 2000. Methane fluxes from a swedish landfill determined by geostatistical treatment of static chamber measurements. Environmental Science & Technology 34, 4044–4050. (Cited on pages 20, 28, and 34.)

Bowman, J., Sly, L., Nichols, P., Hayward, A., 1994. Revised taxonomy of the methantrophs. INTERNATIONAL JOURNAL OF SYSTEMATIC BACTERIOLOGY 44, 375. (Cited on page 9.)

Cabral, A. R., Moreira, J. F. V., Jugnia, L. B., AUG 2010. Biocover Performance of Landfill Methane Oxidation: Experimental Results. JOURNAL OF ENVIRONMENTAL ENGINEERING-ASCE 136 (8), 785–793, 1st Global Waste Management Symposium (GWMS), Copper Mt, CO, SEP 07-10, 2008. (Cited on pages 14, 27, 28, 34, and 90.)

Christophersen, M., Kjeldsen, P., 2001. Lateral gas transport in soil adjacent to an old landfill: factors governing gas migration. WASTE MANAGEMENT & RESEARCH 19, 579–594. (Cited on pages 19, 20, 28, and 29.)

Cossu, R., 2009. From triangles to cycles. EDITORIAL/WASTE MANAGEMENT 29, 2915–2917. (Cited on pages 1 and 3.)

Cossu, R., 2009a. Driving forces in national waste management strategies. EDITORIAL/WASTE MANAGEMENT 29, 2797–2798. (Cited on page 3.)

Czepiel, P., Shorter, J., Mosher, B., Allwine, E., McManus, J., Harriss, R., Kolb, C., Lamb, B., 2003. The influence of atmospheric pressure on landfill methane emissions. WASTE MANAGEMENT 23, 593–598, 2nd Intercontinental Landfill Research Symposium (ICLRS), ASHEVILLE, NORTH CAROLINA, OCT, 2002. (Cited on page 29.)

Dever, S. A., Swarbrick, G. E., Stuetz, R. M., MAY 2011. Passive drainage and biofiltration of landfill gas: Results of Australian field trial. WASTE MANAGEMENT 31 (5, SI), 1029–1048. (Cited on pages 9, 16, 18, 27, 79, 90, 91, and 93.)

Einola, J., Sormunen, K., Lensu, A., Leiskallio, A., Ettala, M., Rintala, J., 2009. Methane oxidation at a surface-sealed boreal landfill. WASTE MANAGEMENT 29, 2105–2120. (Cited on pages 20, 27, and 28.)

Fredenslund, A. M., Scheutz, C., Kjeldsen, P., 2010. Tracer method to measure landfill gas emissions from leachate collection systems. WASTE MANAGEMENT 30, 2146–2152. (Cited on pages 5, 8, 24, 28, and 29.)

Galle, B., Samuelsson, J., 1999. Measurements of methane emissions from landfills using a time correlation tracer method based on ftir absorption spectroscopy. Doktorsavh Chalmers Tek Hogsk, –. (Cited on page 28.)

Gebert, J., Grongroft, A., 2006. Performance of a passively vented field-scale biofilter for the microbial oxidation of landfill methane. WASTE MANAGEMENT 26, 399–407. (Cited on pages 13, 17, 90, and 91.)

Gendebien, A., P. M. L.-D. M. N. E. W. H. B. J. F. R. F. G., 1992. Potential landfill gas damages to vegetation. Landfill Gas from Environment to Energy. Commission of the European Communities, Luxembourg, pp. 35–46. (Cited on pages 6 and 7.)

Geotech, 2011. Biogas 5000 portable gas analyser. Digital Image, Accessed 2 January 2013, <www.geotech.co.uk>. (Cited on pages ix and 31.)

Haubrichs, R., Widmann, R., 2006. Evaluation of aerated biofilter systems for microbial methane oxidation of poor landfill gas. WASTE MANAGEMENT 26, 408–416. (Cited on pages 10, 16, and 92.)

Huber-Humer, M., 2004. Abatement of landfill methane emissions by microbial oxidation in biocovers made of compost. Ph.D. Thesis at the University of Natural Resources and Applied Life Sciences Vienna Institute of Waste Management. (Cited on pages xiv, 89, and 93.)

Huber-Humer, M., Gebert, J., Hilger, H., 2008. Biotic systems to mitigate landfill methane emissions. WASTE MANAGEMENT & RESEARCH 26, 33–46. (Cited on pages ix, 7, 8, 10, and 11.)

Huber-Humer, M., Roeder, S., Lechner, P., 2009. Approaches to assess biocover performance on landfills (vol 27, pg 2092, 2009). WASTE MANAGEMENT 29, 2600. (Cited on page 57.)

Humer, M., Lechner, P., 2001. Design of a Landfill Cover Layer to Enhance Methane Oxidation - Results of a Two Year Field Investigation, 541–550. (Cited on page 9.)

KøbenhavnsAMT, 2006. Miljøgodkendelse. COWI, AV Miljø, <http://www.av.dk/>, –. (Cited on pages ix and 22.)

Kjeldsen, P., 1996. Landfill gas migration in soil. E. & FN Spon, pp. 87–132, 1996; 3.1. (Cited on pages ix, 4, 5, and 6.)

Kjeldsen, P., Fischer, E., 1995. Landfill gas migration - field investigations at Skellingsted landfill, Denmark. Waste Management and Research 13, 467–484. (Cited on page 6.)

LaCrosseTechnology, 2013. Ws-3650 weather station. Digital Image, Accessed 2 January 2013, <http://www.lacrossetechnology.com/>. (Cited on pages x and 36.)

LumaSenseTechnologies, 2012. Photoacoustic gas monitor innova 1412i. Digital Image, Accessed 2 January 2013, <http://www.lumasenseinc.com>. (Cited on pages x, 40, 41, 42, and 43.)

Nagendran, R., Selvam, A., Joseph, K., Chiemchaisri, C., 2006. Phytoremediation and rehabilitation of municipal solid waste landfills and dumpsites: A brief review. WASTE MANAGEMENT 26 (12), 1357–1369. (Cited on page 6.)

NOAA, N. O. . A. A., 2013. Atmospheric carbon dioxide at manua loa observatory. Accessed 10 January 2013, <http://www.esrl.noaa.gov/gmd/obop/mlo/>. (Cited on page 58.)

Pedersen, G. B., Scheutz, C., Kjeldsen, P., 2011. Availability and properties of materials for the Fakse Landfill biocover. WASTE MANAGEMENT 31, 884–894. (Cited on page 77.)

Peter Kjeldsen and Charlotte Scheutz, 2011. Evaluating Gas Emissions From Landfills, Which Methodologies Can Be Used. Environmental Sanitary Engineering Centre. (Cited on pages 28 and 29.)

Philopoulos, A., Felske, C., McCartney, D., SEP 2008. Field-scale treatment of landfill gas with a passive methane oxidizing biofilter. JOURNAL OF ENVIRONMENTAL ENGINEERING AND SCIENCE 7 (5), 531–542. (Cited on pages 15, 16, 17, 27, 90, and 91.)

Poulsen, T. G., Moldrup, P., OCT 2006. Evaluating effects of wind-induced pressure fluctuations on soil-atmosphere gas exchange at a landfill using stochastic modelling. WASTE MANAGEMENT & RESEARCH 24 (5), 473–481. (Cited on page 29.)

Rogner, H.-H., D. Z. R. B. P. C. O. E. B. A. L. K. M. Y., 2007. Introduction. In Climate Change 2007: Mitigation. Contribution of Working Group III to the Fourth Assessment Report of the Intergovernmental Panel on Climate Change [B. Metz, O.R. Davidson, P.R. Bosch, R. Dave, L.A. Meyer (eds)], Cambridge University Press, Cambridge, United Kingdom and New York, NY, USA. (Cited on page 5.)

Roncato, C. D. L., Cabral, A. R., FEB 2012. Evaluation of Methane Oxidation Efficiency of Two Biocovers: Field and Laboratory Results. JOURNAL OF ENVIRONMENTAL ENGINEERING-ASCE 138 (2), 164–173. (Cited on pages 15, 18, 20, 80, 90, and 91.)

Scheutz, C., Fredenslund, A. M., Chanton, J., Pedersen, G. B., Kjeldsen, P., 2011a. Mitigation of methane emission from Fakse landfill using a biowindow system. WASTE MANAGEMENT 31, 1018–1028. (Cited on pages 8, 19, and 25.)

Scheutz, C., Fredenslund, A. M., Nedenskov, J., Samuelsson, J., Kjeldsen, P., 2011b. Gas production, composition and emission at a modern disposal site receiving waste with a low-organic content. WASTE MANAGEMENT 31, 946–955. (Cited on pages 22 and 24.)

Scheutz, C., Kjeldsen, P., Bogner, J. E., De Visscher, A., Gebert, J., Hilger, H. A., Huber-Humer, M., Spokas, K., 2009. Microbial methane oxidation processes and technologies for mitigation of landfill gas emissions. WASTE MANAGEMENT & RESEARCH 27, 409–455. (Cited on pages 9, 10, 27, 28, and 93.)

Scheutz, C., Pedicone, A., Pedersen, G. B., Kjeldsen, P., 2011. Evaluation of respiration in compost landfill biocovers intended for methane oxidation. WASTE MANAGEMENT 31, 895–902. (Cited on pages 5, 9, and 10.)

Scheutz, C., Samuelsson, J., Fredenslund, A. M., Kjeldsen, P., 2011c. Quantification of multiple methane emission sources at landfills using a double tracer technique. WASTE MANAGEMENT 31, 1009–1017. (Cited on pages 24 and 28.)

Spokas, K., Bogner, J., Chanton, J., Morcet, M., Aran, C., Graff, C., Moreau-Le Golvan, Y., Hebe, I., 2006. Methane mass balance at three landfill sites: What is the efficiency of capture by gas collection systems? WASTE MANAGEMENT 26, 516–525. (Cited on page 7.)

Stern, J. C., Chanton, J., Abichou, T., Powelson, D., Yuan, L., Escoriza, S., Bogner, J., 2007. Use of a biologically active cover to reduce landfill methane emissions and enhance methane oxidation. WASTE MANAGEMENT 27, 1248–1258. (Cited on pages 20, 28, 57, 80, and 90.)

Streese, J., Stegmann, R., 2003. Microbial oxidation of methane from old landfills in biofilters. WASTE MANAGEMENT 23 (7), 573–580, 2nd Intercontinental Landfill Research Symposium (ICLRS), ASHEVILLE, NORTH CAROLINA, OCT, 2002. (Cited on pages 9, 14, 17, 27, and 91.)

ThermoScientific, 2008. Fid vapor analyzer 1000b. Digital Image, Accessed 2 January 2013, <http://www.thermo.com/ih>. (Cited on pages x, 37, and 38.)

Vaisala, 2009. Gmp343 carbon dioxide probe. Digital Image, Accessed 2 January 2013, <http://www.vaisala.com>. (Cited on pages x, 37, 38, and 42.)

Wilshusen, J., Hettiaratchi, J., Stein, V., 2004. Long-term behavior of passively aerated compost methanotrophic biofilter columns. WASTE MANAGEMENT 24, 643–653. (Cited on pages 10, 18, 91, and 92.)

DECLARATION

I hereby declare that the project work entitled "Evaluation of the methane mitigation at the AV Miljø pilot biocover system" is the report of the work done by me under the guidance of Professor Kjeldsen Peter, Department of Environmental Engineering, Technical University of Denmark. This project work is submitted in the partial fulfillment of the requirements for the award of the Mater Degree in Environmental Engineering at Padua University.

Candidate:Cassini Filippo, Year 2013

Cassini Filippo